

Aus dem Institut für Immunologie der Ludwig-Maximilians-Universität München  
Direktor: Prof. Dr. Thomas Brocker

# Ppef2 controls the survival and function of CD8<sup>+</sup> dendritic cells

Dissertation

zum Erwerb des Doktorgrades der Naturwissenschaften (Dr. rer. nat.)  
an der medizinischen Fakultät  
der Ludwig-Maximilians-Universität München



vorgelegt von  
Markus Zwick  
aus Bad Friedrichshall

2017



Aus dem Institut für Immunologie der Ludwig-Maximilians-Universität München  
Direktor: Prof. Dr. Thomas Brocker

# Ppef2 controls the survival and function of CD8<sup>+</sup> dendritic cells

Dissertation

zum Erwerb des Doktorgrades der Naturwissenschaften (Dr. rer. nat.)  
an der medizinischen Fakultät  
der Ludwig-Maximilians-Universität München



vorgelegt von  
Markus Zwick  
aus Bad Friedrichshall

München, den 14. Dezember 2017

**Gedruckt mit Genehmigung der Medizinischen Fakultät  
der Ludwig-Maximilians-Universität München**

Betreuer: Prof. Dr. Thomas Brocker

Zweitgutachter: Prof. Dr. Barbara Schraml

Dekan: Prof. Dr. med. dent. Reinhard Hickel

Tag der mündlichen Prüfung: 05.12.2017

# Eidesstattliche Versicherung

Markus Zwick

---

Name, Vorname

Ich erkläre hiermit an Eides statt,  
dass ich die vorliegende Dissertation mit dem Thema

Ppof2 controls the survival and function of CD8<sup>+</sup> dendritic cells

selbständig verfasst, mich außer der angegebenen keiner weiteren Hilfsmittel bedient und alle Erkenntnisse, die aus dem Schrifttum ganz oder annähernd übernommen sind, als solche kenntlich gemacht und nach ihrer Herkunft unter Bezeichnung der Fundstelle einzeln nachgewiesen habe.

Ich erkläre des Weiteren, dass die hier vorgelegte Dissertation nicht in gleicher oder in ähnlicher Form bei einer anderen Stelle zur Erlangung eines akademischen Grades eingereicht wurde.

München, den 18.12.2017

---

Ort, Datum

Markus Zwick

---

Unterschrift Doktorandin/Doktorand

This work contains work presented in the following publication:

M. Zwick, T. Ulas, YL. Cho, C. Ried, V. Buchholz, JL. Schulze, D. Busch, T. Brocker, "Ppef2 controls the survival and function of CD8<sup>+</sup> dendritic cells."

*Manuscript in preparation*

---

# Table of Contents

<b>List of Figures</b>	<b>iii</b>
<b>Abbreviations</b>	<b>iv</b>
<b>1 Summary</b>	<b>1</b>
<b>2 Zusammenfassung</b>	<b>2</b>
<b>3 Introduction</b>	<b>3</b>
3.1 The immune system of higher vertebrates . . . . .	3
3.2 Dendritic Cells . . . . .	4
3.2.1 Development and heterogeneity of DCs <i>in vivo</i> . . . . .	4
3.2.2 DC subsets and their phenotype . . . . .	6
3.2.3 DCs in immunity and tolerance . . . . .	8
3.2.4 DC homeostasis . . . . .	10
3.3 Ppef2 . . . . .	13
3.4 Knockout-first constructs . . . . .	17
3.5 Aim of the project . . . . .	19
<b>4 Results</b>	<b>20</b>
4.1 Ppef2 expression profile analysis . . . . .	20
4.2 Evaluation of Ppef2 deficiency in knockout mice . . . . .	24
4.3 Phenotyping of Ppef2 knockout mice . . . . .	25
4.3.1 Phenotyping of Ppef2 <sup>-/-</sup> DCs . . . . .	25
4.3.2 Phenotyping of other haematopoietic cells . . . . .	29
4.4 Analysis of apoptosis in Ppef2 <sup>-/-</sup> animals . . . . .	30
4.4.1 Apoptosis <i>in vitro</i> . . . . .	30
4.4.2 Apoptosis <i>ex vivo</i> . . . . .	33
4.4.3 Apoptosis <i>in vivo</i> . . . . .	35
4.5 Mixed chimeras . . . . .	36
4.6 Analysis of DC proliferation and turnover . . . . .	38
4.7 <i>In vivo</i> antigen presentation . . . . .	40
4.8 mRNA sequencing and western blot analysis of Ppef2 <sup>-/-</sup> DCs . . . . .	42
<b>5 Discussion</b>	<b>47</b>
5.1 Ppef2 is preferentially expressed by CD8 <sup>+</sup> DCs . . . . .	47

5.2	Expression of Ppef2 is differentially regulated by innate stimuli . . .	48
5.3	The Ppef2 gene trap leads to loss of Ppef2 . . . . .	53
5.4	Ppef2 controls apoptosis of DCs . . . . .	54
5.5	Increase in apoptosis is a CD8 <sup>+</sup> DC intrinsic effect . . . . .	56
5.6	Analyses of DC proliferation and DC precursors do not show com- pensatory effects . . . . .	57
5.7	Ppef2 controls the ability of DCs to transiently activate T cells <i>in</i> <i>vivo</i> . . . . .	58
5.8	Reduced expression of Trim2 leads to accumulation of pro-apoptotic Bim . . . . .	60
5.9	Conclusion and Outlook . . . . .	61
<b>6</b>	<b>Material and Methods</b>	<b>63</b>
6.1	Materials . . . . .	63
6.1.1	Devices . . . . .	63
6.1.2	Consumables . . . . .	64
6.1.3	Chemicals . . . . .	64
6.1.4	Buffer and media . . . . .	64
6.1.5	Antibodies . . . . .	67
6.1.6	Oligonucleotides, peptides and proteins . . . . .	71
6.1.7	Mouse strains . . . . .	72
6.2	Methods . . . . .	74
6.2.1	Immunological and cell biology methods . . . . .	74
6.2.2	Molecular biology . . . . .	82
6.2.3	Statistics . . . . .	85
	<b>References</b>	<b>86</b>
	<b>Acknowledgements</b>	<b>107</b>

---

## List of Figures

3.1	Schematic representation of the Ppef2 protein structure. . . . .	13
3.2	Ppef2 expression profile. . . . .	16
3.3	The knockout-first construct and its conversion. . . . .	18
4.1	Ppef2 is predominantly expressed by CD8 <sup>+</sup> DCs. . . . .	21
4.2	Maturation of DCs leads to downregulation of Ppef2 expression. . .	23
4.3	Verification of the Ppef2 knockout on mRNA level. . . . .	25
4.4	Percentage and total numbers of DC (subpopulations) are not af- fected by the loss of Ppef2. . . . .	26
4.5	Lack of Ppef2 does not influence splenic microarchitecture. . . . .	26
4.6	Ppef2 deficiency does not alter the percentage and total number of DCs in non-lymphoid organs. . . . .	27
4.7	Ppef2 <sup>-/-</sup> mice show a normal cytokine profile. . . . .	28
4.8	Phenotyping of hematopoietic cells does not show abnormalities. . .	30
4.9	Ppef2 <sup>-/-</sup> GM-CSF BMDCs are more prone to apoptosis after grow- th factor withdrawal. . . . .	32
4.10	Ppef2 <sup>-/-</sup> <i>ex vivo</i> cultured splenic DCs show an increase in apoptosis. 35	
4.11	Loss of Ppef2 leads to an increase of apoptotic DCs <i>in vivo</i> . . . . .	36
4.12	Ppef2 <sup>-/-</sup> DCs have a disadvantage in a competitive situation. . . .	37
4.13	Analysis of DC proliferation and turnover. . . . .	39
4.14	<i>In vivo</i> antigen presentation. . . . .	41
4.15	mRNA sequencing of sorted splenic DCs and verification by qPCR. 43	
4.16	Analysis of pro-apoptotic Bim and Dll4 on protein level. . . . .	45
5.1	TLR and CD40 signaling both include TRAF6. . . . .	50

## Abbreviations

<b>AA</b>	Amino acid
<b>APCs</b>	antigen presenting cells
<b>Batf3</b>	basic leucine zipper transcription factor ATF-like 3
<b>Bim</b>	BCL-2-interacting mediator of cell death
<b>BMDCs</b>	bone marrow-derived dendritic cell
<b>BrdU</b>	bromodeoxyuridine
<b>cDCs</b>	classical Dendritic Cells
<b>CDPs</b>	common DC precursors
<b>CLPs</b>	common lymphoid progenitors
<b>CMPs</b>	common myeloid progenitors
<b>cDNA</b>	complementary DNA
<b>DCs</b>	Dendritic Cells
<b>Dll4</b>	Delta-like ligand 4
<b>DTA</b>	diphtheria toxin A
<b>DNA</b>	Deoxyribonucleic acid
<b>e.g.</b>	exempli gratia
<b>ELISA</b>	Enzym-linked immunosorbent assay
<b>ESAM</b>	endothelial cell-selective adhesion molecule
<b>EUCOMM</b>	European Conditional Mouse Mutagenesis Program
<b>Flt3</b>	FMS-like tyrosin kinase 3
<b>Flt3L</b>	FMS-like tyrosin kinase 3 ligand
<b>FITC</b>	Fluorescein isothiocyanate

<b>FDG</b>	fluorescein di-V-galactoside
<b>GFP</b>	green fluorescent protein
<b>GM-CSF</b>	granulocyte-macrophage colony-stimulating factor
<b>GMPs</b>	granulocyte-macrophage precursors
<b>IRFs</b>	IFN regulatory factors
<b>KO</b>	knockout
<b>LCs</b>	Langerhans cells
<b>LPS</b>	lipopolysaccharide
<b>mAb</b>	monoclonal antibody
<b>MDPs</b>	macrophage/DC precursors
<b>mRNA</b>	messenger RNA
<b>MHCII</b>	major histocompatibility complex class II
<b>Ppef2</b>	Protein phosphatase with EF-hands 2
<b>pDCs</b>	plasmacytoid Dendritic Cells
<b>PBS</b>	phosphat buffered saline
<b>PCR</b>	Polymerase Chain Reaction
<b>PRRs</b>	pathogen recognition receptors
<b>qPCR</b>	Quantitative PCR
<b>RNA</b>	Ribonucleic acid
<b>TLR</b>	toll-like receptor
<b>Trim2</b>	tripartite motif protein 2
<b>WTSI</b>	Wellcome Trust Sanger Institute
<b>WT</b>	wild type

# 1 Summary

Programmed apoptotic cell death is critical not only for the development and the life cycle of multi-cellular organisms, but also for maintaining the balance between immunity and self-tolerance.

Several diseases like Systemic Lupus erythematosus, Autoimmune lymphoproliferative syndrome, Rheumatoid arthritis, as well as Thyroiditis have been linked to alterations of apoptosis.

For Dendritic Cells (DCs) it was shown that inhibition of caspases by the baculoviral p35, expressed under the control of a DC specific CD11c promoter, causes a defect in DC apoptosis which leads to their accumulation, and results in autoimmunity [1]. This and other studies interfering with DC death suggested that DC apoptosis is an important regulator for maintaining immune self-tolerance [2, 3, 4]. However, a lot of the proteins investigated in the context of apoptosis in DCs are not unique for DCs but show a broad expression throughout many different haematopoietic cell types, or are not expressed naturally in DC (like p35).

Recent comparative promoter analyses published by our group revealed previously unknown genes that share promoter organization with the promoter region of the DC marker CD11c [5]. One of those genes encodes for the “Protein Phosphatase with EF-Hands 2” (Ppef2); a rarely described phosphatase with three EF-hands and an IQ motif. The expression of Ppef2 was DC-specific and downregulated rapidly after activation with toll-like receptor (TLR) ligands.

Here we further characterized the expression of Ppef2 and generated mice deficient for this phosphatase to investigate its role in the context of DC biology. We found that Ppef2<sup>-/-</sup> DCs displayed increased apoptosis *in vitro* and *in vivo*. We also showed that the reduced longevity of DCs caused by the loss of Ppef2 corresponded to a decreased transient T cell activation *in vivo*.

In order to find the mechanism by which Ppef2 influences DC apoptosis, we performed an mRNA sequencing assay and identified tripartite motif protein 2 (Trim2) as differently expressed in Ppef2<sup>-/-</sup> CD8<sup>+</sup> cDCs. Trim2 drives apoptosis by modulating the abundance of BCL-2-interacting mediator of cell death (Bim), which was also increased in Ppef2<sup>-/-</sup> mice.

In conclusion, we showed that Ppef2, specifically expressed by CD8<sup>+</sup> DCs and downregulated after maturation, is a driver of DC apoptosis through Trim2 and Bim.

## 2 Zusammenfassung

Programmierter Zelltod (Apoptose) ist nicht nur für die Entwicklung mehrzelliger Organismen, sondern auch für die Aufrechterhaltung des Gleichgewichts zwischen der Ausbildung einer immunologischen Antwort und der Toleranz gegenüber Selbst von immenser Bedeutung.

Krankheiten wie Systemischer Lupus erythematoses, rheumatoide Arthritis, das autoimmun-lymphoproliferative Syndrom und Thyreoiditis wurden mit der Veränderung apoptotischer Prozesse in Verbindung gebracht. Dass Apoptose auch im Kontext von Dendritischen Zellen (DCs) eine maßgebliche Rolle spielt wurde unter anderem durch die Zell-spezifische Inhibition von Caspasen gezeigt. Die so herbeigeführte Akkumulation von DCs führte schlussendlich zur Ausbildung von Autoimmunität [1]. Diese und andere Studien die sich mit der Langlebigkeit von DCs befassten legten den Schluss nahe, dass die Apoptose von DCs ein wichtiger Regulator für die Aufrechterhaltung der immunologischen Toleranz ist [2, 3, 4]. Viele der in diesem Zusammenhang untersuchten Proteine sind jedoch nicht spezifisch für Dendritische Zellen, sondern zeigen vielmehr ein breites Auftreten in den verschiedensten Zelltypen.

Durch kürzlich veröffentlichten Analysen des Promotorbereichs von DC spezifischen Genen fand unsere Gruppe weitere bislang weitgehend unbekannte Gene, die dieselbe Promotorstruktur wie der weitläufig verwendete DC Marker CD11c aufwiesen [5]. Eines dieser Gene kodiert für die Phosphatase Ppef2 (*Protein Phosphatase EF-Hand 2*). Erste Analysen der Expression von Ppef2 zeigten ein DC spezifisches Expressionsmuster, welches auf Aktivierung von DCs durch TLR Liganden mit der Herunterregulation der Ppef2 Expression reagierte.

In der vorliegenden Arbeit charakterisierten wir die Expression von Ppef2 detailliert und generierten Mäuse, die diese Phosphatase nicht mehr exprimieren, um so ihre Rolle im Kontext von Dendritischen Zellen weiter zu erarbeiten.

Wir konnten so *in vitro* und *in vivo* zeigen, dass Ppef2 defiziente DCs vermehrt apoptotisch sind. Weiterhin konnten wir zeigen, dass die so verkürzte Lebenszeit von CD8<sup>+</sup> DCs zu einer verminderten T Zell Proliferation führte. Durch Sequenzierungsanalysen von Ppef2 defizienten DCs war es uns schlussendlich möglich Trim2 als differentiell exprimiert in CD8<sup>+</sup> DCs identifizieren. Mechanistisch führt Trim2 wiederum durch eine Erhöhung von Bim, welche wir ebenso in Ppef2 defizienten Tieren nachweisen konnten, zur verstärkten Apoptose von CD8<sup>+</sup> DCs.

Zusammenfassend weisen unsere Daten darauf hin, dass Ppef2 ein Regulator für das Überleben von DCs ist.

## 3 Introduction

### 3.1 The immune system of higher vertebrates

The human organism is facing a broad range of potential pathogens. However, only in rare cases these infections lead to the outbreak of a disease. Humans therefore developed a variety of defense mechanisms during evolution as a reaction to new, emerging pathogens.

The immune system of higher vertebrates is separated into two branches, the evolutionary older innate immune system, and the adaptive immune system. When a potentially harmful pathogen breaks through the naturally existing barriers like skin or the gastrointestinal tract, the innate immune system orchestrates the first protective response against the pathogen. Together with antibacterial peptides like  $\alpha$ -defensins, the complement system, and cellular components like NK cells and granulocytes, the innate immune system also has an extensive variety of defense mechanisms that act mostly by recognizing foreign molecular structures or patterns with only a limited repertoire of receptors for the respective antigens (reviewed in [6, 7]).

The other arm of the immune system is the so called adaptive immune system, which consists of B cells and T cells. Adaptive immunity is activated by the innate immune system and therefore acts chronologically later than innate immunity with high affinity and specificity. The wide array of specific antigen receptors of B and T cells are generated by combining a limited number of gene segments in a process called V(D)J-recombination. This somatic recombination occurs semi-randomly and generates a very high variety of antigen receptors, not only against unknown structures of all different kind, but also against self antigens. As a consequence, the developmental process of these antigen receptors has to be tightly controlled and there is a need for mechanisms by which potential self-reactive cells have to be controlled or deleted. Another hallmark of the adaptive immune system is the acquirement of an immunological memory. In case of a second infection with the same pathogen this leads to a faster and better reaction, with antibodies of higher affinity.

In the end, innate immunity has a smaller antigen receptor repertoire than the adaptive immune system but acts faster and is also necessary to activate the latter.

## 3.2 Dendritic Cells

DCs were first described in the 1970s by Ralph Steinman and Zanvil Cohn [8, 9]. Their morphology was described as a “*variety of cell shapes ranging from bipolar elongate cells to elaborate, stellate or dendritic ones*” [8] which led to their name as Dendritic cells. Over the past forty years and a Nobel Prize later it became evident that DCs are unique antigen presenting cells (APCs) that link innate and adaptive immunity [10]. Their location in lymphoid and non-lymphoid organs together with the expression of several pathogen recognition receptors (PRRs) leads to an early recognition of pathogens. This results in the maturation of DCs, which is characterized by upregulation of major histocompatibility complex class II (MHCII), production of costimulatory molecules, expression and secretion of cytokines, as well as enhanced migratory capacities. All of these characteristics are described in more detail in the following chapters.

### 3.2.1 Development and heterogeneity of DCs *in vivo*

Comprehensive studies of DC biology led to the identification of distinct DC subtypes and their respective biogeneses. Several studies tried to clarify the developmental origin of the different DC subtypes, facing the problem that DC subsets of different organs can have different origins. Most insight in classical DC (cDC) development was gained through animal models that were deficient in certain transcription factors, cytokines, cytokine receptors, or by transferring specific precursors into irradiated mice.

By now the cDC lineage is considered as a distinct hematopoietic branch. One of the early progenitor transfer experiments led to the conclusion that common myeloid progenitors (CMPs) can give rise to CD8<sup>+</sup> and CD8<sup>-</sup> DCs [11]. The authors also found that common lymphoid progenitors (CLPs) can give rise to CD8<sup>+</sup> and CD8<sup>-</sup> DCs in the spleen and the thymus but only if transferred in higher numbers. The fact that CMPs are 10 times more numerous than CLPs suggested that, on a per cell basis, CMPs are the major producers of splenic and lymph node DCs, whereas CLPs are more potent in producing thymic DCs [12]. Other studies focusing on Lin<sup>-</sup>c-kit<sup>+</sup>Thy-1<sup>low</sup>CD4<sup>low</sup> intrathymic lymphoid-restricted precursors showed that also those cells can develop into thymic CD8<sup>+</sup> DCs in an irradiated thymus [13], distinguishing thymic CD8<sup>+</sup> DCs development from CD8<sup>+</sup> DCs of other organs. Commitment to the mononuclear phagocyte lineage takes place when CMPs further differentiate into granulocyte-macrophage precursors (GMPs) or macrophage/DC precursors (MDPs) [14]. MDPs were shown to be able to dif-

differentiate into spleen macrophages, lymphoid tissue resident classical Dendritic Cells (cDCs), non-lymphoid tissue-resident cDCs, and some plasmacytoid Dendritic Cells (pDCs), but not granulocytes [14]. Macrophage potential is lost when MDPs differentiate into common DC precursors (CDPs), which were initially defined as  $\text{Lin}^- \text{c-kit}^{\text{int}} \text{Flt3}^+ \text{Csf-1R}^+$  and shown to be able to generate cDCs and pDCs in cultures supplemented with FMS-like tyrosin kinase 3 ligand (Flt3L) [15]. *In vivo* transferred CDPs produced spleen and LN cDCs and pDCs but showed no potential to develop into macrophages [15]. The last differentiation step of DC progenitors takes place after the CDP stage, when  $\text{CD11c}^+ \text{MHCII}^-$  proliferative precursors (pre-cDC) are able to differentiate into  $\text{CD8}^+$  and  $\text{CD11b}^+$  cDCs but not into pDCs. Pre-DCs were shown to migrate from the bone marrow along high endothelial venules to home to lymphoid and non-lymphoid organs [16].

Monocytes were also believed to be precursors of cDCs but studies showed that monocytes generate only very few cDCs when transferred in steady-state recipient mice. However, in mice with an ongoing granulocyte-macrophage colony-stimulating factor (GM-CSF) dependent inflammation, monocytes were able to give rise to  $\text{CD11c}^{\text{int}} \text{CD11b}^{\text{hi}} \text{Mac-3}^+$  DCs in various organs, including the spleen [17]. This finding reflected the ability of monocyte to convert into DCs *in vitro* when cultured in GM-CSF containing medium. Later studies investigating the role of the Notch2 receptor revealed that the blockade of Notch signaling in DCs affected a population within the  $\text{CD11b}^+$  DCs compartment that was distinguished by the expression of the endothelial cell-selective adhesion molecule (ESAM).  $\text{ESAM}^{\text{hi}} \text{CD11b}^+$  DCs were ablated after blocking Notch2 signaling, whereas  $\text{ESAM}^{\text{lo}}$  DCs were unaffected. Closer investigation of the  $\text{ESAM}^{\text{lo}}$  cells revealed a more monocyte-specific expression profile suggesting that these cells arise from monocytes in the steady state [18].

Regulation of the developmental pathways mentioned above is affected extrinsically by hematopoietic cytokines and intrinsically by transcription factors. With regard to control by cytokines, it was shown that FMS-like tyrosin kinase 3 (Flt3), which is expressed by CLPs, MLPs, and steady state DCs in spleen, thymus and epidermis [19], is necessary for DC lineage commitment, as precursors that lack Flt3 expression also lose the potential to differentiate into DC [19]. Another cytokine used to generate cDC from monocytes and hematopoietic progenitors *in vitro* is GM-CSF. Surprisingly, mice lacking GM-CSF, or its corresponding receptor, showed normal development of spleen and LN cDCs [20]. However, it was shown that GM-CSF is necessary for the survival and homeostasis of non-lymphoid tissue-resident  $\text{CD103}^+$  and  $\text{CD11b}^+$  DCs [21].

Transcriptional control of DC development involves, amongst others, IFN regulatory factors (IRFs), basic leucine zipper transcription factor ATF-like 3 (Batf3), and PU.1. IRFs show a subset-specific expression and regulation profile. IRF4, for example, is expressed by CD4<sup>+</sup> DCs, while IRF8 is expressed in CD8<sup>+</sup> DCs. Consequently, lack of IRF4 leads to loss of CD4<sup>+</sup> DCs, whereas loss of IRF8 results in failure to generate spleen-resident CD8<sup>+</sup> DCs and pDCs [22]. In the case of Batf3 the expression pattern doesn't match the effect observed in knockout (KO) strains. Batf3 is expressed in all cDCs, but mice lacking Batf3 showed a background-specific impact only on splenic CD8<sup>+</sup> DCs and CD103<sup>+</sup> DCs [23].

### 3.2.2 DC subsets and their phenotype

DCs are a heterogeneous population of cells. Thus, it is important to distinguish between the different DC subtypes in regard to their development and functional specializations. As already discussed in section 3.2.1, with regard to their origin, we can differentiate between cDCs and pDCs. Conventional DCs include both migratory and lymphoid-resident subsets.

pDCs were first described by Lennert and Remmele in 1958 as plasma cell-like cells that were missing B cell and plasma cell markers and were characterized by the ability to produce large amounts of type I interferons in response to viruses [24]. They express low levels of MHCII and costimulatory molecules, as well as intermediate levels of CD11c in the steady state. As one of the hallmarks of pDCs is the reaction to viral infections, they also express a range of pattern-recognition receptors that include TLR 7 and 9, sensing the presence of viral DNA and RNA [25]. Based on the expression of pDC specific markers like mPDCA-1 [26] and others, pDCs were found in lymphoid organs and also in liver, lung, and skin [27, 28].

The other branch of DCs are conventional DCs. cDCs include all DCs except pDCs. They are a small population of hematopoietic origin (see section 3.2.1) found in lymphoid and non-lymphoid tissues. As major APCs, distributed through several different tissues, DCs have an enhanced capacity to capture and subsequently process and present environmental- and cell-associated antigens to T cells. These key features of DC biology will further be discussed in section 3.2.3. Despite their broad distribution, DCs from different tissues can all be defined by a set of common markers, such as the integrin CD11c, and MHCII. They also lack surface expression of T cell, B cell, NK cell, granulocyte, and erythrocyte lineage markers. CD11c as it is the marker broadly used for the definition of cDCs, is also used in many mouse models to control the DC-specific expression of the Cre transgene

[29]. However, CD11c expression is also found on several macrophage populations, especially in the lung and intestine, and therefore other more cDC specific markers have been recently investigated. One of these is the transcription factor *Zbtb46* [30, 31]. Diphtheria toxin receptor or green fluorescent protein (GFP) reporter-based studies could distinguish cDCs from macrophages. Interestingly, the *Zbtb46* GFP reporter mice showed some heterogeneity of the GFP signal in the CD103<sup>-</sup> CD11b<sup>+</sup> cDC subset of the lung, where only 42% of cells were positive for GFP [31]. TNF- $\alpha$ /iNOS-producing Dendritic Cells (TIP-DCs) displayed little to no tissue expression of *Zbtb46*, which makes them less likely to be DCs and instead potentially have macrophage identity. For this reason, these cells will not be further discussed in detail in this and the following chapters. Epidermal Langerhans cells (LCs) on the other hand did also show expression of *Zbtb46* [32]. However, since LCs differ not only in their ontogeny, yolk sac-derived instead of bone marrow-derived, but also in their homeostasis from cDCs they will not be discussed in greater detail in the following chapters which will focus more on classical DCs.

cDCs can be further subdivided into CD8<sup>+</sup>/CD103<sup>+</sup> and CD11b<sup>+</sup> subsets [33, 34, 35]. Both subsets are discussed below.

### 3.2.2.1 CD8<sup>+</sup>/CD103<sup>+</sup> DCs

The first flow cytometric analyses of splenic and thymic DCs revealed a heterogeneity concerning the surface expression of CD8 [36, 37]. Therefore this cDC subset was the first to be described in more detail. CD8<sup>+</sup> DCs account to 20–40% of spleen, LN, and thymus cDCs. However, thymic cDCs differ in their expression of CD8 from spleen and LN cDCs in regard to the expression of the  $\alpha$  and  $\beta$  chains. Thymic cDCs express both the CD8  $\alpha$  and  $\beta$  chains, whereas splenic cDCs exclusively express the  $\alpha$  chain [37].

In non-lymphoid tissues CD8 expression is not found on DCs, but instead the equivalent subset to CD8<sup>+</sup> DCs are characterized by surface expression of CD103 [38, 39]. The transcriptomes of lymphoid tissue CD8<sup>+</sup> and non-lymphoid tissue CD103<sup>+</sup> DCs are closely related and are clearly distinguishable from CD11b<sup>+</sup> DCs [33]. Furthermore, both CD8<sup>+</sup> and CD103<sup>+</sup> DCs express the cytokine receptor *Xcr1* [40, 41] which makes it a unifying marker for these DC subtypes. The CD8<sup>+</sup>/CD103<sup>+</sup> DC-specific expression of several lectin receptors like DEC205 [42] and Clec9A [43] also makes these surface proteins useful markers. Functionally, CD8<sup>+</sup> and CD103<sup>+</sup> DCs are characterized by the production of high amounts of IL-12p70 after stimulation with TLR ligands [44]. The production of IL-12 by

CD8<sup>+</sup> cDCs differs from that by macrophages because of the requirement of c-Rel in the former [45].

### 3.2.2.2 CD11b<sup>+</sup> DCs

The CD11b<sup>+</sup> DC compartment is characterized by a higher heterogeneity as compared to CD8<sup>+</sup>/CD103<sup>+</sup> DCs. They express CD11b and DCIR2 (also called 33D1) [42], and lack the expression of CD8<sup>+</sup> and CD103<sup>+</sup>. Markers for further subdivision are CD4 and ESAM [18]. High expression of ESAM correlates with an increased expression of CD4, CD11c, and Flt3, whereas low expression of ESAM corresponds to a monocyte-like expression signature, although they do not seem to derive from monocytes [18]. However, this subdivision according to ESAM expression still does not result in a homogeneous population, as shown by parallel single-cell transcriptome analysis [46]. Probably the most functionally relevant difference between CD11b<sup>+</sup> and CD8<sup>+</sup>/CD103<sup>+</sup> cDCs is that the former are not capable of cross-presenting antigens (described in section 3.2.3) [42], but are superior in the induction of CD4 T cell responses.

### 3.2.3 DCs in immunity and tolerance

A hallmark of DCs is their high functional plasticity, which allows them to either initiate immunity or tolerance. In steady state, DCs are located in the subcapsular sinus of the LN, or the T cell zones and the marginal zone of the spleen. Both positions enable DCs to sense circulating pathogens: in the subcapsular sinus as the entry site of afferent lymphatic vessels, or in the spleen by filtering blood antigens [47, 48], with new publications showing also an important role of macrophages in filtering blood antigens in the spleen [49]. These DCs can be distinguished into two developmental stages (mature and immature), which are defined by their expression of costimulatory molecules [50, 51], and their phagocytic activity [52]. Most spleen DCs in steady state show low levels of costimulatory molecules and, in contrast to tissue-migratory cDCs which are in a more mature state, can still present newly encountered antigens [53, 52]. Furthermore, other features, except for their superior location for the induction of immunity or tolerance, are their exceptional antigen processing and presentation machinery, their remarkable capability of migrating to T cell zones of LNs, and finally their notable competence in priming naive T cells [47, 48, 54].

The transcriptome of CD8<sup>+</sup> DCs suggests that they are better equipped to present antigens via MHCI than CD11b<sup>+</sup> DCs [42]. Indeed, *ex vivo* studies re-

led the superior ability of CD8<sup>+</sup> and CD103<sup>+</sup> cDCs to present microbial [55] and cell-associated antigens [23, 56, 57, 58] to CD8<sup>+</sup> T cells, when compared to CD11b<sup>+</sup> DCs. CD11b<sup>+</sup> DCs on the other hand show higher expression of genes encoding for proteins involved in the MHCII processing and presenting machinery [42]. Another feature of CD8<sup>+</sup> and CD103<sup>+</sup> DCs is their ability to load exogenous antigens onto MHCI and presenting them to CD8<sup>+</sup> T cells, a process called cross-presentation [42, 57, 59]. Although cross-presentation seemed to be limited to CD8<sup>+</sup> and CD103<sup>+</sup> DCs, it was shown that also CD11b<sup>+</sup> DCs can be induced to cross-present OVA/anti-OVA immune complexes to CD8<sup>+</sup> T cells in an Fcγ receptor dependent fashion [60]. For viral infection models the question still persists whether CD11b<sup>+</sup> DCs are able to present viral antigens to CD8<sup>+</sup> T cells. For example, in the case of influenza infection, it was shown that the CD103<sup>-</sup> CD11b<sup>high</sup> DCs controlled antigen presentation at the peak of infection [61]. However, it is questionable whether the MHCI dependent presentation in such cases is the result of cross-presentation of infected cell-associated antigens, or direct presentation. Mechanistically, cross-presentation is dependent on endocytosis and a phagosome-to-cytosol transport system. This requires the endocytic pathway to have a low lysosomal proteolytic activity [62, 63], and the intracellular transport system has to ensure antigen trafficking from the phagosome to the cytosol and subsequently the loading onto MHCI molecules [64].

Tolerance can be subdivided in central tolerance and peripheral tolerance, based on the induction site. In primary lymphoid organs, like the thymus and the bone marrow, T cells or B cells, respectively, are tested for autoreactivity after they rearrange their corresponding receptor. In the thymus, T cells that react strongly with MHC-self peptide complexes either have to be converted in regulatory T cells (T<sub>regs</sub>), or undergo apoptosis in order to be removed as potentially harmful autoreactive T cells. Central tolerance induction in the thymus is mediated by endogenous CD8<sup>+</sup> DCs or circulating CD11b<sup>+</sup> DCs from the blood (reviewed in [65, 66]). Although this mechanism is very efficient in ridding the organism of potentially harmful autoreactive T cells, some still leave the thymus and are found in the periphery. In this case, CD8<sup>+</sup> cDCs of the periphery take up self antigens, e.g. in form of dying cells, and present them by cross-presentation to antigen-specific CD8<sup>+</sup> T cells [47, 67, 68], a process termed cross-tolerance induction. The same was shown for migratory CD103<sup>+</sup> DCs in the lamina propria, where DCs were able to induce peripheral T<sub>regs</sub> *in vivo*. The conversion of naive T cells into T<sub>reg</sub> cells is dependent on TGF-β and retinoic acid. CD103<sup>+</sup> DCs express high levels of aldehyde dehydrogenase (ALDH), which converts dietary vitamin A into retinoic

acid [69, 70], as a basis for  $T_{\text{reg}}$  cell conversion.

### 3.2.4 DC homeostasis

Since DCs are the major APCs and are able to initiate either immunity or tolerance, multiple mechanisms control maturation and life span of DCs to guarantee a balanced immunological state.

Early experiments addressing DC turnover were carried out by bromodeoxyuridine (BrdU) labeling of DCs or their respective precursors *in vivo*. BrdU, a chemically modified thymidine analog, enters dividing cells and is incorporated into the DNA, where it can be stained with specific antibodies and analyzed by flow cytometry. It was shown that  $CD8^+$  DCs have a turnover rate of 1.5 days, whereas  $CD8^-$  DCs have a slower turnover of 3 days in the spleen of mice [52]. Skin resident Langerhans cells (LCs) are an exception among DCs, as they showed a remarkable 3- to 4-fold slower BrdU labeling rate [71]. In contrast with the long-held belief that tissue DCs are terminally differentiated non-dividing cells, short time BrdU labeling revealed that about 5% of lymphoid-resident DCs are undergoing cell division at any given time [72]. Furthermore, parabiosis experiments where two CD45 allotypic mice were surgically joined in order to obtain a shared blood circulation revealed that the majority of DCs were not exchanged between hosts after 6 weeks (10–30% being parabiotic partner derived), whereas T and B cells reached equilibrium distribution [72]. This argued in favor of a local renewal capacity for cDCs.

However, this has to be considered carefully since cells and proteins with short half-lives in circulation never reach equilibrium in parabiotic mice and DC precursors are known to have a short half-life. Additionally, chimerism in the blood of parabiotic mice reflected the DC chimerism in lymphoid organs [73]. Ten to fourteen days following separation of parabiotic mice, DCs of spleen and lymph nodes were completely replaced by endogenous bone marrow-derived cells [73]. These findings rather argue for a half-life of 5 to 7 days than the half-lives estimated by short time BrdU labeling. However, in steady state homeostasis, the maintenance of DC populations relies on constant replenishment by blood-borne cells [73, 74] (with a rate of precursor input of nearly 4,300 cells per hour [73]), as well as *in situ* cell division.

The first evidences of factors regulating DC division and homeostasis were found in 1996, when Maraskovsky and colleagues observed that administration of the ligand for the receptor tyrosin kinase Flt3 *in vivo* led to an increase in the number of peripheral DCs [75, 76]. At the same time, inhibition of Flt3-mediated signals

resulted in a reduction of peripheral DCs [77, 78]. Flt3 seemed to be an essential regulator of homeostatic DC division, since mixed bone marrow chimeras of Flt3-deficient and -sufficient mice showed fewer Flt3<sup>-/-</sup> DCs and pDCs. Finally, BrdU experiments revealed the necessity of Flt3 for DC *in situ* proliferation [74].

Mice deficient in the lymphotoxin (LT)- $\beta$  receptor (LT $\beta$ R), a family member of TNF receptors, or its membrane-associated ligand, LT $\alpha$ 1 $\beta$ 2, have reduced numbers of DCs in the spleen [79], but at the same time show an increase in DCs in non-lymphoid tissues; this fact, and the known role of LT $\alpha$ 1 $\beta$ 2 in promoting chemokine and adhesion molecule expression, led researchers to hypothesize a secondary recruitment or retention effect [79]. Others however, hypothesized that LT $\alpha$ 1 $\beta$ 2 might instead act as a growth or survival factor. Indeed, studies of BM chimeras and BrdU incorporation experiments showed such an effect on DCs of spleen and lymph nodes. However, this effect appears to be limited to CD11b<sup>+</sup> DCs as CD8<sup>+</sup> DCs were unaffected by the loss of LT $\beta$ R [72, 80].

Another player in DC homeostasis is the TNF family member TRANCE (tumor necrosis factor [TNF]-related activation-induced cytokine). Unlike Flt3 and LT $\beta$ , TRANCE does not have much influence on steady state DCs, since TRANCE-deficient mice do not show a deficiency of DCs [81]. However, the TRANCE receptor is highly expressed in DCs and studies on TRANCE-treated, mature bone marrow-derived DCs showed enhanced survival through inhibition of apoptosis, which was mediated by upregulation of Bcl-x<sub>L</sub> [82]. The increased survival of TRANCE-treated DCs also resulted in a stronger induction of T cell responses after DC vaccination [2], suggesting that the abundance and longevity of mature DCs influences the strength of T cell immunity *in vivo*.

GM-CSF, a cytokine used for the *in vitro* generation of DCs [83], is a hematopoietic growth factor that controls the differentiation of the myeloid lineage [84]. In consideration of the usage of GM-CSF for DC *in vitro* studies, it came as a surprise that mice lacking expression of this cytokine or its receptor showed only a minor impairment in the development of spleen and LN cDCs [20]. More recent studies showed that GM-CSF plays a role in the survival of non-lymphoid tissue cDCs, which were decreased in the intestine, lung, and dermis of GM-CSF-deficient mice. Furthermore, remaining tissue cDCs in these mice showed a more proapoptotic phenotype [21].

The importance of DC homeostasis, *in situ* proliferation, and DC death becomes obvious when the system is disturbed. After microbial stimulation, *in vivo* BrdU labeling revealed increased DC turnover [52, 85]. Inhibition of caspases by expression of the baculoviral p35 under the control of a CD11c promoter leads to

a defect in DC apoptosis followed by their accumulation and autoimmunity as a result of chronic lymphocyte activation [1]. The same group showed that systemic autoimmunity observed in Bim-deficient mice is not exclusively explained by a defect in negative selection of T cells in the thymus, but also by the ability of Bim-deficient DCs to actively induce autoimmunity [86]. Similar to these findings, systemic autoimmunity detected in mice lacking the receptor on all cells was traced back to DCs, which seemed to be sufficient for the induction of autoimmunity and the production of autoantibodies when loss of the Fas receptor was DC specific [87]. Another regulator of DC survival is Bcl-2, which, when constitutively expressed in DCs, enhances survival [3]. Prolonging the lifespan of DCs by a constitutive, “functionally optimized”, Akt allele enhanced immunogenicity, exempli gratia (e.g.) against tumors [88].

### 3.3 Ppef2

The gene family of mammalian serine-threonine phosphatases with EF-hand protein motifs was first described in 1997, and named Ppef, short for Protein Phosphatase with EF calcium-binding domain [89]. In the original study, the phosphatase investigated showed high homology with *Drosophila* retinal degeneration C (rdgC), which was known to be important to prevent retinal degeneration in *Drosophila* [90]. Amino acid (AA) sequence comparison with rdgC showed homology with other members of the protein phosphatase family. The identified catalytic phosphatase domain ranges in case of murine Ppef2 from AA 128–544 (Fig. 3.1). The sequence of human Ppef showed two EF-hand motifs, which consist of a helix-loop-helix domain found in a large family of calcium-binding proteins [89]. Ppef2, which was described afterwards together with Ppef1 [91], contains three EF-hand domains with two potential  $\text{Ca}^{2+}$  binding sites (Fig. 3.1).

Because of the expression pattern, with highest levels in the retina (Fig. 3.2 A), Ppef2 was long believed to play a role in sensory neurons. Surprisingly, mice deficient for Ppef2 did not show any signs of a defect of rod function or alterations of retina integrity. Even a Ppef1 and Ppef2 double knockout appeared to have normal rhodopsin phosphorylation and dephosphorylation, as well as no signs of retinal degeneration [92]. The study of protein organization and functional domains showed that Ppef2 of *Caenorhabditis elegans* (rdgC) is able to bind to  $\text{Ca}^{2+}$  [93], while the human Ppef2 is able to bind to calmodulin [94]. However, binding of calmodulin to the closely related human recombinant Ppef1 did not influence its phosphatase activity [95]. Furthermore, different microarray studies suggest a role of Ppef2 in stress-protective responses and a possibly positive participation in cell survival, growth, proliferation and oncogenesis (reviewed in [96]).

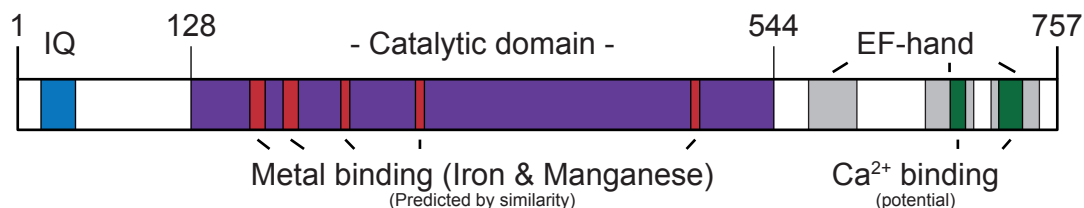


**Figure 3.1: Schematic representation of the Ppef2 protein structure.** Displayed is a schematic representation of the Ppef2 protein as provided by uniprot.org. The most N-terminal motif is an IQ motif starting at amino acid (AA) 21. The catalytic phosphatase domain ranges from AA 128 to 544 and is shown in purple. Three EF-hand domains are located between AA 544 and 757 with two potential  $\text{Ca}^{2+}$ -binding domains within the EF-hands.

The first and so far only functional report of Ppef2 in mammalian cells showed

evidence of a strong interaction of human *Ppef2* with the pro-apoptotic MAP kinase kinase kinase Apoptosis signal-regulating kinase 1 (Ask1) [97], after the same group performed large scale expression analyses and found that expression of *Ppef* phosphatases was influenced by apoptosis-inducing or apoptosis-inhibiting treatments and had a tendency to be elevated in apoptosis-resistant cells [96]. The interaction of *Ppef2* with Ask1 led to dephosphorylation of Ask1 at the threonine residue 838 in COS-7 or HEK 293 A cells after treatment with H<sub>2</sub>O<sub>2</sub>. Phosphorylation at this residue was previously shown to be important for Ask1 activity and therefore serves as indicator of Ask1 activity [98]. *Ppef2* seemed to be more potent in dephosphorylating Ask1 than the already known inhibitor serine/threonine protein phosphatase 5 (PP5) after oxidative stress. Finally, in a system where Ask1 and *Ppef2* were either individually or co-expressed in HEK 293 A or COS-7 cells, suppression of Ask1 by *Ppef2* led to an increase in caspase-3 activation. However, this was not seen when *Ppef2* was expressed without Ask1, in which case the basal level of caspase-3 activity did not change [97].

Genetic and molecular characterization of the promoter region of DC specific genes, particularly CD11c and DC-STAMP, led to the identification of an evolutionary conserved promoter framework consisting of 4 transcription factor binding sites [5]. This motif spanning about 250 base pairs, which was sufficient to drive DC specific gene expression, was further used for a proactive promoter database search, leading to the identification of two genes, *Pftk1* and *Ppef2*, that shared the previously found promoter motif and are preferentially expressed in DCs, according to microarray data (Fig. 3.2). Quantitative PCR (qPCR) of sorted spleen DCs and bone marrow-derived dendritic cell (BMDCs) confirmed the expression in DCs. Interestingly, expression of *Ppef2* was higher in CD8<sup>+</sup> DCs compared to CD8<sup>-</sup> DCs, and stimulation of BMDCs with lipopolysaccharide (LPS) led to a reduction of *Ppef2* expression [5]. In accordance with this finding, the data sets of the Immgen Consortium [99] and BioGPS [100], generated from high throughput data, show the same expression pattern for *Ppef2* (Fig. 3.2). BioGPS (Fig. 3.2 A) focuses on the different organs and offers a broad overview of the distribution of expression, while the Immgen Consortium datasets are restricted to immunologically relevant cell types (Fig. 3.2 B & C). Across the different organs, expression of *Ppef2* is highest in the eye, or more precisely in the Retina, the retinal pigment epithelium, and to a lesser extent the iris (Fig. 3.2 A). Notably, lymphoid CD8<sup>+</sup> DCs (Fig. 3.2 A, shown in red) also show measurable expression of *Ppef2*. Focusing on immunologically relevant cell types, like B cell and their precursors, DCs, Macrophages, Monocytes, NK cells, Neutrophils and T cells of different organs

(Fig. 3.2 B), *Ppef2* expression is highest in CD8<sup>+</sup> DCs of the spleen and thymus (Fig. 3.2 B and C, red), though a similar expression is found also in CD8<sup>-</sup> DCs of thymus (Fig. 3.2 B and C, blue). Blood monocytes (Fig. 3.2 B, yellow) are the only other cells that show expression above background. Taking a closer look at the different DC subtypes (Fig. 3.2 C), *Ppef2* expression seems to be limited to CD8<sup>+</sup> DCs (Fig. 3.2 C, red) across several organs, and CD8<sup>-</sup> DCs (Fig. 3.2 B and C, blue) of the thymus. The closely related CD103<sup>+</sup> DCs (Fig. 3.2 C, green) of liver, lung, lung draining lymph node, and small intestine also show expression above background.

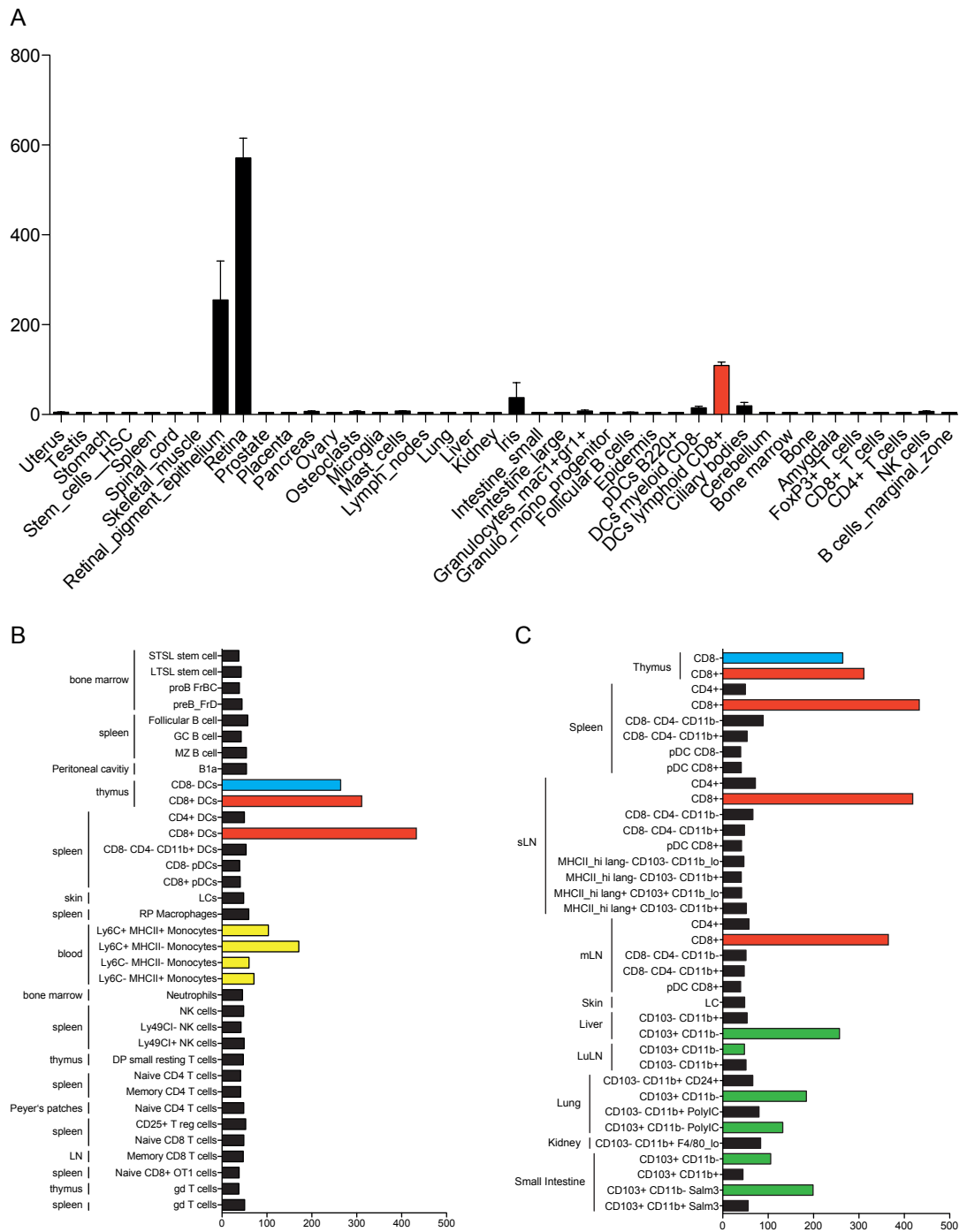


**Figure 3.2: Ppef2 expression profile.** Expression data of Ppef2 was provided by biogps.prg [100] (A) and the Immgen Consortium [99] (B & C). sLN, skin draining lymph node; mLN, mesenteric lymph node; LuLN, lung draining lymph node.

### 3.4 Knockout-first constructs

To study the roles of Ppef2 *in vivo* we generated Ppef2<sup>-/-</sup> mice. Embryonic stem cells targeting Ppef2 with the so called “knockout-first” approach were therefor purchased at the European Conditional Mouse Mutagenesis Program (EUCOMM) and blastocyst microinjection was performed.

Differently from the traditional conditional approach, where an exon is flanked by loxP sites and deleted after exposure to the Cre recombinase, the “knockout-first” constructs act as gene trap by inserting an additional splice acceptor site after an exon, which is followed by a polyadenylation site [101]. The major difference between the Cre-lox system and gene traps is the possibility to delete a gene only in certain cell types. This can be achieved by using a cell specific promoter for the expression of the Cre recombinase, whereas gene traps act on all cell types. The knockout-first construct in the locus of Ppef2 is shown in figure 3.3, together with the possible breeding schemes to generate conditional Ppef2 knockout mice.

The so called targeted mutation 1a (tm1a) allele contains an IRES:lacZ trapping cassette with a splice acceptor from *engrailed-2* (EN2SA) after exon 4 (Fig. 3.3, yellow boxes), as well as the highly effective SV40 polyadenylation signal downstream of a  $\beta$ -Galactosidase (lacZ) reporter, leading, in homozygous mice, to a null allele with lacZ as reporter for promoter activity. This trapping cassette, together with a loxP site and a neomycin (neo) resistance, driven by an autonomous promoter (hBactP), is flanked by Frt sites. Additional loxP sites are flanking exon 5. Crossing of mice containing the tm1a allele with mice expressing the Cre recombinase leads to loss of exon 5 and/or the neomycin selection cassette (tm1b). This construct, leading to Ppef2 deficiency, still functions as lacZ reporter for promoter activity.

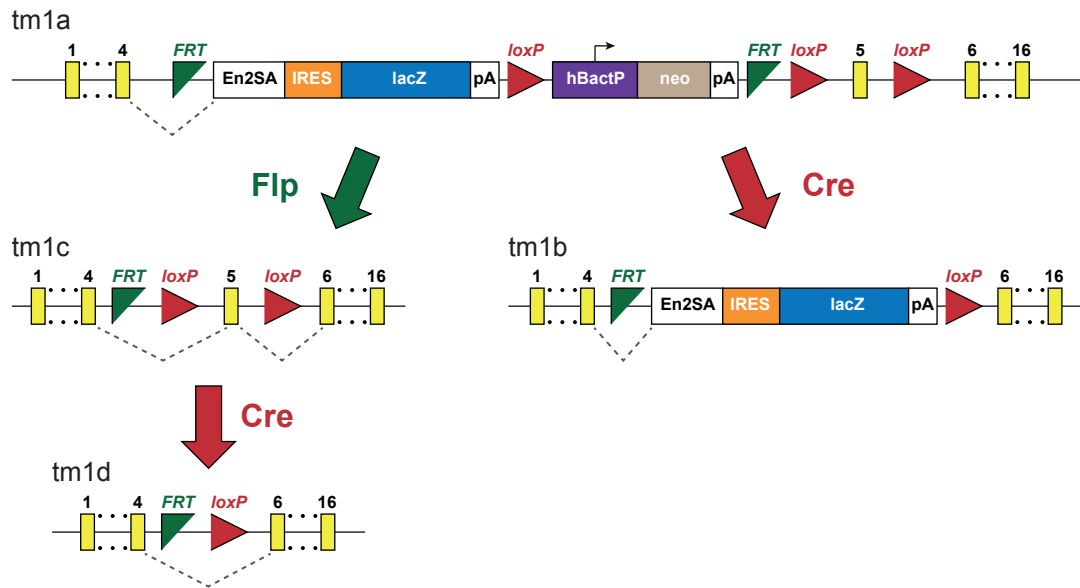


**Figure 3.3: The knockout-first construct and its conversion.** The knockout-first construct inserted within the Ppof2 locus consists of a gene trap cassette containing an EN2 splice acceptor (EN2SA), fused with a Internal Ribosomal Entry Site (IRES), followed by the gene coding for beta-galactosidase (*lacZ*), and a polyadenylation (pA) signal. The selection cassette, consisting of a neomycin (*neo*) resistance driven by an autonomous promoter (*hBactP*), follows the gene trap cassette, and together they are flanked by FRT sites. Additional loxP sites are found between the two cassettes, flanking exon 5. Exons are depicted as yellow boxes and possible splicing is indicated by dashed lines. The figure was modified from Skarnes *et al.* [102].

Exposure of the tm1a allele to a source of (ubiquitously expressed) Flp recombinase deletes the trapping cassette and restores normal gene activity, leaving a “conditional-ready” allele with a floxed exon 5 (tm1c). Subsequent crossing to a mouse line expressing the Cre recombinase under organ or cell type specific promoter control leads to a loss of exon 5 resulting in frameshift and null mutation (tm1d).

### **3.5 Aim of the project**

DCs are professional antigen presenting cells that shape adaptive immune responses. The process of antigen capturing, processing, presenting to T cells, and finally priming a T cell response is tightly controlled. DCs are replenished constantly from a pool of hematopoietic stem cells and have a relatively short half-life. Consistently, it was shown that control of DC survival, turnover, and longevity also serves as a regulator of the priming of adaptive immune responses.

Ppef2, a phosphatase with EF-hands, was recently shown by our group to be expressed in a DC specific manner and to be downregulated after maturation of DCs. The biological function of Ppef2 in DCs is not known albeit its DC specific expression.

The goal of this study was to further characterize the DC specific expression of Ppef2 in various cell types and organs, as well as the analysis of the role of this phosphatase in the context of DC biology.

To this end, we generated a mouse model that allowed us to track the promoter activity of Ppef2 and to investigate the influence of Ppef2 deficiency on DC longevity, survival, turnover, as well as the ability to transiently activate T cells.

## 4 Results

### 4.1 Ppef2 expression profile analysis

Very little is known about Ppef2 in the context of DCs. Early studies showed expression in the CD8<sup>+</sup> DC subset [5]. Therefore we performed qPCR analyses on sorted splenic DC subsets to characterize the expression of Ppef2 in more detail (Fig. 4.1 A). We also FACS-sorted classical blood monocytes, due to their expression profile shown by the Immgen database (Fig. 3.2 B). In accordance with the Immgen data (Fig. 3.2), we found the highest expression in CD8<sup>+</sup> DCs. CD11b<sup>+</sup> ESAM<sup>lo</sup> DCs, together with monocytes of the blood, expressed Ppef2 to a smaller extent, close to background signal. pDCs, T cells, and B cells on the other hand did not show expression of Ppef2.

To test the abundance of Ppef2 not only on mRNA, but also on a protein level, we took advantage of the knockout-first construct described in chapter 3.4. Direct measurement of protein levels, e.g. by western blot, were not possible due to lack of a functional antibody against Ppef2. In the knockout-first system, expression of Ppef2 is directly coupled to the expression of  $\beta$ -galactosidase (*lacZ*). Enzymatic activity of  $\beta$ -galactosidase can be measured by FACS using the fluorescein di-V-galactoside (FDG) substrate [103]. When FDG gets cleaved by the  $\beta$ -galactosidase it releases the fluorescent product fluorescein isothiocyanate (FITC). The FITC signal-intensity can be used as readout for the abundance of Ppef2 on a protein level since accumulation of the FITC signal is linear and directly correlated to enzymatic activity of the  $\beta$ -galactosidase [103]. Therefore, hematopoietic cells of the spleen of Ppef2<sup>-/-</sup> *lacZ*-reporter mice were isolated and *lacZ* activity measured as described above (Fig. 4.1 B). Consistent with the findings on mRNA level (Fig. 4.1 A), we detected *lacZ* activity mostly in CD8<sup>+</sup> DCs.

Furthermore, *lacZ* activity was measured in different cDC subsets of thymus, skin draining lymph nodes (sLN), lung, lamina propria and the mesenteric lymph nodes (mLN) (Fig. 4.1 C). cDC populations of lymph nodes were further separated in resident or migratory cDCs, based on their expression of CD11c and MHCII. Expression was restricted to CD8<sup>+</sup> DCs with the exception for CD11b<sup>+</sup> DCs of the thymus.

Taken together, our data on *lacZ* protein expression matched the expression profile of Ppef2 published in the Immgen database (Fig. 3.2 C), with the exception of CD103<sup>+</sup> DCs which did not display *lacZ* expression in our experiments.

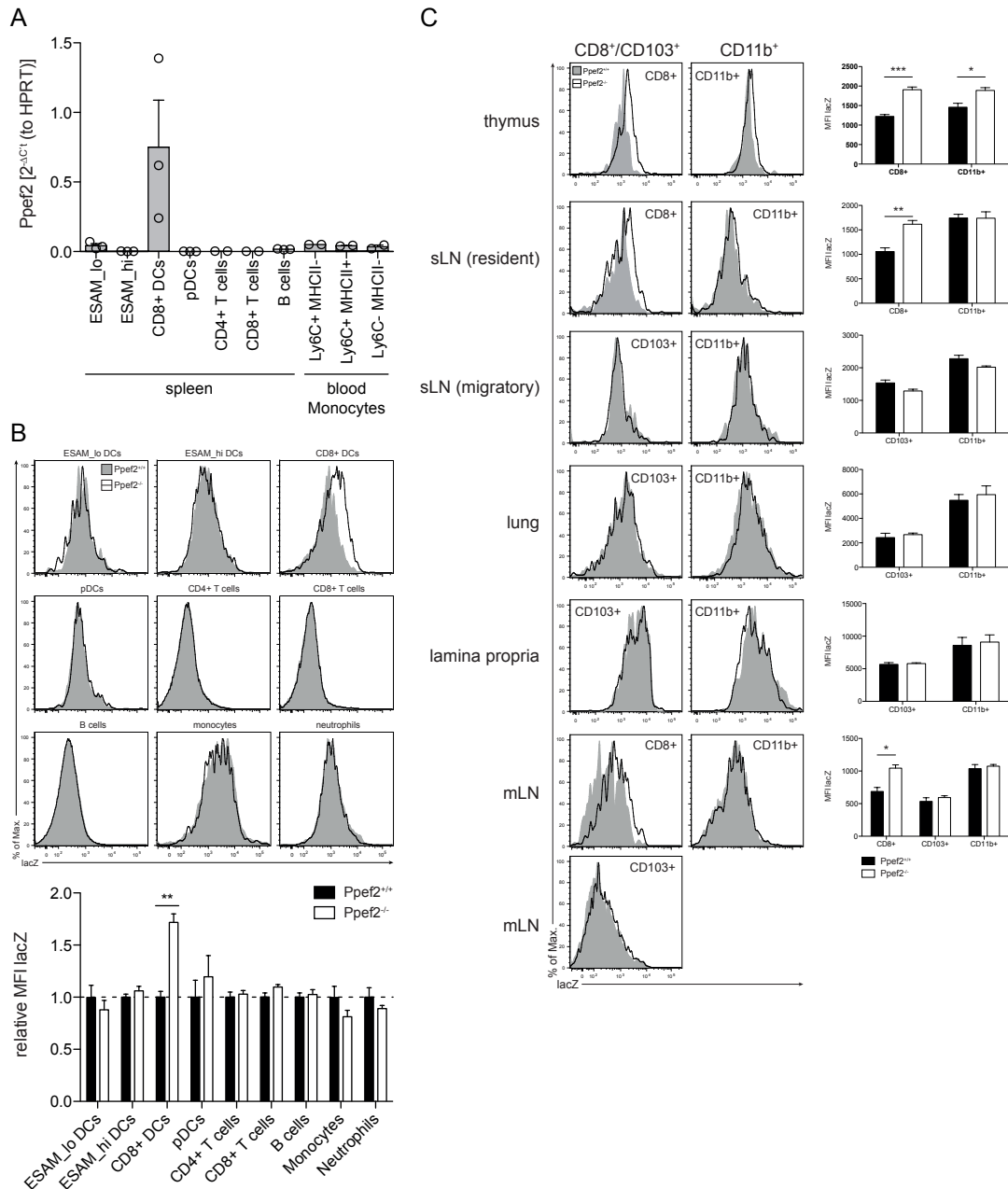


**Figure 4.1: Ppef2 is predominantly expressed by CD8<sup>+</sup> DCs.** (A) Gene expression profiling of spleen and blood cells after sorting. Shown is the quantitative real-time PCR result for Ppef2 of three independent sort experiments (n=3 pooled mice per sort) analyzed by the  $2^{-\Delta C_t}$  method [104, 105] with HPRT as housekeeping gene. (B) & (C) Measurement of lacZ activity by flow cytometry in different cell types of the spleen (B) and DCs of various other organs (C). Shown are representative FACS-plots with the corresponding statistics (n=3 mice per group). Statistical analysis was performed using Student's *t*-test, with \*:  $p < 0.05$ , \*\*:  $p < 0.01$  and \*\*\*:  $p < 0.001$ .

It was previously shown that Ppef2 expression decreased in BMDCs after stimulation with lipopolysaccharide (LPS) [5]. To test whether this effect was limited to TLR4 stimulation or whether other TLR ligands would lead to a similar decre-

ase, we stimulated GM-CSF-generated BMDCs with TLR agonists against TLR4 (LPS), TLR5 (Flagellin), TLR3 (Poly(I:C)), TLR1/2 (Pam3CSK4), and TLR7/8 (CLO97) (Fig. 4.2 A). We also included stimulation with anti-CD40 monoclonal antibody (mAb), because it was shown that ligation of CD40 led to DC activation, marked by the upregulation of MHCII, costimulatory molecules, and cytokine production [106, 107]. We also combined the CD40-stimulus with TNF $\alpha$ , since anti-CD40 antibody alone did not induce DC maturation to an extent similar to the stimulation with LPS (data not shown). TNF $\alpha$  is commonly used as a maturation agent for DCs [108, 109, 110], and CD40 also belongs to the TNF-receptor superfamily. Combination of anti-CD40 antibody with TNF $\alpha$  led to high percentages of fully mature DCs, at levels comparable to LPS stimulation. However, the influence of CD40 on DCs is controversial and some studies claim that the CD40 signal has to be accompanied by TLR stimulus to fully mature DCs [111]. For this reason, we also combined the anti-CD40 stimulus with the TLR4 stimulus LPS (Fig. 4.2 A).

Every TLR stimulation tested led to downregulation of *Ppef2* expression, whereas stimulation with anti-CD40 mAb, or the combination of anti-CD40 mAb and TNF $\alpha$ , did not alter the expression of *Ppef2*, even when different concentrations of the antibody were tested in a titration experiment (data not shown). Combining CD40 and LPS stimulus led to a decrease of *Ppef2* expression comparable to LPS alone.

To broaden this analysis, and because GM-CSF BMDCs do not show the diversity of splenic DCs, we performed the same stimulation experiment in a Flt3L dependent BMDC culture (Fig. 4.2 B). Maturation of BMDCs in both culture conditions was verified by flow cytometric staining of MHCII and CD86 (data not shown). The Flt3L dependent BMDC culture displayed the same expression pattern of *Ppef2* as the GM-CSF BMDCs for all of the tested stimuli.

To test the differential regulation of *Ppef2* expression after DC maturation *in vivo*, we took advantage of the lacZ reporter mice described previously. Reporter and control mice were intravenously injected with 10  $\mu$ g LPS either 4h (Fig. 4.2 C, in blue) or  $\sim$ 16h (Fig. 4.2 C, 16h in black) before sacrifice. Non-reporter control mice provided the background measurements for detection of lacZ activity in each experimental group (empty line histograms in Figure 4.2 C). In accordance with the data obtained *in vitro*, LPS injection led to rapid downregulation of *Ppef2* expression already after 4 hours and decreasing further over time.

*In vitro* generated GM-CSF BMDCs show to some degree spontaneous maturation in the absence of stimuli, accompanied by upregulation of MHCII and costimula-

tory molecules on the surface.

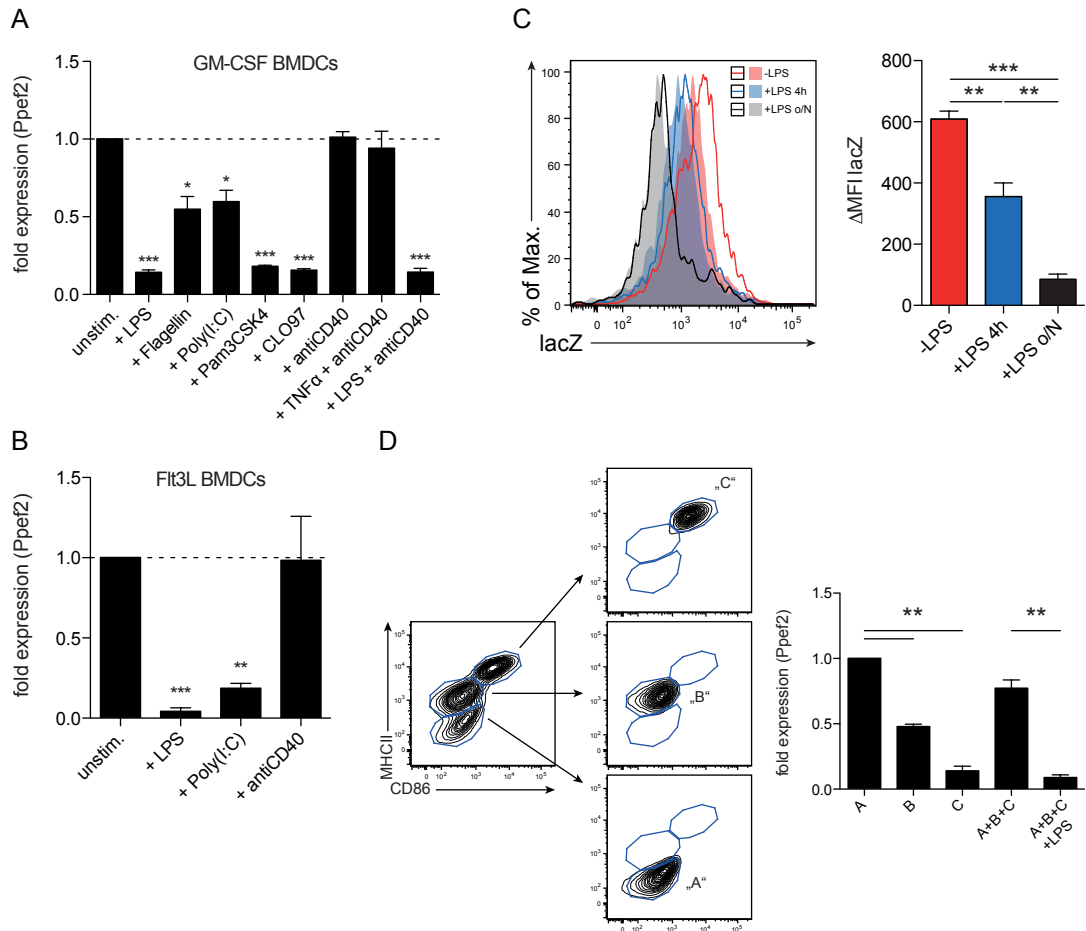


**Figure 4.2: Maturation of DCs leads to downregulation of Ppef2 expression.**

(A) Ppef2 expression in GM-CSF BMDCs of C57BL/6 mice 18h after stimulation as determined by qPCR. Bar graphs with SEM represent pooled data from independently performed cell cultures (unstim., LPS n=5; Flagellin, Poly(I:C), Pam3CSK4, CLO97, n=4; antiCD40, LPS+antiCD40, n=3; TNF $\alpha$ +antiCD40, n=2). (B) Expression of Ppef2 (qPCR) in Flt3L BMDCs 18h after addition of LPS, Poly(I:C), or antiCD40 mAb. Bar graphs with SEM represent pooled data of 3 independently performed cell cultures. (C) Flow cytometric measurement of lacZ activity in splenic CD8<sup>+</sup> DCs. Ppef2<sup>-/-</sup> reporter and control Ppef2<sup>+/+</sup> mice were injected intravenously with LPS either 4h or the day before analysis. Shown are representative FACS-plots (open histograms: lacZ-reporter mice; solid histograms: background from non-reporter controls) and statistics, where the lacZ signal of reporter mice was subtracted from the lacZ background signal of control mice who received the same treatment (no LPS, 4h LPS, or o/N LPS). Statistical analysis was performed on n=3 mice per group using Student's *t*-test. (D) Ppef2 expression in GM-CSF BMDCs of C57BL/6 mice after cell sorting based on the expression of CD11c, MHCII, and CD86. Unsorted samples containing all three populations were incubated with or without LPS for 7h. Error bars represent SEM of 3 independent experiments and statistical analysis was performed using Student's *t*-test, with \*: p<0.05, \*\*: p<0.01 and \*\*\*: p<0.001.

One possible explanation for this behavior is the disruption of E-cadherin mediated DC-DC clusters, which was shown to cause this phenotypical maturation. However, DCs stimulated this way failed to produce immunostimulatory cytokines [112] and spontaneous maturation within a GM-CSF BMDC culture can have other, possibly additional, reasons. To evaluate the effect of spontaneous maturation on *Ppef2* expression we generated GM-CSF dependent DCs *in vitro* and sorted CD11c<sup>+</sup> DCs in three populations according to their expression of MHCII and CD86 (Fig. 4.2 D). *Ppef2* expression decreased with BMDCs gaining a more (spontaneous) mature phenotype. *Ppef2* expression level of fully mature MHCII<sup>hi</sup> CD86<sup>hi</sup> reflected LPS matured BMDCs.

Taken together, we detected *Ppef2* expression in CD8<sup>+</sup> DCs of lymphoid organs on mRNA level by qPCR of sorted cells and on protein level by lacZ assays. Expression of *Ppef2* decreased when DCs were matured by TLR ligands *in vitro* and *in vivo* as well as in the case of spontaneous maturation *in vitro*, whereas maturation of DCs by CD40 ligation did not alter *Ppef2* expression.

## 4.2 Evaluation of *Ppef2* deficiency in knockout mice

To further examine the effects of *Ppef2* on DC biology we generated KO mice from embryonic stem cells (JM8A3.N1) produced by EUCOMM. Blastocyst injection into C57BL/6 mice was performed by the Transgenic Core Facility at the MPI of Molecular Cell Biology and Genetics in Dresden. Since the stem cell line JM8A3.N1 is of C57BL/6 background but has a agouti coat color, chimerism was determined by coat color and germline transmission was verified by genotyping pups of breedings with C57BL/6 mice.

Using the knockout-first approach described in chapter 3.4, we needed to verify whether homologous recombination was occurring, replacing the endogenous *Ppef2* locus (Fig. 4.3 A). We also had to exclude that the promoter driving the neomycin resistance gene would cause expression of the gene exons located downstream of the gene trap cassette.

To verify the knockout on transcript level we magnetically enriched CD11c<sup>+</sup> spleen cells and isolated messenger RNA (mRNA). Quantitative PCR of complementary DNA (cDNA) was performed with intron-spanning primers upstream of the gene trap, on the the floxed exon 5, or downstream, on exons 11-12 (Fig. 4.3 B).

Compared to *Ppef2*<sup>+/+</sup> control mice, mRNA upstream of the gene trap was decreased two-fold, whereas mRNA downstream of the gene trap (spanning the gene trap or downstream of its polyadenylation signal) was completely absent.

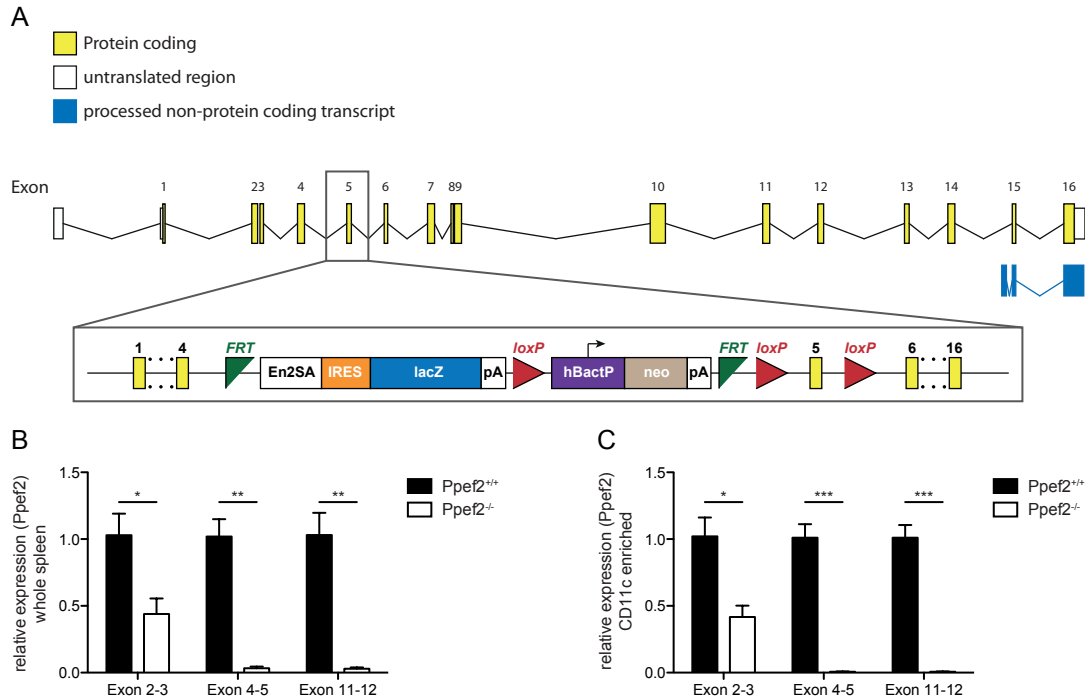


**Figure 4.3: Verification of the *Ppef2* knockout on mRNA level.** (A) Shown is the *Ppef2* locus with its splicing pattern and different transcripts as stated by the ensembl project. The knockout-first construct containing the gene trap between exon 4 and 5, as well as the floxed exon 5, is displayed below. (B) & (C) *Ppef2* expression analysis of whole spleen lysates (B) or CD11c enriched splenocytes (C) in *Ppef2*<sup>+/+</sup> and *Ppef2*<sup>-/-</sup> mice by quantitative real-time PCR. Three sets of intron spanning primer pairs were used to amplify fragments from exons 2 to 3, 4 to 5 and 11 to 12. The latter corresponds to the previously shown qPCR experiments of Figure 4.1 and 4.2. The  $\Delta\Delta\text{Ct}$  Method was used to calculate the fold expression compared to *Ppef2*<sup>+/+</sup> control samples. Data was normalized to HPRT. Statistical analysis was performed (n=3 mice) using Student's *t*-test, with \*:  $p < 0.05$ , \*\*:  $p < 0.01$  and \*\*\*:  $p < 0.001$ .

## 4.3 Phenotyping of *Ppef2* knockout mice

### 4.3.1 Phenotyping of *Ppef2*<sup>-/-</sup> DCs

Due to its DC specific expression (Fig. 4.1), we hypothesized that *Ppef2* may play a role in DC biology. To analyze for alterations within different DC subsets we performed flow cytometric analyses of DCs in primary lymphoid organs (Fig. 4.4). Frequencies of DCs in spleen, skin-draining lymph nodes, and thymus were not influenced by the knockout of *Ppef2* (Fig. 4.4 A). Total cell numbers of DC subpopulations within these primary lymphoid organs were also unaffected by the loss of *Ppef2* (Fig. 4.4 B).

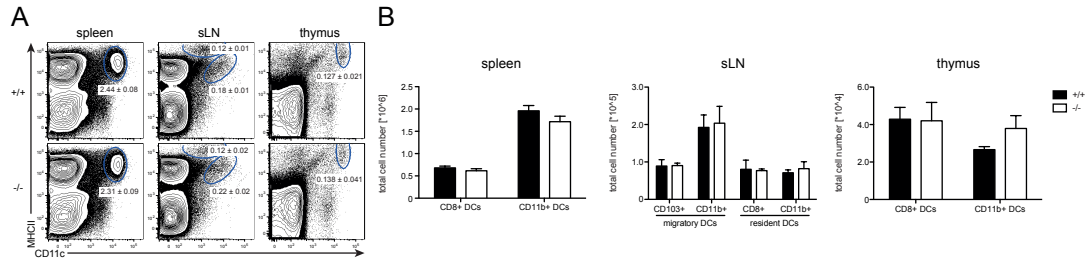


**Figure 4.4: Percentage and total numbers of DC (subpopulations) are not affected by the loss of *Ppef2*.** (A) DCs of spleen, sLN, and thymus were identified as CD11c<sup>+</sup>MHCII<sup>+</sup>. Shown are representative FACS plots and numbers indicate average DC percentages ± SEM of pooled data (spleen: n=36 mice; sLN: n=23 mice; thymus: n=6 mice). (B) Total cell numbers were calculated for DC subtypes of spleen, sLN and thymus (identified with CD8, CD103 and CD11b) and shown is pooled data ± SEM (spleen: n=36 mice; sLN: n=23 mice; thymus: n=6 mice). Statistical analysis was performed using Student's *t*-test and all p-values were above 0.05.

Flow cytometric analyses provide information about the frequencies of different cell populations and consequently their total cell number. However, this does not consider the local distribution of different cell types and/or splenic microarchitecture. Therefore, we performed histological analyses of spleens of *Ppef2*<sup>+/+</sup> and *Ppef2*<sup>-/-</sup> mice (Fig. 4.5). Splenic microarchitecture was not influenced by the loss of *Ppef2*. Analyzed spleen sections of *Ppef2*<sup>-/-</sup> mice showed intact T and B cell zones, a clear staining for the marginal zone (metallophilic macrophages; MOMA), and DCs that were located in the marginal zone and the T cell zone.

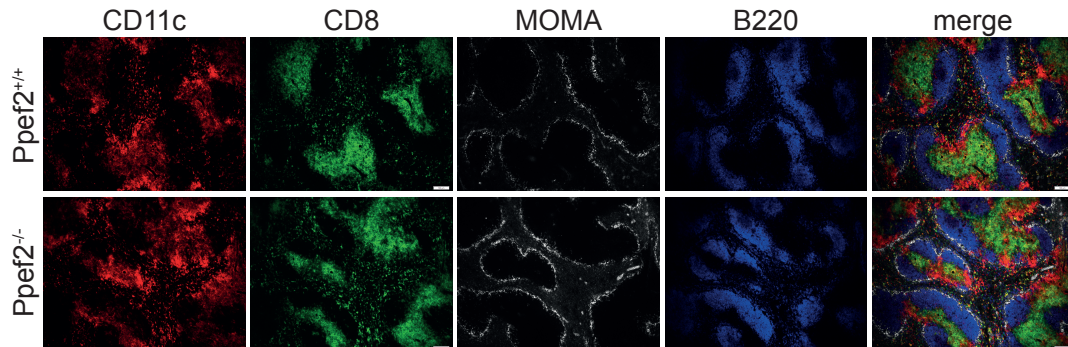


**Figure 4.5: Lack of *Ppef2* does not influence splenic microarchitecture.** Acetone fixed spleen sections of *Ppef2*<sup>+/+</sup> and *Ppef2*<sup>-/-</sup> mice were stained with antibodies against CD11c (red), CD8 (green), MOMA (white), and B220 (blue). Scale bars represent 100 μm.

Since DCs of non-lymphoid organs also displayed expression of *Ppef2* in the Immgen dataset (Fig. 3.2 C), we isolated DCs from the lung, the lamina propria, the skin, and the liver, in order to evaluate the effect of the knockout on the DC compartments of these non-lymphoid organs (Fig. 4.6). The identification and gating

of DC (subpopulations) in the non-lymphoid organs was, together with the CD103 surrogate marker CD24, carried out like in [21].

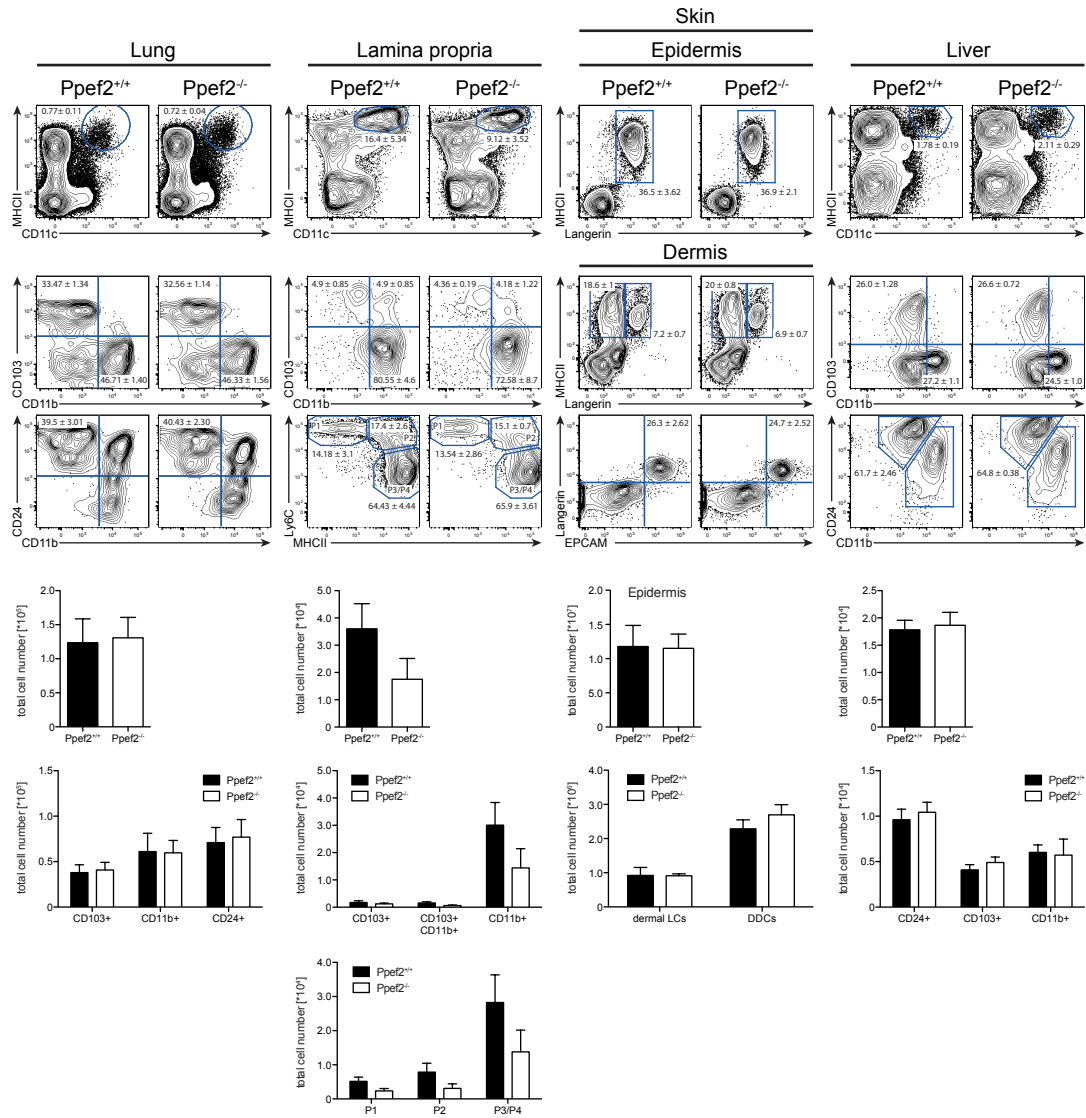


**Figure 4.6: *Ppef2* deficiency does not influence the percentage and total number of DCs in non-lymphoid organs.** DCs of lung, lamina propria, and liver were identified by their expression of CD11c and MHCII after gating on viable CD45<sup>+</sup> cells and further distinguished by their expression of CD8, CD103, CD11b and CD24. DCs and LCs of the skin were identified by staining for Langerin and MHCII on CD45<sup>+</sup> cells. Dermal cell populations were further distinguished based on Langerin and EpCAM, on CD45<sup>+</sup>MHC II<sup>+</sup> cells. Monocytes differentiating into macrophages in the gut were distinguished by the expression of Ly6C and MHCII after gating on viable CD11b<sup>+</sup> CD64<sup>+</sup> cells as described in [113]. Shown are representative FACS-plots of pooled data (lung stainings: n=10; lamina propria and skin: n=4; liver: n=10) with the percentages of DCs ± SEM and the corresponding total numbers in the bar graphs below. Statistical analysis was performed using Student's *t*-test. All p-values were above 0.05.

In addition, expression of *Ppef2* was also observed on circulating blood monocy-

tes on mRNA level (Fig. 4.1 A); we therefore wondered whether monocytes, or monocyte derived macrophages, showed any alterations. To this end, we applied a staining panel designed by the group of Bernard Malissen [113] to the lamina propria samples. After gating on viable  $CD11b^+ CD64^+$  cells, monocytes from the circulation (gate P1, Fig. 4.6) can be distinguished by their expression of Ly6C and MHCII on their way to finally become anti-inflammatory macrophages (gate P3/4, Fig. 4.6). However, we did not observe any changes in DC subsets concerning their percentage (representative FACS-plots) or their total numbers (bar graphs). One of the hallmarks of DC biology is the production and secretion of different kinds of cytokines.

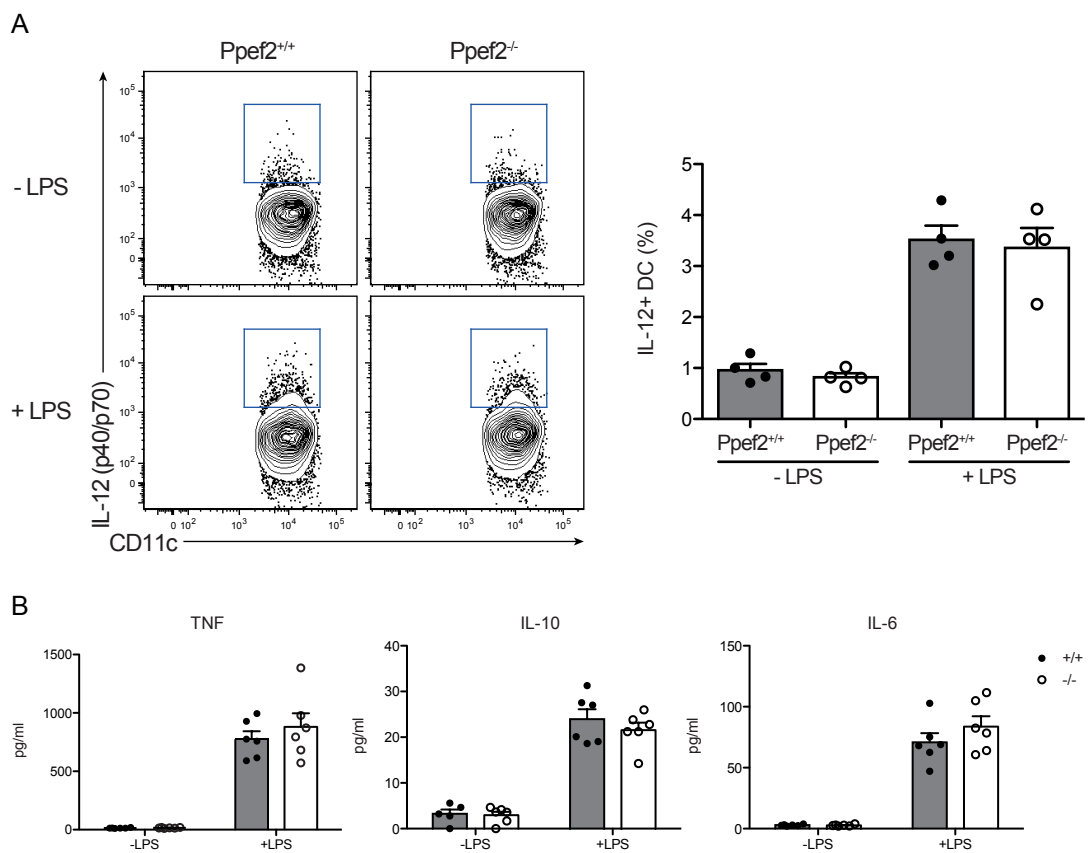


**Figure 4.7: *Ppef2*<sup>-/-</sup> mice show a normal cytokine profile.** (A) Splenocytes were stimulated with LPS *in vitro* for 3h and IL-12 production was measured by intracellular staining of IL-12 (p40/p70). Cells were gated on viable  $CD11c^+ MHCII^+$  DCs. Shown are representative FACS-plots and the corresponding statistics (n=4 mice; Student's *t*-test) in bar graphs. (B)  $CD11c$  enriched spleen DCs were cultured for 4h with or without LPS. The amount of TNF, IL-10 and IL-6 was measured in the supernatant with the Cytokine Bead Array Kit. Shown is pooled data of two experiments (n=4 mice each). Statistical analysis was performed using Student's *t*-test. All p-values were above 0.05.

Matured cDCs produce the proinflammatory cytokine IL-12 [44] (reviewed in

[114]), which we also assessed in order to perform a functional phenotyping of the *Ppef2*<sup>-/-</sup> mice. To test the ability of splenic DCs to produce IL-12, we isolated splenocytes and cultured them for three hours, with or without addition of LPS. We used a fluorescently labeled antibody detecting the p40 monomer and p70 heterodimer of IL-12 for intracellular staining.

Addition of LPS increased the level of IL-12 measured by flow cytometry both in the *Ppef2*<sup>+/+</sup> and *Ppef2*<sup>-/-</sup> DCs (Fig. 4.7 A). Production and secretion of TNF, IL-10, and IL-6 was measured by culturing magnetically enriched CD11c<sup>+</sup> splenocytes with or without the addition of LPS. Secreted cytokines were measured by cytokine bead array on the collected supernatants. Addition of LPS led in all cases to an increase in secreted cytokines (Fig. 4.7 B), and no significant difference was observed between mice lacking *Ppef2* and controls.

### 4.3.2 Phenotyping of other haematopoietic cells

Although *Ppef2* expression seemed, within the haematopoietic system, to be limited to CD8<sup>+</sup> DCs, we sought to rule out whether the complete knockout used in this study has any impact on the abundance of other immune cells. Together with the Centre d'Immunophénomique (CIPHE) we performed a high-throughput flow cytometry analysis to measure several different cell types at once in the spleens of *Ppef2*<sup>+/+</sup> and *Ppef2*<sup>-/-</sup> mice (Fig. 4.8). To highlight systematic differences across all populations, hierarchical clustering was performed (Fig. 4.8 A). The lack of defined clustering among *Ppef2*<sup>+/+</sup> and *Ppef2*<sup>-/-</sup> samples within cell populations, as well as among samples, indicates that absence of *Ppef2* does not impact specific cell "families". However, this does not rule out the possibility that only one or a few cell types, independent of each other, are affected. To evaluate each cell type individually, we looked at their percentages (Fig. 4.8 B) and total cell number (Fig. 4.8 C). The lack of *Ppef2* did not significantly influence the abundance of any cell type investigated.

Taken together, the lack of *Ppef2* did neither affect the abundance of cDCs in lymphoid and non-lymphoid organs, nor the frequency of other hematopoietic cells investigated. Histological analysis of spleens also revealed an intact spleen microarchitecture with cDCs confined to the marginal zone and the T cell zone. Functionally, *Ppef2*<sup>-/-</sup> DCs were still able to produce cytokines after stimulation at levels comparable to *Ppef2*<sup>+/+</sup> DCs.

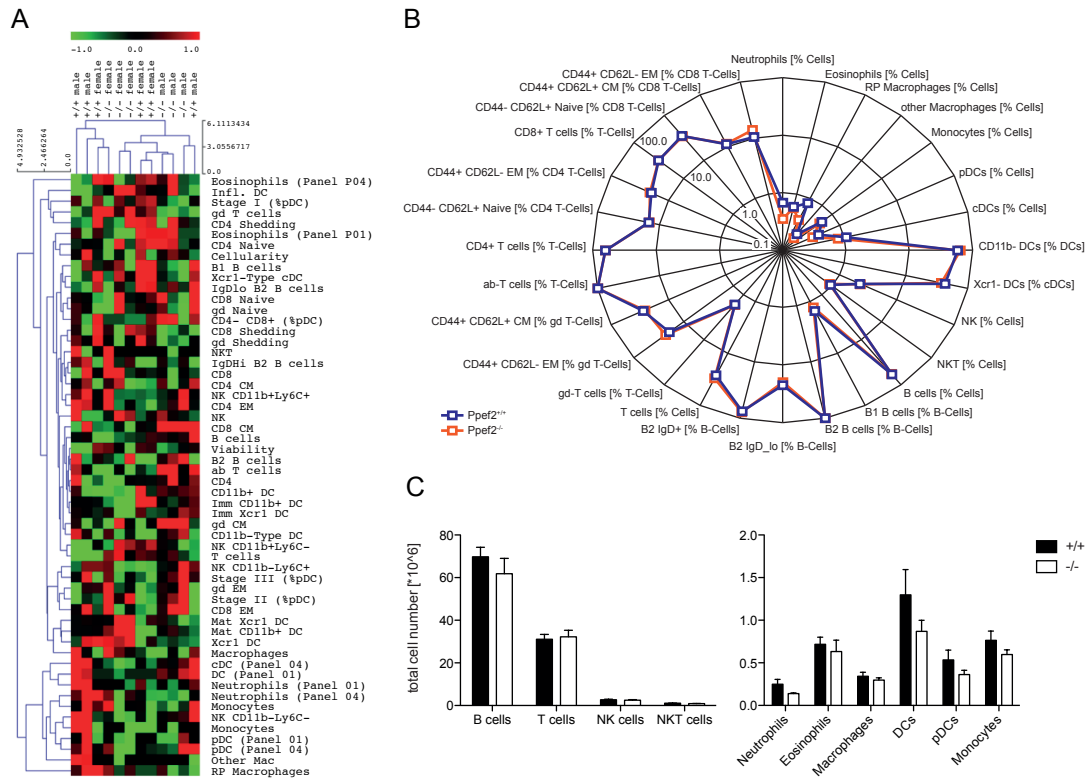


**Figure 4.8: Phenotyping of hematopoietic cells does not show abnormalities.** Splens of *Ppef2*<sup>+/+</sup> or *Ppef2*<sup>-/-</sup> mice were analyzed by the Centre d’Immunophénomique (CIPHE) for various cell populations by flow cytometry (n=6 mice per group). The marker used for the identification of every population is listed in section 6.2.1.3. (A) Hierarchical clustering (HC) analysis of all 56 parameters tested in two different staining panels. THE Dataset was therefore imported into TIGR MultiExperiment Viewer (TMeV), normalized based on the median value of each row and reduced based on the SD of the values of the given row. A hierarchical clustering tree was built based on these signal intensities (Euclidean Complete). (B) Radar plot of the frequencies of different (sub-) populations (as percent of total or percent of parent, indicated in squared brackets) and their corresponding total cell numbers (C). Analysis was performed with cohoused groups of six mice.

## 4.4 Analysis of apoptosis in *Ppef2*<sup>-/-</sup> animals

Although *Ppef2*<sup>-/-</sup> mice did not display any change, neither in the abundance of DCs nor in the spleen microarchitecture, we wondered whether cDCs might be more prone to apoptosis, as suggested by previous studies on the role of *Ppef2* *in vitro* in different cell lines [97].

### 4.4.1 Apoptosis *in vitro*

To address the question of enhanced susceptibility to apoptosis, we performed GM-CSF BMDC cultures from *Ppef2*<sup>+/+</sup> and *Ppef2*<sup>-/-</sup> mice. After six days of

culture, growth factor was removed and survival of DCs was monitored by flow cytometry for the following six days (Fig. 4.9 A).

As long as BMDCs were cultured in the presence of GM-CSF (Fig. 4.9 A; days -6 to 0), *Ppef2*<sup>+/+</sup> and *Ppef2*<sup>-/-</sup> DCs showed normal frequencies and survival, as shown in Figure 4.9 B (day 0 without GM-CSF). However, at the first day after GM-CSF withdrawal both BMDC cultures showed an increase in the percentage of viable DCs, although the frequency of *Ppef2*<sup>-/-</sup> BMDCs was decreased compared to control. This reduction of viable *Ppef2*<sup>-/-</sup> DCs was maintained the following days of culture until day six, where the amount of living *Ppef2*<sup>+/+</sup> and *Ppef2*<sup>-/-</sup> DCs were identical.

In relation to the increase in viable DCs one day after the removal of GM-CSF, we wondered whether the observed discrepancy in viability between *Ppef2*<sup>+/+</sup> and *Ppef2*<sup>-/-</sup> DCs could be due to differences in proliferation rather than apoptosis. To this end, we analyzed proliferation by adding BrdU to the culture at day 0 of GM-CSF withdrawal. BrdU incorporation was measured the following day (day 1 after removal of growth factor) by flow cytometry (Fig. 4.9 C). Approximately 20% of both, *Ppef2*<sup>+/+</sup> and *Ppef2*<sup>-/-</sup> DCs, incorporated BrdU into the DNA. This made changes in proliferation after GM-CSF removal unlikely and we went on to look for apoptotic alterations.

The cleavage of caspase-3, a critical player of the execution-phase of cell apoptosis, is necessary for its activation and function. This cleavage can be used as a measure of apoptotic activity, by means of intracellular staining with antibodies targeting specifically the cleaved subunit. In our experiment, this staining revealed an increase in active caspase-3 after removal of growth factor in both, *Ppef2*<sup>+/+</sup> and *Ppef2*<sup>-/-</sup> BMDCs (Fig. 4.9 D). However, *Ppef2* deficiency resulted in a significantly higher increase in cleaved caspase-3 when compared to *Ppef2*<sup>+/+</sup> control BMDCs. The increase caused by *Ppef2* deficiency was not visible with normal culture conditions in the presence of GM-CSF (day 0).

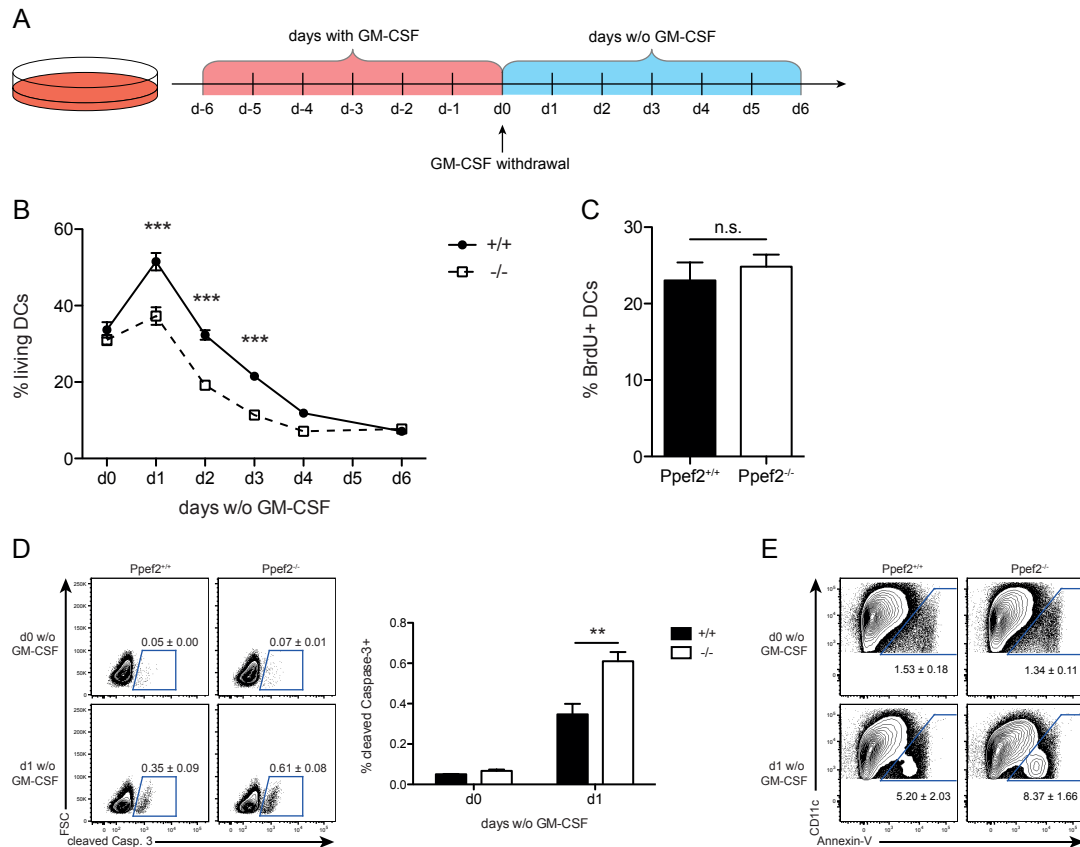


**Figure 4.9: *Ppef2*<sup>-/-</sup> GM-CSF BMDCs are more prone to apoptosis after growth factor withdrawal.** (A) Survival of *Ppef2*<sup>+/+</sup> and *Ppef2*<sup>-/-</sup> *in vitro* generated GM-CSF BMDCs after withdrawal of growth factor. BMDCs were extensively washed after 6 days (“day 0”) and  $2 \cdot 10^6$  cells were again plated in a 6 well plate with 3 ml of medium lacking GM-CSF. (B) The amount of viable CD11c<sup>+</sup> MHCII<sup>+</sup> DCs was monitored over time by FACS analysis. Representative result of 3 repetitions with n=3 mice. (C) At day 0 of GM-CSF withdrawal 5-bromo-2'-deoxyuridine (BrdU) was added to the culture at final concentration of 1mM. BrdU incorporation was monitored the following day by FACS analysis (n=3). (D) Intracellular staining of cleaved caspase-3 in day 0 (of GM-CSF withdrawal) CD11c<sup>+</sup> MHCII<sup>+</sup> BMDCs or BMDCs after one day of GM-CSF withdrawal (n=3). (E) Annexin-V staining of *in vitro* generated CD11c<sup>+</sup> MHCII<sup>+</sup> DCs after withdrawal of GM-CSF (n=3). Statistical analysis was performed using Student's *t*-test, with \*\*:  $p < 0.01$  and \*\*\*:  $p < 0.001$ .

Caspase-3 activation is an early event of apoptosis and lastly leading to several cellular changes. One of them is the exposure of phosphatidylserine on the outer plasma membrane leaflet. This translocation of phosphatidylserine from the inner to the outer membrane leaflet promotes phagocytosis of apoptotic cells and can be stained with the phosphatidylserine-binding protein Annexin-V [115] as a marker of early and late apoptosis. Staining of phosphatidylserine on BMDCs at day 0 or day 1 without GM-CSF reflected the active caspase-3 staining and increased in both groups after removal of the growth factor. However, this increase

in phosphatidylserine on the cell surface was elevated after loss of *Ppef2* (Fig. 4.9 E).

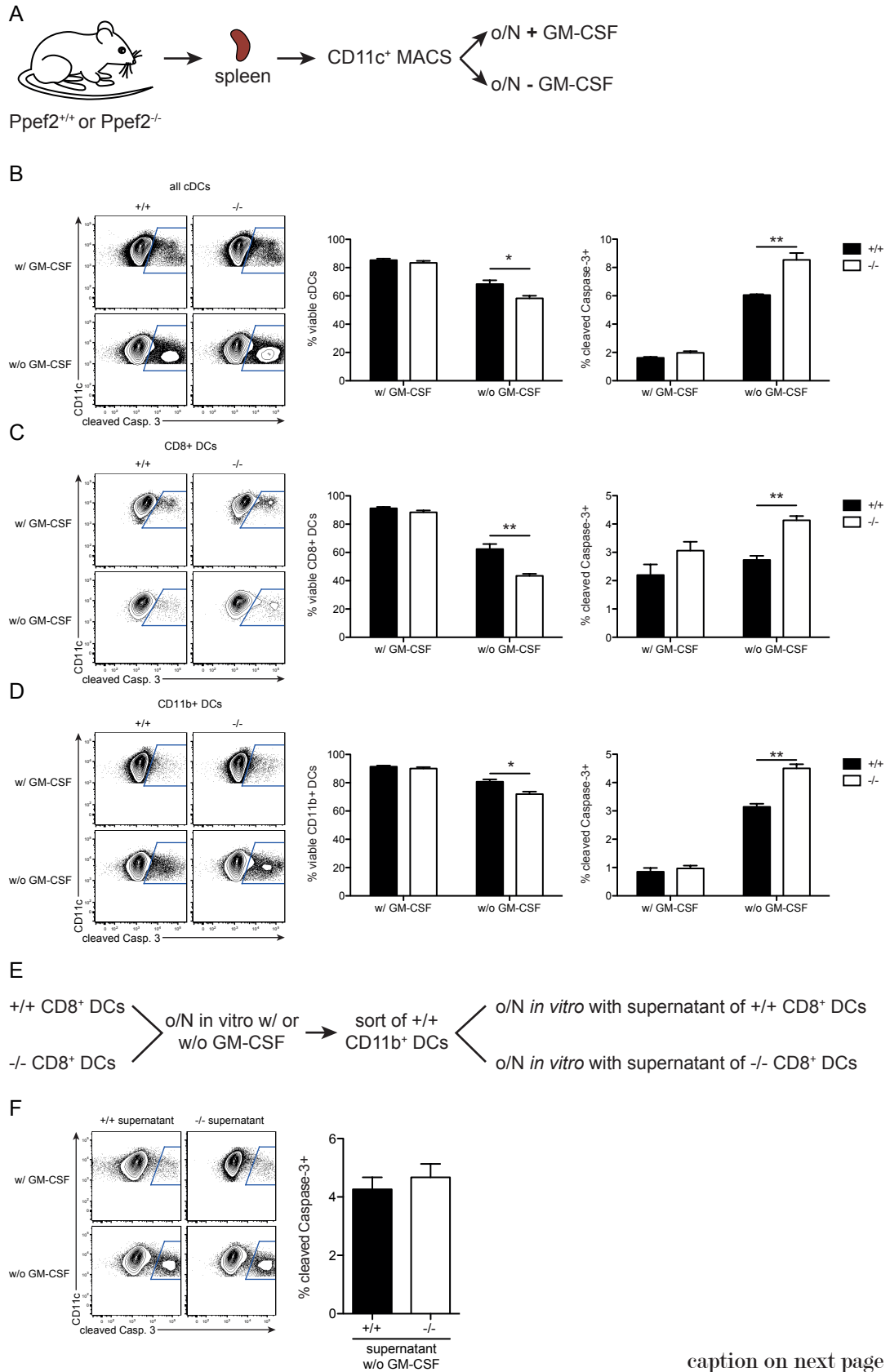
#### 4.4.2 Apoptosis *ex vivo*

We asked whether these findings also hold true for *ex vivo* sorted, primary splenocytes. To this end, we isolated splenocytes from *Ppef2*<sup>+/+</sup> and *Ppef2*<sup>-/-</sup> mice and magnetically purified the CD11c<sup>+</sup> cells. Cleaved caspase-3 staining was used as a readout for apoptosis after culturing the enriched DCs over night with or without GM-CSF (Fig. 4.10 A).

Gating on all viable cDCs, without differentiating subpopulations (Fig. 4.10 B), revealed that the lack of growth factor caused an increase of cleaved caspase-3 in both *Ppef2*<sup>-/-</sup> and control mice. However, cDCs of *Ppef2*<sup>-/-</sup> mice showed higher levels of active caspase-3 compared to *Ppef2*<sup>+/+</sup> control mice. Concomitantly, the percentage of viable cDCs was also reduced compared to control.

To broaden this analysis, we discriminated the CD8<sup>+</sup> (Fig. 4.10 B) and CD11b<sup>+</sup> (Fig. 4.10 C) DC subpopulations. Already in the presence of growth factor, control and *Ppef2*<sup>-/-</sup> mice showed more caspase-3 activity in CD8<sup>+</sup> compared to CD11b<sup>+</sup> DCs (Fig. 4.10 B and C). The general increase of cleaved caspase-3 without GM-CSF was more pronounced in CD11b<sup>+</sup> DCs (Fig. 4.10 C) than in CD8<sup>+</sup> DCs (Fig. 4.10 B). Nevertheless, both cDC subpopulation showed more active caspase-3 in the knockout condition compared to wild type after cytokine withdrawal. In line with this result, the frequency of viable *Ppef2*<sup>-/-</sup> cells was reduced in both cDCs subsets, although this difference was more pronounced in the CD8<sup>+</sup> DCs.

Because of the restricted expression pattern of *Ppef2* (Fig. 3.2 and 4.1), which showed almost no expression in CD11b<sup>+</sup> DCs, we wondered whether a soluble factor secreted by CD8<sup>+</sup> DCs might be the cause of elevated caspase activity in CD11b<sup>+</sup> DCs, lacking *Ppef2*. To this end, we sorted spleen CD8<sup>+</sup> DCs of *Ppef2*<sup>+/+</sup> and *Ppef2*<sup>-/-</sup> mice and kept in culture over night, with or without the addition of GM-CSF (Fig. 4.10 E). The following day, the supernatants of these cultures were collected and sorted splenic CD11b<sup>+</sup> DCs of *Ppef2*<sup>+/+</sup> mice were cultured with either the supernatant of the *Ppef2*<sup>+/+</sup> or *Ppef2*<sup>-/-</sup> CD8<sup>+</sup> DCs. In accordance with previous results, medium lacking GM-CSF led to increased caspase activity but the source of supernatant, *Ppef2*<sup>+/+</sup> or *Ppef2*<sup>-/-</sup> CD8<sup>+</sup> DCs, had no effect on the extent of this increase (Fig. 4.10 F).



caption on next page

**Figure 4.10: *Ppef2*<sup>-/-</sup> *ex vivo* cultured splenic DCs show an increase in apoptosis.** (A) Spleen DCs of *Ppef2*<sup>+/+</sup> or *Ppef2*<sup>-/-</sup> mice were purified by magnetic labeling and cultured overnight in the presence or absence of GM-CSF. DCs were intracellularly stained for cleaved caspase-3 and analyzed by flow cytometry, gated either on all CD11c<sup>+</sup> MHCII<sup>+</sup> (B), on the CD8<sup>+</sup> DCs (C), or on the CD11b<sup>+</sup> DCs (D). Shown are representative FACS-plots of n=3 mice. (E) *Ppef2*<sup>+/+</sup> or *Ppef2*<sup>-/-</sup> magnetically purified CD8<sup>+</sup> DCs were cultured overnight with or without GM-CSF. The next day, *Ppef2*<sup>+/+</sup> CD11b<sup>+</sup> DCs were FACS sorted and cultured overnight with the supernatant of the *Ppef2*<sup>+/+</sup> or *Ppef2*<sup>-/-</sup> CD8<sup>+</sup> DCs. Caspase-3 activity was measured by intracellular staining of cleaved caspase-3 (F). Shown is combined data of two experiments. Statistical analysis was performed using Student's *t*-test, with \*: p<0.05 and \*\*: p<0.01.

#### 4.4.3 Apoptosis *in vivo*

After observing an increased susceptibility to apoptosis *in vitro* and *ex vivo*, we wondered whether this effects are truly dependent of GM-CSF or are also detectable in a more physiological environment *in vivo*, where GM-CSF is known to be dispensable for the development and homeostasis of DCs in lymphoid organs [20]. Therefore we isolated spleen cells of *Ppef2*<sup>+/+</sup> and *Ppef2*<sup>-/-</sup> mice and stained intracellular, active caspase-3. Flow cytometric analyses revealed an increase of active caspase-3 in *Ppef2*<sup>-/-</sup> cDCs compared to control cDCs (Fig. 4.11 A). Surprisingly, we could observe this increase in both cDCs subsets of the spleen, CD8<sup>+</sup> and CD11b<sup>+</sup> DCs, although CD8<sup>+</sup> DCs showed generally more caspase activity than CD11b<sup>+</sup> DCs. Since *Ppef2* expression was limited to DCs, we checked whether the observed increase in caspase activity was truly specific for DCs by also staining other cells of the haematopoietic system (Fig. 4.11 B). Caspase-3 activity was highest in pDCs and only marginally detectable in B cells, (CD4<sup>+</sup> and CD8<sup>+</sup>) T cells, macrophages, and monocytes of the spleen. However, in none of the cell types investigated we found a statistically significant increase of cleaved caspase-3 in *Ppef2*<sup>-/-</sup> mice.

Furthermore, we performed Annexin-V stainings to also examine later stages of apoptosis than those observed with cleaved caspase-3 staining (Fig. 4.11 C). We found that the frequency of Annexin-V<sup>+</sup> *Ppef2*<sup>-/-</sup> cells was elevated in CD8<sup>+</sup> and CD11b<sup>+</sup> DCs.

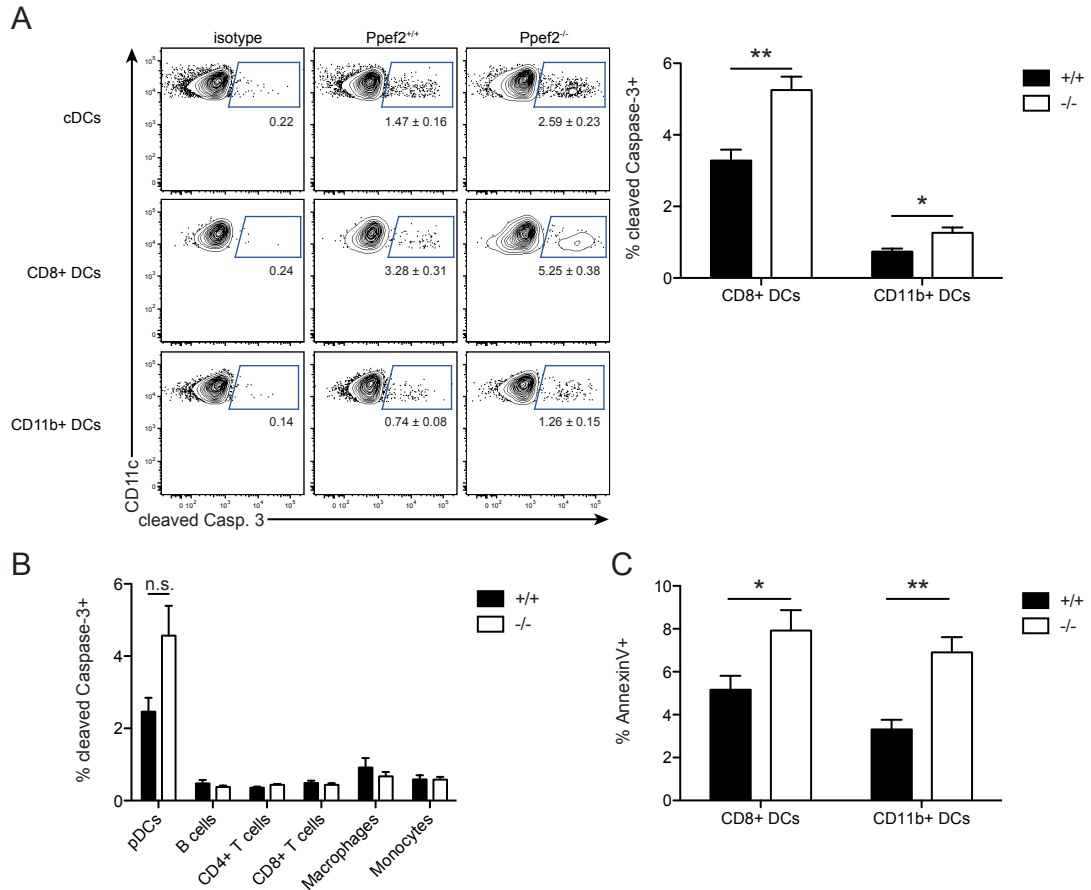


**Figure 4.11: Loss of Ppef2 leads to an increase of apoptotic DCs *in vivo*.** (A) Spleen DCs were intracellularly stained for cleaved caspase-3 and analyzed by flow cytometry. Shown are representative FACS-plots of two experiments (with  $n=4$  mice each) and the corresponding pooled statistics. (B) Analysis of cleaved caspase-3 in different spleen subsets ( $n=4$  mice). (C) Annexin-V staining of spleen DCs defined as viable  $CD11c^+$   $MHCII^+$ . Shown are representative FACS-plots of  $n=5$  mice and the corresponding statistics. All statistical analyses were performed using Student's *t*-test, with \*:  $p < 0.05$  and \*\*:  $p < 0.01$ .

Taken together,  $Ppef2^{-/-}$  DCs showed an increase in apoptosis *in vitro* and *ex vivo* when not supplied optimally with growth factor. This was also seen *in vivo* with freshly isolated spleen  $CD8^+$  and  $CD11b^+$  cDCs.

## 4.5 Mixed chimeras

Congenic animals differ in only one locus and a linked segment of chromosome but are otherwise genetically identical. CD45.1 and CD45.2 are congenic variants of CD45 and can be used to identify cells of distinct origins in transfer experiments. To test whether the increase in apoptosis would lead to a disadvantage of  $Ppef2^{-/-}$  DCs in a competitive situation we reconstituted lethally irradiated  $Ppef2^{+/+}$  mice

(CD45.1) with a 1:1 bone marrow mixture derived from Ppef2<sup>+/+</sup> (CD45.1) and Ppef2<sup>-/-</sup> (CD45.2) mice (Fig. 4.12 A). In such mixed bone marrow chimeras haematopoietic Ppef2<sup>+/+</sup> derived cells and non-haematopoietic cells of the recipient can provide all extrinsic factors like cytokines. This allows to investigate whether the observed increase in apoptosis is an intrinsic or extrinsic effect for CD8<sup>+</sup> and CD11b<sup>+</sup> DCs, respectively.

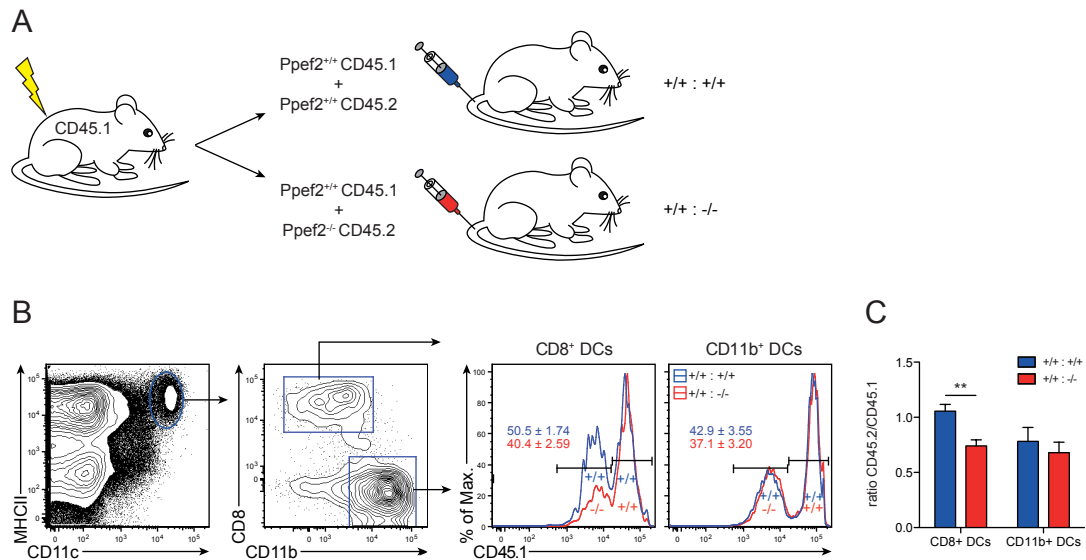


**Figure 4.12: Ppef2<sup>-/-</sup> DCs have a disadvantage in a competitive situation.** (A) Mixed bone marrow chimeras were produced by reconstitution of irradiated CD45.1<sup>+</sup> recipients with mixed CD45.1<sup>+</sup> and CD45.2<sup>+</sup> bone marrow of either Ppef2<sup>+/+</sup> mice, or Ppef2<sup>+/+</sup> and Ppef2<sup>-/-</sup> mice. (B) Mixed bone marrow chimera were analyzed earliest at 6 weeks after reconstitution by staining of CD45.1. DCs of the spleen were identified by staining of CD11c and MHCII and DCs subsets were distinguished by staining of CD8 and CD11b. FACS-plots shown are representative of three independently performed experiments with similar outcome (n=11). (C) The ratios of CD45.2<sup>+</sup> to CD45.1<sup>+</sup> DCs were calculated and statistical analysis was performed using Student's *t*-test, with \*\*: p < 0.01.

Analyses of the congenic composition of splenic CD8<sup>+</sup> DCs revealed that DCs of Ppef2<sup>-/-</sup> origin showed a disadvantage compared to Ppef2<sup>+/+</sup> DCs (Fig. 4.12 B). On the other hand, the congenic distribution in CD11b<sup>+</sup> DCs was not altered compared to control chimeras, that received a mixture of Ppef2<sup>+/+</sup> bone marrow (Fig. 4.12 B). Statistical analysis was performed calculating the ratio between DCs of CD45.2 (Ppef2<sup>-/-</sup>) and CD45.1 (Ppef2<sup>+/+</sup>) origin to determine the chimerism. Those ratios were compared to control chimeras (Fig. 4.12 C). CD8<sup>+</sup> DCs showed a 29.78% reduction in the ratio, whereas CD11b<sup>+</sup> DCs did not display any significant changes, arguing for a CD8<sup>+</sup> DC intrinsic effect of Ppef2, as assumed by the expression pattern of Ppef2 (Fig. 4.1).

## 4.6 Analysis of DC proliferation and turnover

We observed that Ppef2 deficiency led to increased susceptibility to apoptosis if not supplied optimally with growth factor *in vitro*, as well as *ex vivo*. Furthermore, Ppef2<sup>-/-</sup> DC of the spleen also showed an increase in apoptosis *in vivo*. Intriguingly, we did not observe any changes in DC numbers or percentages in various organs, albeit the observed increase in apoptosis. This led us to the question, whether Ppef2 deficiency also leads to an increase in proliferation of DCs to compensate for their increased apoptosis. To analyze *in vivo* proliferation of DCs we performed BrdU pulse-chase experiments with an initial bolus of intraperitoneally applied BrdU, followed by administration of BrdU in the drinking water for three consecutive days. During this so called “pulse phase” newly dividing cells incorporate the thymidine analog into the Deoxyribonucleic acid (DNA). After these three days of pulsing, mice were again given normal drinking water and BrdU labeling was followed for another 9 days. When BrdU supply stops and BrdU gets cleared out of the system, the decrease of BrdU positive cells corresponds to cell turnover in the “chase phase”. Investigating the effect of cDC proliferation in the “pulse phase” (Fig. 4.13 A) showed inconsistent results. In one experiment (filled blue and open blue data-points) we observed an increase in DC proliferation at day 3, although more pronounced on CD11b<sup>+</sup> DCs compared to CD8<sup>+</sup> DCs. In another repetition we saw effects on day 9 rather than day 3. In particular we observed a reduced percentage of BrdU<sup>+</sup> Ppef2<sup>-/-</sup> DCs. However, pooling the two individually performed experiments did not highlight any statistically significant differences when it comes to BrdU incorporation or turnover.

To focus on the BrdU incorporation “pulse phase” we also performed short time BrdU labeling, where mice were sacrificed two hours after intraperitoneal injection of 1 mg BrdU (Fig. 4.13 B). Also this experiment displayed contradictory data and did not show any significant differences between Ppef2<sup>+/+</sup> and Ppef2<sup>-/-</sup> DCs, when data from three experiments were pooled.

cDCs and their precursors are well known consumers of Flt3L and we therefore wondered whether the increase in apoptotic DCs in Ppef2<sup>-/-</sup> would lead to increased Flt3L levels in the serum, which was seen in some mouse models with reduced cDC numbers [116, 117]. To this end, we performed an ELISA to test whether the observed increase in apoptosis translates in changes of the serum level of Flt3L in Ppef2<sup>+/+</sup> and Ppef2<sup>-/-</sup> mice (Fig. 4.13 C).

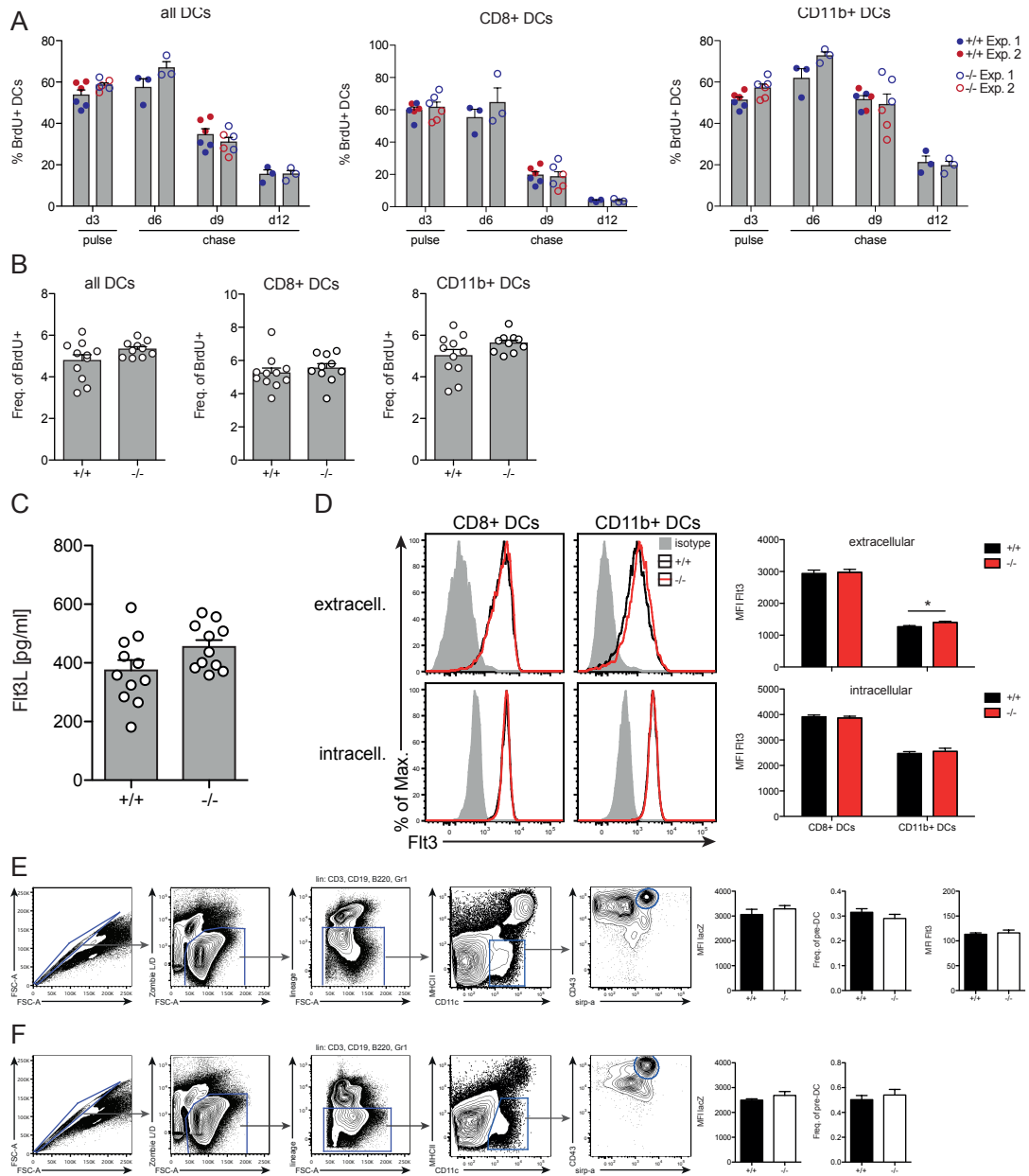


**Figure 4.13: Analysis of DC proliferation and turnover.** (A) Ppof2<sup>+/+</sup> and Ppof2<sup>-/-</sup> mice were injected i.p. with 1 mg of BrdU and given 0.8 mg/ml BrdU in the drinking water for three consecutive days. After that mice were switched back to normal drinking water and BrdU turnover was followed for another 9 days. Shown is the pooled data of two different experiments (n=3 each) (on day 3 and 9) or one experiment (n=3 on day 6 and 12). Filled and open blue data-points indicate one experiment, whereas filled and open red represents a second experiment. (B) Mice were injected i.p. with 1 mg of BrdU and sacrificed 2h after injection. Shown is pooled data from three experiments (with n=11 mice in total). (C) Serum level of Flt3L was measured by ELISA (n=11). (D) Protein level of Flt3 was measured by extra- and intracellular staining of the receptor in spleen cDCs. Shown are representative FACS-plots of three experiments with n=4 mice each. (E) and (F) The frequency of DC precursors was determined for spleen and bone marrow (n=3 for (E) and n=4 for (F)), together with their expression of lacZ. (E) Flt3 surface expression was measured on splenic DC precursors. Statistical analysis was performed using Student's *t*-test, with \*: p<0.05.

We found only a small tendency of increased Flt3L in the serum with a p-value of 0.0735 (Fig. 4.13 C). However, once Flt3L binds to its receptor, Flt3 forms a homodimer and the whole complex gets internalized starting within 5 minutes of ligation and reaching a maximum after 15 minutes, leading to rapid degradation [118]. Because of the trend observed in serum Flt3L, we wondered whether DCs or their precursors might display differences in the expression of the receptor Flt3, which could sum up with the tendency in serum Flt3L. To this end, we performed surface and intracellular stainings of the receptor on spleen cDCs (Fig. 4.13 D). Because of the role of Flt3 in the development of DCs [19] we investigated its expression on DC precursors of the spleen (Fig. 4.13 E). To exclude effects caused by differences in DC precursors we checked their frequency and their expression of Ppef2 by performing a lacZ-FACS-assay in the spleen (Fig. 4.13 E) and the bone marrow (Fig. 4.13 F). No major differences between Ppef2<sup>+/+</sup> or Ppef2<sup>-/-</sup> cDCs or their precursors were detected.

Taken together, BrdU incorporation experiments did not show any changes in DC proliferation which would compensate for the increased apoptosis. Serum levels of Flt3L were normal, as well as the surface expression of its receptor (Flt3) on cDC precursors and terminally differentiated cDCs.

## 4.7 *In vivo* antigen presentation

Since it was already shown that the life-span of DCs directly influences the priming of T cells [1], we wondered whether the increase in DC apoptosis would lead to a diminished T cell activation under limiting conditions. To this end, we took advantage of OT-I cells, which are monoclonal CD8<sup>+</sup> T cells that carry a transgenic T cell receptor which specifically recognizes the OVA<sub>257-264</sub> peptide SIINFEKL in the context of H2-K<sup>b</sup>. We adoptively transferred OT-I T cells into Ppef2<sup>+/+</sup> or Ppef2<sup>-/-</sup> host mice and injected the mice OVA protein one day later. Mice were then sacrificed three days later at the peak of OT-I proliferation and spleens were analyzed by flow cytometry (Fig. 4.14 A and B).

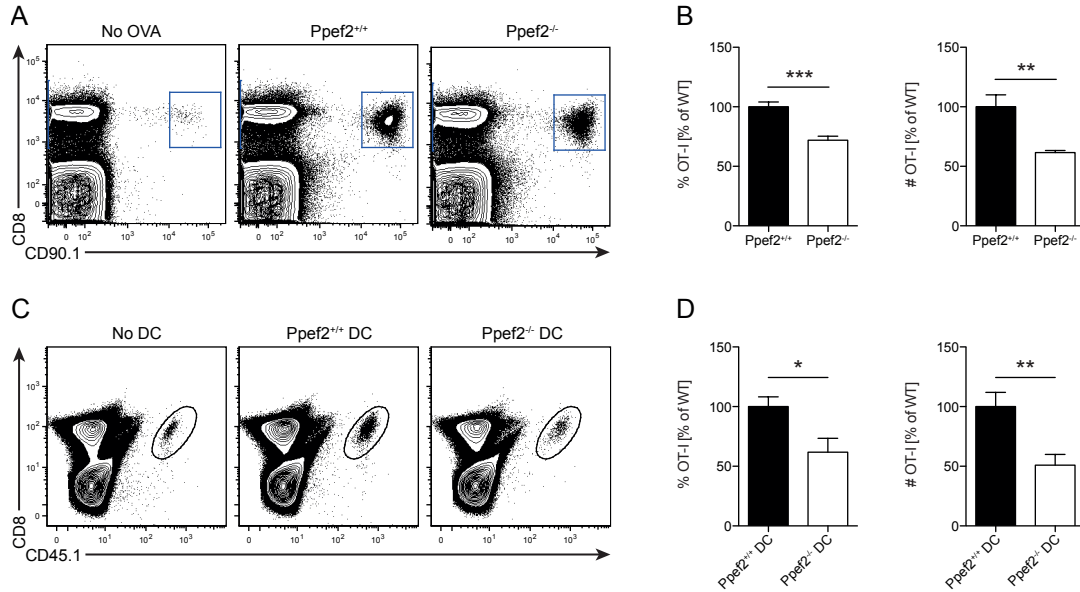


**Figure 4.14: *In vivo* antigen presentation.**  $5 \cdot 10^5$  congenically marked (CD90.1) OT-I T cells were adoptively transferred either in Ppef2<sup>+/+</sup> or Ppef2<sup>-/-</sup> mice, which received 100  $\mu$ g OVA protein intravenously one day later. Mice were sacrificed three days after OVA administration and spleens were analyzed by flow cytometry for OT-I T cell proliferation. Shown are representative FACS-plots of OT-I T cells (A). (B) Two independent experiments (with  $n=3$  mice each) were pooled by calculating the percent of WT for the percentage and total cell number of OT-I T cells. (C) and (D)  $1.5 \cdot 10^5$  Ppef2<sup>+/+</sup> or Ppef2<sup>-/-</sup> DCs were pulsed with OVA peptide (SIINFEKL) and transferred into  $K^{bm1}$  recipient mice. 24 h later  $K^{bm1}$  OT-I T cells were transferred and mice were analyzed 3 days later for OT-I T cell proliferation by flow cytometry. (C) Shown are representative FACS-plots of the gated OT-I T cells. (D) Two different independently performed experiments (with  $n=3$  mice each) were pooled by calculating the percent of WT for total cell number and percentage of OT-I T cells. Statistical analysis was performed using Student's *t*-test, with \*:  $p < 0.05$ , \*\*:  $p < 0.01$  and \*\*\*:  $p < 0.001$ .

Transferred OT-I T cells were identified by their surface expression of CD8 and the congenic marker CD90.1 (Fig. 4.14 A). Mice lacking Ppef2 showed a 28% reduction in the percentage of OT-I T cells and a 38% reduction in the total cell number of OVA specific T cells (Fig. 4.14 B).

As this effect can be explained by several different reasons, like defects in OVA protein uptake, processing of antigen, MHC loading, and proper presentation of antigen, we wanted to exclude some of these factors by transferring peptide pulsed DCs in  $K^{bm1}$  recipient mice. Pulsing DCs with the OVA peptide SIINFEKL avoids the need of protein processing and using  $K^{bm1}$  mice as recipients bypasses the possibility that the peptide is presented by any other cell type of the host mice, as the *bm1* mutation of the H2- $K^b$  gene leads to a failure to present SIINFEKL on MHC I [119].

To this end, we isolated cDCs of Ppef2<sup>+/+</sup> or Ppef2<sup>-/-</sup> mice that were previously expanded *in vivo* by administering a Flt3L secreting tumor cell line.  $1.5 \cdot 10^5$  magnetically enriched cDCs were then pulsed with SIINFEKL for one hour *in vitro* and transferred into K<sup>bm1</sup> recipient mice. One day after the transfer, recipient mice received  $10^5$  congenitally marked (CD45.1) K<sup>bm1</sup> OT-I T cells, and mice were analyzed by flow cytometry three days after OT-I transfer. OT-I T cell proliferation was assessed by gating on CD8<sup>+</sup> CD45.1<sup>+</sup> T cells (Fig. 4.14 C) and calculating the percentage and total number of OT-I cells in the spleen (Fig. 4.14 D). The percentage of OT-I T cells was reduced by 38.2% in the mice that received Ppef2<sup>-/-</sup> peptide-pulsed DCs compared to control and the total cell number of OT-I cells were reduced by half (49.1%).

In conclusion, we were able to show that Ppef2 influences the transient T cell activation, as transfer of SIINFEKL-pulsed Ppef2<sup>-/-</sup> DCs resulted in reduced numbers and frequencies of antigen specific T cells. The same was seen for cross-primed T cells when full OVA protein was injected in Ppef2<sup>-/-</sup> mice.

## 4.8 mRNA sequencing and western blot analysis of Ppef2<sup>-/-</sup> DCs

To understand mechanistically how Ppef2 might influence DC survival, we conducted mRNA sequencing of sorted spleen cDCs (Fig. 4.15). FACS-sorting of Ppef2<sup>+/+</sup> and Ppef2<sup>-/-</sup> splenocytes was performed according to the gating strategy depicted in Figure 4.15 A. After gating on living lymphocytes, excluding cell aggregates, we identified cDCs as CD11c<sup>+</sup> MHCII<sup>+</sup> and distinguished cDC subpopulations according to their expression of CD8 and CD11b.

A total of 10766 genes were detected in CD8<sup>+</sup> DCs and 10947 in CD11b<sup>+</sup> DCs. The read counts for Ppef2 in the two subsets were used as internal control for sorting and genotype (Fig. 4.15 B). Ppef2<sup>+/+</sup> mice showed about 200 reads of Ppef2 in the sorted CD8<sup>+</sup> but not in the CD11b<sup>+</sup> DCs, whereas the sorted Ppef2<sup>-/-</sup> DCs did not show any reads above background, neither in the CD8<sup>+</sup> nor in the CD11b<sup>+</sup> DCs.

Analysis of differentially expressed genes in the CD8<sup>+</sup> DC compartment (Fig. 4.15 C) revealed 13 genes that were downregulated compared to control, and 8 genes that were upregulated more than at least two-fold with a p-value  $\leq 0.01$ . Ppef2 showed the strongest downregulation (84.4 fold compared to control), followed by an uncharacterized transcript (LOC100503496), which was downregulated 9.2 fold.

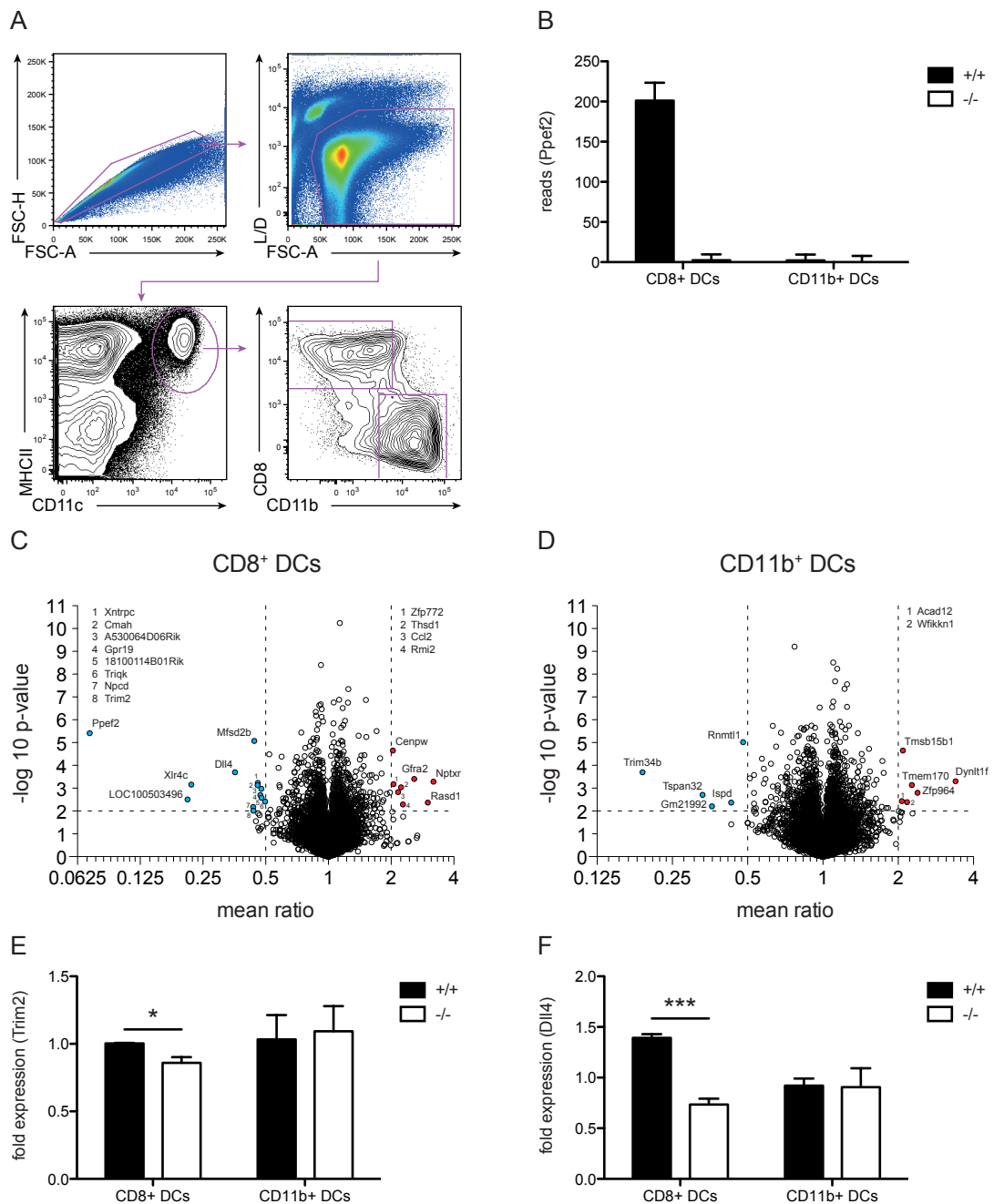


**Figure 4.15: mRNA sequencing of sorted splenic DCs and verification by qPCR.** (A) Splenic CD8<sup>+</sup> and CD11b<sup>+</sup> DCs were FACS sorted five times independently with  $\geq 3$  pooled mice per group. The average sort purity of all 5 sorts reached  $\geq 95\%$  for each sample. RNA processing and sequencing was performed by the group of Joachim Schultze (LIMES, Bonn). (B) The reads of *Ppef2* served as internal control. (C) & (D) Volcano plot analyses of sorted DC subpopulations. Fold change of -2 and +2, and a p-value  $\leq 0.01$  were chosen as cut-off. qPCRs of another three independently performed sorts were done for *Trim2* (E) and *Dll4* (F). Statistical analysis was performed using Student's *t*-test, with \*:  $p < 0.05$ , \*\*:  $p < 0.01$  and \*\*\*:  $p < 0.001$ .

The other significantly downregulated genes were *Xlr4c*, *Dll4*, *Trim2*, *Npcd*,

Mfsd2b, Cmah, Xntrpc, Gpr19, A530064D06Rik, 1810014B01Rik, and Triqk. Among the upregulated genes, *Nptxr* was the highest, with a 3.3 fold increase, followed by *Rasd1*, *Gfra2*, *Rmi2*, *Thsd1*, *Ccl2*, *Zfp772*, and *Cenpw*.

Although CD11b<sup>+</sup> DCs do not express *Ppef2* and effects showed for the CD11b<sup>+</sup> DCs were indirect rather than intrinsic effects, we also performed mRNA sequencing on sorted CD11b<sup>+</sup> DCs of the spleen (Fig. 4.15 D). The volcano plot analysis displayed, showed five downregulated and six upregulated transcripts. Among the reduced transcripts, *Trim34b* was the most downregulated, with an 8.1-fold reduction. *Tspan32*, *Gm21992*, *Ispd*, and *Rnmt1l* were downregulated between 3.2 to 2.1 fold. From the six upregulated transcripts, *Dynlt1f* (3.7 fold) was the one with the highest increase. *Zfp964*, *Tmem170*, *Wfikkn1*, *Tmsb15b1*, and *Acad12* were increased between 2.4 to 2.1 fold.

In CD8<sup>+</sup> DCs, *Trim2* was downregulated 2.5 fold; this gene is of particular interest because it is known to bind to the pro-apoptotic protein Bim, mediating the p42/p44 MAP kinase-dependent ubiquitination of Bim [120].

To validate the mRNA sequencing results, we performed a qPCR of *Trim2* on sorted DC subpopulations of the spleen (Fig. 4.15 E). The results showed a reduction of 14.3% in CD8<sup>+</sup> DCs compared to control, whereas expression of *Trim2* was not altered in CD11b<sup>+</sup> DCs.

*Dll4* was downregulated 2.8 fold in the mRNA sequencing of CD8<sup>+</sup> DCs and is a ligand of Notch1 and Notch4 [121]. Notch signaling is known to be crucial for lymphocyte development and function (reviewed in [122]). It was also shown that signaling via Notch is crucial for the maintenance of CD8<sup>-</sup> DCs [29]. Therefore, we also verified the downregulation of the *Dll4* transcript by qPCR (Fig. 4.15 F). Compared to control, *Dll4* expression was reduced 47.4% in *Ppef2*<sup>-/-</sup> CD8<sup>+</sup> DCs, whereas expression was not altered in CD11b<sup>+</sup> DCs.

To test whether the decrease of *Trim2* mRNA could be the driver of apoptosis by a pathway leading to accumulation of pro-apoptotic Bim, we performed western blot analyses of Bim in GM-CSF BMDCs (Fig. 4.16 A & B) and primary sorted spleen DCs (Fig. 4.16 C & D). We also performed FACS analysis of *Dll4* to test whether the altered expression of *Dll4* would translate into changed amounts of protein.

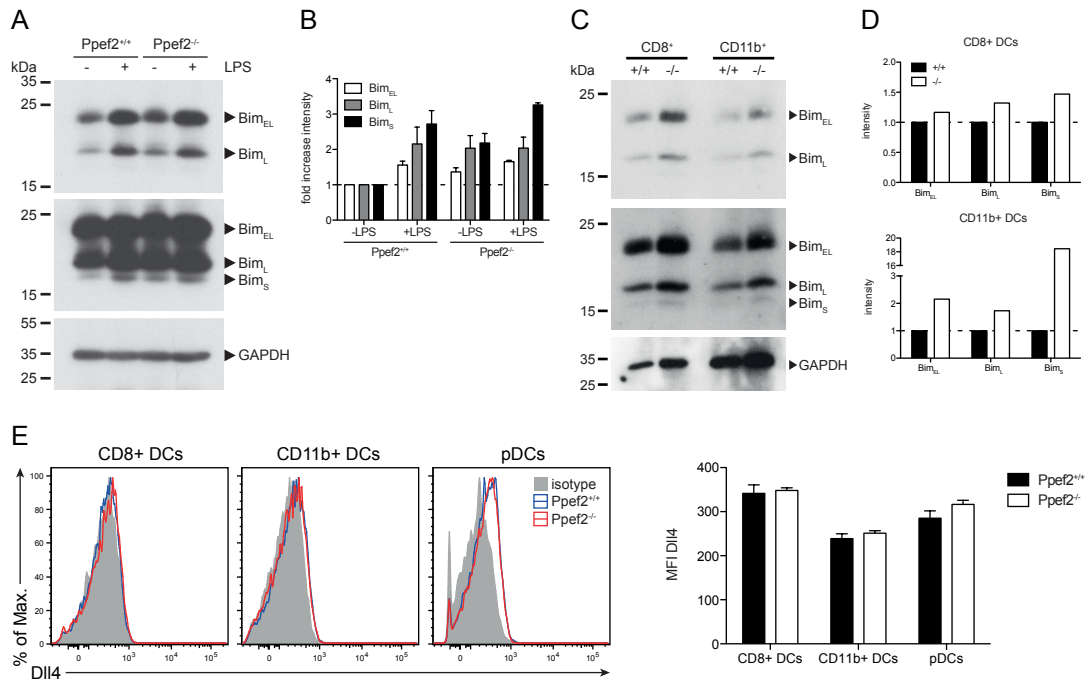


**Figure 4.16: Analysis of pro-apoptotic Bim and Dll4 on protein level.** (A) Western blot for Bim was performed with 30  $\mu$ g cell lysates of GM-CSF BMDCs either unstimulated or LPS matured. The membrane was exposed for 30 seconds to detect gradual levels of the Bim<sub>EL</sub> and Bim<sub>L</sub> isoforms. To detect the Bim<sub>S</sub> isoform the membrane was exposed for 5 minutes. GAPDH with an exposure time of less than a second served as loading control. (B) Intensities of the bands for all three Bim isoforms were quantified relative to the GAPDH loading control by using ImageJ and fold increase was calculated relative to the untreated Ppef2<sup>+/+</sup> control. Two western blots were performed and shown is the pooled normalized intensity of both. (C) Western blot for Bim was performed with 30  $\mu$ g cell lysates of FACS-sorted CD8<sup>+</sup> and CD11b<sup>+</sup> DCs of the spleen of Ppef2<sup>+/+</sup> and Ppef2<sup>-/-</sup> mice. Exposure of the membrane was performed like in (A). (D) Intensities of the bands for all three Bim isoforms were quantified relative to the GAPDH loading control by using ImageJ and fold increase was calculated relative to the untreated Ppef2<sup>+/+</sup> control. Shown is the result of one experiment with pooled samples of three mice per group. (E) Surface staining of Dll4 was performed with fluorescently labeled antibody and protein abundance was measured by flow cytometry. Shown are representative FACS plots of n=3 mice.

It was shown previously that cytoplasmic Bim increases after stimulation with TLR ligands like LPS [86]. Therefore we stimulated parts of the BMDC culture over night with LPS as positive control for an increase of Bim, which comes in three isoforms: Bim<sub>EL</sub>, Bim<sub>L</sub>, and Bim<sub>S</sub>. All three isoforms are generated by alternative splicing and are promoting apoptosis [123]. The shortest isoform, Bim<sub>S</sub>, is the most cytotoxic and only transiently expressed during apoptosis. Due to the different abundance of the three Bim isoforms the western blot was exposed either 30 seconds for detection of the larger and more abundant isoforms Bim<sub>EL</sub> and

Bim<sub>L</sub>, or 5 minutes for detection of the small isoform Bim<sub>S</sub> (Fig. 4.16 A & C). GAPDH was used as loading control for every sample with an exposure of less than a second to not get a fully saturated signal. To quantify the increase in Bim protein, the intensities of the western blot bands were quantified and normalized to the intensities of the respective GAPDH bands. Fold increase of Bim protein was then calculated relative to *Ppef2*<sup>+/+</sup> (non LPS-treated) DCs for each Bim isotype respectively (Fig. 4.16 B & D). The intensity of all of the three Bim isoforms increased in the *Ppef2*<sup>-/-</sup> BMDCs compared to control. This increase was comparable to the increase caused by LPS in *Ppef2*<sup>+/+</sup> BMDCs. Stimulation of *Ppef2*<sup>-/-</sup> DCs with LPS increased cytoplasmic Bim only marginally (Fig. 4.16 B). Also in primary spleen cDCs protein abundance of all three Bim isoforms was increased in *Ppef2*<sup>-/-</sup> CD8<sup>+</sup> and CD11b<sup>+</sup> DCs (Fig. 4.16 C & D).

Although expression of Dll4 is generally low in cDCs but high in pDCs (immgen.org), we saw alterations of expression in CD8<sup>+</sup> cDCs of *Ppef2*<sup>-/-</sup> mice (Fig. 4.15 C & F). Therefore, we performed surface stainings with an antibody directed against Dll4 (Fig. 4.16 D). In accordance with the expression profile of Dll4, splenic cDCs showed only minor staining compared to an isotype control, whereas pDCs showed a clear staining of Dll4. However, *Ppef2*<sup>+/+</sup> and *Ppef2*<sup>-/-</sup> DCs showed the same extent of Dll4 staining and the difference in expression was not seen on a (surface) protein level.

In conclusion, we detected decreased Trim2 mRNA by mRNA sequencing of *Ppef2*<sup>-/-</sup> CD8<sup>+</sup> DCs, which we were able to verify by qPCR. Trim2 is known to influence the protein abundance of pro-apoptotic Bim, which was upregulated in *Ppef2*<sup>-/-</sup> BMDCs and splenic DCs.

## 5 Discussion

Currently very little is known about Ppef2. In this project we were able to show that haematopoietic cells express this phosphatase in a CD8<sup>+</sup> DC specific manner and that expression is changed upon maturation of DCs. By generating Ppef2<sup>-/-</sup> mice we were the first to demonstrate a role of Ppef2 in DC biology. We were able to show that Ppef2 controls DC apoptosis by mechanisms involving Trim2 and Bim, influencing the priming of naive T cells.

### 5.1 Ppef2 is preferentially expressed by CD8<sup>+</sup> DCs

Previous work by our group identified a transcription factor binding motif in the promoter region of CD11c, that is responsible for driving expression of DC specific genes. An *in silico* search for other genes with the same promoter module identified Ppef2 as gene potentially expressed in a DC specific manner. To test this, we purified DCs, T cells, and B cells of the spleen, as well as circulating blood monocytes. Ppef2 expression, as determined by qPCR, was highest in CD8<sup>+</sup> DCs, with an 17.7 fold increase compared to ESAM<sup>lo</sup> DCs. With a  $2^{-\Delta C^t}$  value of 0.04, the expression in ESAM<sup>lo</sup> DCs was similar to blood monocytes (0.03 to 0.05). pDCs, CD4<sup>+</sup>, and CD8<sup>+</sup> T cells showed a  $2^{-\Delta C^t}$  value of less than 0.003, which can be seen as background (Fig. 4.1 A). As the expression in ESAM<sup>lo</sup> DCs and monocytes is also very modest and close to background, it is hard to say whether the expression measured here is of biological significance, or not. Interestingly, ESAM<sup>lo</sup> DCs are supposed to be more closely related to monocytes than to cDCs, as they express several monocyte related genes [18]. Overall, the expression profile of Ppef2 in sorted spleen cells reflected the microarray data available from the Immgen consortium (Fig. 3.2 B), showing Ppef2 expression largely specific for CD8<sup>+</sup> DCs.

The abundance of a certain transcript does not necessarily predict protein quantity. As shown by several genome-wide studies, only about 40% of the variation in protein concentration can be explained by knowing mRNA abundance [124, 125]. To further elucidate the expression profile of Ppef2 at the protein level, we took advantage of the  $\beta$ -galactosidase (lacZ) included in the gene trap cassette of Ppef2<sup>-/-</sup> mice (Fig. 3.3). In the spleen, lacZ activity was only measured in CD8<sup>+</sup> DCs, but not in ESAM<sup>lo</sup> DCs, ESAM<sup>hi</sup> DCs, pDCs, CD4<sup>+</sup> T cells, CD8<sup>+</sup> T cells, B cells, monocytes, and neutrophils (Fig. 4.1 B). Thus we can conclude that expression of Ppef2 mRNA in ESAM<sup>lo</sup> DCs and monocytes (Fig. 4.1 A) is indistinguishable

from background, or that it is not translated into biologically relevant amount of protein. However, due to technical limitations of the *lacZ* assay we can not rule out to not miss very small amounts of protein being expressed. Checking *Ppef2* on protein level by other methods, e.g. by western blot, was not possible due to a lack of a functional antibody against *Ppef2*.

Due to the fact that the  $CD103^+$  DCs of the periphery are the equivalent to splenic  $CD8^+$  DCs [38, 39], we wondered whether those cells also express *Ppef2*. According to the Immgen database (Fig. 3.2 C),  $CD103^+$  DCs show some expression of *Ppef2*, although to a lesser extent than  $CD8^+$  DCs. Interestingly, the Immgen data set also showed expression of *Ppef2* in thymic  $CD11b^+$  DCs, which differ in their development from cDCs of the spleen as they arise from CLPs instead of CMPs [12]. Indeed, we observed *Ppef2* promoter activity in  $CD8^+$  and  $CD11b^+$  DCs of the thymus, whereas  $CD11b^+$  DCs of sLN, lung, lamina propria, and mLN did not show expression of *Ppef2* (Fig. 4.1). Although the above mentioned close relationship of  $CD103^+$  to  $CD8^+$ , the  $CD103^+$  DCs of sLN, lung, lamina propria, and mLN did not express *Ppef2*. This was not completely in accordance with the microarray data provided by the Immgen consortium.

In conclusion, we were able to show expression of *Ppef2* in  $CD8^+$  DCs of the spleen on mRNA and protein level, whereas there was no expression in  $CD11b^+$  (with the exception of the thymus) or  $CD103^+$  DCs. Based on the finding that *Ppef2* shares promoter organization with the promoter region of *CD11c* [5], it is surprising that  $CD11c^+$   $CD11b^+$  DCs do not express *Ppef2*. Although the promoter motif described above is sufficient to drive DC specific expression, the expression of *Ppef2* is most probably controlled on additional levels. Different methylation status, *Ppef2* specific silencer, *Ppef2* targeting miRNAs, and many other pre- and post-transcriptional modifications can explain the differential expression in DC subpopulations.

## 5.2 Expression of *Ppef2* is differentially regulated by innate stimuli

Already the first work describing the presumably DC specific expression of *Ppef2* revealed a downregulation of mRNA in BMDCs after stimulating the cells with LPS [5]. To test whether other TLR ligands than LPS would also lead to *Ppef2* downregulation, we stimulated BMDCs with TLR1/2, TLR3, TLR5 and TLR7/8 agonists. After incubation of BMDCs with LPS the expression was downregulated by 85.7%, which was the strongest downregulation observed (Fig. 4.2 A). TLR5

(Flagellin) and TLR3 (Poly(I:C)) stimulation led to a statistically significant decrease in *Ppef2* expression of 41.2 to 45.1% compared to a unstimulated BMDC control. Stainings for DC maturation with the costimulatory molecule CD86 and MHCII revealed that of all TLR stimuli used in this study, the TLR5 and TLR3 stimuli were the weakest. Still clearly leading to distinct DC maturation, those stimuli led to about 50% fully matured DCs, whereas all other TLR stimuli showed about 70% of fully matured DCs (data not shown). BMDC stimulation with TLR2/TLR1 (Pam3CSK4) and TLR7/TLR8 (CL097) agonists again showed a downregulation of *Ppef2* expression and an extent of phenotypical maturation comparable to stimulation with LPS. The extent of *Ppef2* downregulation thus correlated with the amount of fully matured DCs in culture.

Another common tool to stimulate DCs *in vitro* and *in vivo* is ligation of CD40, a member of the TNF-receptor superfamily. Stimulation with anti-CD40 leads to signaling via TRAFs (TNF receptor-associated factors) [126]. In DCs TRAF6 is necessary for both, LPS- and CD40-mediated signaling [127]. Schematic TLR and CD40 signaling pathways are shown in Figure 5.1. For myeloid differentiation primary-response protein 88 (MYD88) dependent signaling of TLRs TRAF6 can signal via different pathways, leading e.g. to activation of the transcription factors like AP1, cAMP response element-binding protein (CREB), or NF- $\kappa$ B. The latter can also be activated by CD40 signaling involving TRAF6 [128]. CD40 and TLR signaling leading to activation of NF- $\kappa$ B are different, although both utilise TRAF6. In contrast to TLR signaling, CD40 mediated TRAF6 signaling involves TRAF2 and TRAF3, which altogether bind to the cytoplasmic tail of CD40 and contribute independently to canonical NF- $\kappa$ B activation [129], whereas TRAF6 dependent TLR signaling involves IL-1R-associated kinases (IRAKs). NF- $\kappa$ B activation by CD40 signaling is only one way of signaling, but it was also shown that CD40 signaling can result in protein kinase B (Akt) activation [130]. However, we did not observe any changes in *Ppef2* expression after stimulation with a monoclonal antibody directed against CD40. Even when the anti-CD40 antibody was combined with TNF $\alpha$ , also triggering the TNF-receptor superfamily, DCs did not display any change in *Ppef2* expression, although the percentage of matured DCs was comparable to stimulation with LPS.

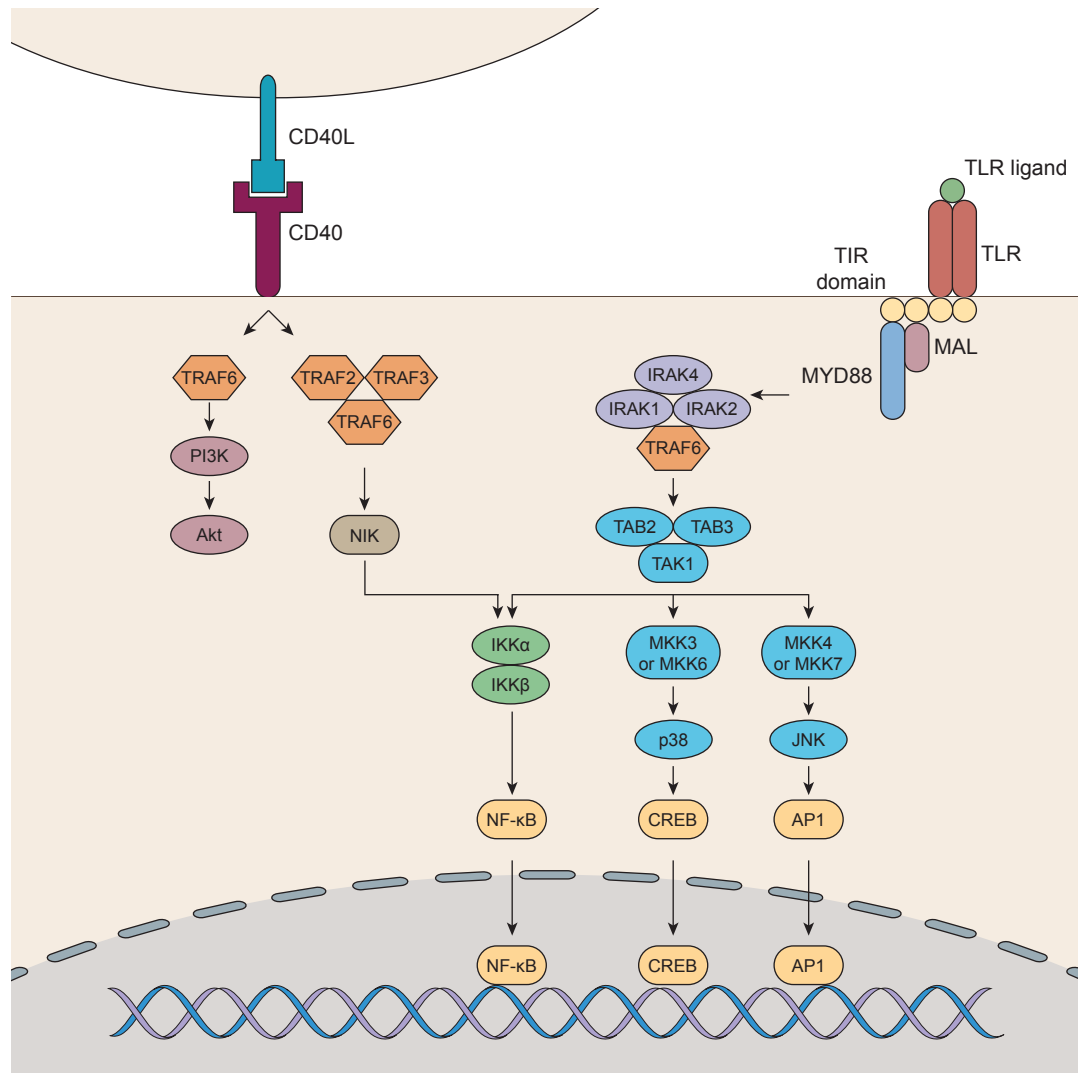


**Figure 5.1: TLR and CD40 signaling both include TRAF6.** Shown are signaling pathways of TLRs and CD40. Binding of TLR ligands leads to dimerization of their receptors which initiates signaling. In a first signaling step of TLRs, the Toll-IL-1-resistance (TIR) domains engage the myeloid differentiation primary-response protein 88 (MYD88). This stimulates downstream signaling pathways involving IL-1R-associated kinases (IRAKs) and the adaptor molecule TNF receptor-associated factor 6 (TRAF6), which can lead to the activation of the mitogen-activated protein kinases (MAPKs) JUN N-terminal kinase (JNK) and p38, or to the activation of the transcription factor NF- $\kappa$ B. Signaling via CD40 also involves TRAFs, like TRAF6. Signaling of CD40 via TRAF6 can, like TLR signaling, lead to the activation of NF- $\kappa$ B, or to protein kinase B (Akt) signaling via the phosphoinositide 3-kinase (PI3K). MAL, MYD88-adaptor-like protein; CD40L, CD40 ligand; CREB, cAMP response element-binding protein; NIK, NF- $\kappa$ B-inducing kinase; IKK, inhibitor of NF- $\kappa$ B kinase; MKK, MAP kinase kinase; TAB, TAK1-binding protein; TAK, TGF $\beta$ -activated kinase. Modified from [131, 130, 132].

In conclusion, TRAF6 is important for signaling of CD40 and MYD88 dependent TLRs and triggering of both can lead to activation of NF- $\kappa$ B, but those are not the only signaling pathways triggered by TRAF6. Especially for CD40 signaling it was

shown that Akt is a downstream target and known as a candidate for the promotion of survival [130]. Interestingly, it was also shown that JUN N-terminal kinase (JNK) signaling induced by LPS results in apoptosis [133]. These data fits to the hypothesis that CD40 signaling acts pro-survival whereas TLR signaling acts pro-apoptotic. Considering the downregulation of *Ppef2* expression after TLR stimuli, TLR induced TRAF6 signaling might involve mitogen-activated protein kinases that e.g. lead to the activation of p38 and the cAMP response element-binding protein (CREB), which was shown to be a repressor of transcription [134] and therefore could be responsible for the downregulation of *Ppef2* expression as additional pro-apoptotic factor next to activation of JNK [133]. CD40 signaling on the other hand might signal via Akt, acting pro-survival and not altering the expressing of *Ppef2*. However, the physiological role of CD40 ligation in DC maturation is controversial and studies showed that LPS alone is not sufficient to generate Ag-specific CTL responses *in vitro*, but that CD40 ligation is [135]. To test for synergistic or antagonistic effects of LPS and anti-CD40, we combined the two stimuli. LPS stimulation was dominant when used in combination with anti-CD40 and resulted in a degree of *Ppef2* downregulation comparable with stimulation of LPS alone.

GM-CSF generated BMDCs lack the heterogeneity of splenic DCs and recent studies showed that bone marrow cultured in GM-CSF generates both, DCs and macrophages, which both express CD11c and MHCII [136]. Especially CD8 is a marker that is missing on GM-CSF BMDCs. The fact that mice lacking GM-CSF or the corresponding receptor show normal DC development *in vivo* [20] raises the question of how well GM-CSF generated BMDCs resemble *in vivo* found DC (and their subsets). Another method to generate mouse BMDCs *in vitro* is by supplementing bone marrow cells with Flt3 ligand [137]. Flt3L generated BMDCs show a higher variety of DC subsets, which resemble splenic CD8<sup>+</sup> DCs, CD11b<sup>+</sup> DCs, and pDCs in the surface marker expression (except the expression of CD8), the expression pattern of TLRs and the production of cytokines [138]. Especially the BMDCs resembling CD8<sup>+</sup> DCs in such a culture were shown to be able to cross-present exogenous antigens to CD8<sup>+</sup> T cells and were developmental dependent on IRF8 [138], which corresponds to *in vivo* found CD8<sup>+</sup> DCs. For this reason, we also evaluated in Flt3L generated BMDCs whether stimulation would lead to downregulation of *Ppef2* expression, which was the case for all the TLR ligands tested (Fig. 4.2 B). In accordance with the GM-CSF BMDCs, stimulation of the Flt3L BMDCs with anti-CD40 did not alter the expression of *Ppef2*. We analyzed *Ppef2* expression in the whole bone marrow culture, which does not allow con-

clusions on different subpopulations which normally come up in Flt3L cultures. Still some conclusions of *Ppef2* expression in Flt3L BMDC subpopulations can be drawn from these results. Taking the extent of *Ppef2* downregulation after addition of LPS to Flt3L BMDCs argues that the pDCs present in this culture do not express *Ppef2*, otherwise there should be *Ppef2* expression left, since pDCs in such a culture do not express the TLR responsible for recognizing LPS [138]. The TLR triggered by Poly(I:C), TLR3, on the other hand, is only expressed by the splenic CD8<sup>+</sup> DCs and their Flt3L BMDC counterparts [138]. Also in this case, *Ppef2* expression is downregulated to a level similar to LPS treated Flt3L BMDCs. Since the Flt3L BMDC culture is largely composed of CD11b<sup>+</sup> DCs, expression in this latter subtype within the Flt3L BMDC culture is unlikely. However, we can not rule out that cytokines or other inflammatory molecules secreted or produced by matured subpopulations within this culture influence the other subpopulations and led to their maturation.

To evaluate the downregulation of *Ppef2* expression in a more physiological setting, we took advantage of the *lacZ* reporter and looked for  $\beta$ -galactosidase abundance after LPS administration *in vivo* (Fig. 4.2 C). Administration of LPS decreased the quantity of  $\beta$ -galactosidase already after 4h. Considering  $\beta$ -galactosidase protein stability and turnover rate, expression of *Ppef2* expression has to be downregulated quickly after DC maturation. After  $\sim$ 16h the  $\beta$ -galactosidase activity was decreased by 86.99%. This reduction is remarkably close to the downregulation of *Ppef2* seen by qPCR (Fig. 4.2 A). The strong correlation between qPCR data and *lacZ* expression, while relying on different methods and quantifying different products, mRNA and protein, respectively, argues in favor of a linear and specific correlation between *lacZ* activity and *Ppef2* expression.

Spontaneous maturation, observed and described mostly in *in vitro* systems, is an alternative way of DC maturation. Factors shown to contribute to spontaneous maturation include adhesion molecules like E-cadherin and integrins [112, 139, 140], soluble factors [141], as well as integrin mediated cell-cell contact not mediated by  $\beta$ -catenin but Swap-70 and RhoA [142]. To check whether the spontaneous maturation occurring in a GM-CSF BMDC culture could also lead to downregulation of *Ppef2* expression, we sorted CD11c<sup>+</sup> BMDCs according to their surface expression of MHCII and CD86 and performed qPCR analyses (Fig. 4.2 D). Completely immature DCs, identified as CD11c<sup>+</sup> MHCII<sup>low</sup> CD86<sup>low</sup>, expressed *Ppef2*, although it is questionable whether these cells are truly related to fully differentiated DCs because of their low expression of MHCII. Interestingly, DC precursors of the spleen do not display *Ppef2* expression (Fig. 4.13 E) and *Ppef2* expression

increases during DC differentiation, as shown by analyses in a GM-CSF BMDC culture over time with little to no expression in early stages of the culture [5]. Nonetheless, the expression decreases by half when the cells increase surface MHCII expression to MHCII<sup>int</sup>. Spontaneous maturation, leading to CD11c<sup>+</sup> MHCII<sup>high</sup> CD86<sup>high</sup> DCs, further decreases the expression of *Ppef2*. Following the argument that only CD11c<sup>+</sup> MHCII<sup>int</sup> DCs would reflect fully differentiated immature DCs, the expression still decreases in fully matured MHCII<sup>high</sup> CD86<sup>high</sup> DCs by 70.83% (p-value=0.0122) compared to the latter. In conclusion, we observed a downregulation of *Ppef2* expression after spontaneous maturation that parallels the expression profile of the whole unsorted culture stimulated with LPS. Indeed, other independent studies have shown similarities between LPS activated and spontaneously activated cells when looking at microarray data of e.g. miRNAs [143].

Taken together, we observed that the maturation status of DCs strongly correlates with the expression of *Ppef2*. Expression decreased when DCs were matured with TLR ligands or underwent spontaneous maturation. DC maturation with anti-CD40 monoclonal antibody (even combined with TNF $\alpha$ ), on the other hand, did not alter the expression of *Ppef2*. Anti-CD40 mediated DC maturation is not fully understood. Several studies showed that CD40 ligation is able to fully mature DCs only in combination with a TLR stimulus [135, 144, 145]. This combination led to downregulation of *Ppef2* expression.

The maturation of DCs is a complex process that leads to numerous changes in cellular morphology, physiology and phenotype, with several factors controlling the process on several levels. Studies have shown that the majority of changes in gene expression during maturation are reductions of expression [146]. Therefore, it is difficult to conclude whether the expression profile of *Ppef2* is simply a consequence of co-downregulation with hundreds other genes, which are dispensable for mature DCs, or whether it is a specific regulation due to a functionally relevant role of the protein in the maturation of DCs.

### 5.3 The *Ppef2* gene trap leads to loss of *Ppef2*

We generated *Ppef2*<sup>-/-</sup> mice to further investigate the role of this phosphatase in the context of DC biology. The knockout-first approach used for this is described in more detail in chapter 3.4.

To exclude differential splicing or short/modified transcript versions we performed qPCRs with amplified fragments upstream and downstream of the inserted cassette. mRNA downstream of the cassette was gone completely whereas the mRNA upstream of the gene trap was reduced by over 55%.

This remaining truncated and non-functional version of the transcript should undergo nonsense mediated mRNA decay (NMD) caused by premature stop codons. The rate or speed of NMD, as well as the expression rate of *Ppef2*, determine the abundance of mRNA upstream of the gene trap. The finding that upstream mRNA is reduced by half, instead of being completely abrogated, could argue for constitutive expression at higher rates in immature DCs, but this would need further investigation of mRNA turnover rates, speed of NMD and other factors influencing RNA stability and integrity. Another important finding is that mRNA downstream of the gene trap is completely absent. Expression of the neomycin resistance gene located after the *lacZ* reporter gene and the premature stop codon is driven by an autonomous promoter and also terminated by a polyadenylation signal. If this stop codon, terminating the expression of the neomycin resistance, was leaky or not functional, it could lead to expression of a transcript including exon 5, which would correspond to the catalytic domain of *Ppef2*. This was not the case in our *Ppef2*<sup>-/-</sup> mice.

## 5.4 *Ppef2* controls apoptosis of DCs

The only functional study of *Ppef2* published so far investigated its role in oxidative stress in COS-7 and HEK 293 A cells [97]. *Ppef2* was shown to be anti-apoptotic by a mechanism involving H<sub>2</sub>O<sub>2</sub>-induced suppression of Ask1.

Cytokine withdrawal in a GM-CSF BMDC culture is a commonly used method to test for the susceptibility of DCs to apoptosis. GM-CSF withdrawal at a stage where precursors already differentiated in DCs (Fig. 4.9 A) leads to apoptosis by mechanisms involving Bim [86], PI3K/mTOR [147], and Jak3 [148].

*Ppef2*<sup>-/-</sup> DCs were more sensitive to apoptosis after GM-CSF withdrawal compared to *Ppef2*<sup>+/+</sup> DCs. There are two possible explanations for the difference observed between *Ppef2*<sup>+/+</sup> and *Ppef2*<sup>-/-</sup> cells during the interim expansion. Either *Ppef2*<sup>-/-</sup> DCs have a reduced proliferation capacity (1), or deficiency of *Ppef2* leads to an increase in apoptosis (2). Since we could not observe any changes in proliferation as measured by BrdU incorporation, but on the other hand could detect an increase in active caspase-3, as well as phosphatidylserine, these data suggest an increase in apoptosis (Fig. 4.9).

In summary, we observed increase in apoptosis in *Ppef2*<sup>-/-</sup> BMDCs after growth factor removal. Interestingly, the interim increase in living DCs was not observed by other groups using the same apoptosis model of cytokine withdrawal [3, 148]. The cause of this expansion of DCs could be remaining trace amounts of GM-CSF in the culture, although cells have been washed extensively. Another reason could

be found in the kinetics of BMDC differentiation. There still may be precursors after 6 days of the culture that already received signals to differentiate into DCs, or are currently undergoing differentiation, and therefore are causing the increase in the percentage of viable DCs before induction of apoptosis takes over. However, the increase in apoptosis after cytokine withdrawal observed *in vitro* led us to question whether primary cells show the same phenotype, as GM-CSF seems to be dispensable for DC development and maintenance *in vivo* [20].

To this end, we magnetically enriched CD11c<sup>+</sup> splenocytes and kept them in culture over night with or without the supplement of GM-CSF (Fig. 4.10 A). By using magnetically enriched CD11c<sup>+</sup> splenocytes, different DC subpopulations and other CD11c expressing cells were cultured together and distinguished later by flow cytometry. Overall, cDCs showed a marked increase in intracellular active caspase-3 when cultured without GM-CSF (Fig. 4.10 B). *Ppef2* deficiency enhanced the apoptosis induced by the lack of GM-CSF, measurable by a reduction in the percentage of viable cDCs and by an increase in the amount of active caspase-3. Interestingly, we observed the same effects of enhanced apoptosis in *Ppef2*<sup>-/-</sup> CD8<sup>+</sup> and CD11b<sup>+</sup> DCs (Fig. 4.10 C and D). However, the decrease in the percentage of living cells after GM-CSF withdrawal was markedly more pronounced in CD8<sup>+</sup> DCs (30.3% reduction) compared to CD11b<sup>+</sup> DCs (10.9% reduction), although both populations showed a similar increase in active caspase-3 (51.4% increase in CD8<sup>+</sup> DCs and 43.2% increase in CD11b<sup>+</sup> DCs). This difference may reflect the different turnover rates of CD8<sup>+</sup> and CD11b<sup>+</sup> DCs which was shown to be higher in CD8<sup>+</sup> DCs [52]. Nonetheless, it is puzzling why the *Ppef2*<sup>-/-</sup> CD11b<sup>+</sup> DCs also show an increase in apoptosis, lacking expression of the protein (Fig. 4.1).

Several scenarios can explain this finding: Most probably are secondary effects, e.g. the deprivation of survival factors by dying CD8<sup>+</sup> DCs that are important for the maintenance of CD11b<sup>+</sup> DCs, or the uptake of apoptotic CD8<sup>+</sup> DCs (positive for cleaved caspase-3) by CD11b<sup>+</sup> DCs. Also the crosstalk between CD8<sup>+</sup> and CD11b<sup>+</sup> DCs could provide a possible explanation. DC-DC interactions were shown mostly between pDCs and cDCs [149, 150]; They can be mediated by soluble factors like IL-15 [150], or by direct cell-cell contact, as in the case of antigen transfer from migratory DCs to resident LN DCs [151]. With the methods used in this study it was not possible to identify a soluble factor in the supernatant of CD8<sup>+/+</sup> *Ppef2*<sup>-/-</sup> DCs that would induce apoptosis in CD11b<sup>+</sup> DCs.

To investigate the increase in apoptotic cells observed *in vitro* in a more physiological setting, and without depending on exogenous cytokines (GM-CSF), we stained primary splenocytes for active caspase-3 and surface phosphatidylserine

(Fig. 4.11). As seen *in vitro* and *ex vivo* in the absence of GM-CSF, also *in vivo* the amount of apoptotic cells was increased in the Ppef2<sup>-/-</sup> DCs. In concordance with the turnover rate of cDC subpopulations reported in the literature [52], CD8<sup>+</sup> DCs showed a higher caspase activity than CD11b<sup>+</sup> DCs (Fig. 4.11 A). However, also *in vivo* we observed the surprising increase of caspase activity in CD11b<sup>+</sup> DCs already seen when *ex vivo* cultured, despite the physiological absence of Ppef2 expression. Nonetheless, the enhancement of apoptosis was anyway limited to cDCs, as none of the other cell types investigated showed any signs of increased caspase activity (Fig. 4.11 B). Due to the exclusive expression of Ppef2 in CD8<sup>+</sup> DCs, the increase in apoptosis in CD11b<sup>+</sup> is most likely caused by secondary effects. Data from mixed bone marrow chimeras, discussed in the following sections, will provide further evidence for this assumption.

In conclusion, we observed an increase in apoptosis in Ppef2<sup>-/-</sup> DCs *in vitro* and *ex vivo* under suboptimal culture conditions. The same effect was observed *in vivo* as shown by caspase and Annexin-V staining. The biological significance of this increased apoptosis can be explained by the findings that artificially prolonged DC longevity causes exaggerated T cell responses leading to autoimmune disorders [1, 3, 86, 87, 88]. Ppef2 would therefore act as a molecular timer that regulates the lifespan of DCs after their activation. This fits to our data that Ppef2 expression decreases rapidly after maturation of DCs with TLR ligands (Fig. 4.2). Also the finding that Ppef2 expression does not change after stimulation with anti-CD40 is in line with this hypothesis as it was shown that ligation of CD40, as well as ligation with other members of the TNF family [2, 152], promotes DC survival [153].

## 5.5 Increase in apoptosis is a CD8<sup>+</sup> DC intrinsic effect

To evaluate whether the increase in apoptosis would lead to a disadvantage in a competitive situation we generated mixed bone marrow chimeras (Fig. 4.12). Analysis of the distribution of congenic markers in CD8<sup>+</sup> and CD11b<sup>+</sup> DCs revealed that Ppef2<sup>-/-</sup> CD8<sup>+</sup> DC had a competitive disadvantage over Ppef2<sup>+/+</sup> CD8<sup>+</sup> DCs. This did not hold true for CD11b<sup>+</sup> DCs, where DCs of Ppef2<sup>+/+</sup> or Ppef2<sup>-/-</sup> origin were distributed equally.

This exclusivity of the competitive disadvantage observed for CD8<sup>+</sup> but not CD11b<sup>+</sup> DCs strengthens the hypothesis that the enhanced apoptosis in CD11b<sup>+</sup> DCs is a secondary effect and that Ppef2 deficiency directly influences only the survival and competitiveness of CD8<sup>+</sup> DCs.

In conclusion, we were able to demonstrate a role of Ppef2 in keeping the cellular

fitness and survival of CD8<sup>+</sup> DCs intact and that loss of Ppef2 led intrinsically to a competitive disadvantage of Ppef2<sup>-/-</sup> CD8<sup>+</sup> DCs, mediated through an increase of apoptosis. However, CD11b<sup>+</sup> DCs were not influenced by the loss of Ppef2 in the competitive situation of mixed bone marrow chimeras, which argues for extrinsic signals causing enhanced apoptosis in CD11c<sup>+</sup> CD11b<sup>+</sup> DCs. Possible extrinsic signals, like soluble factors [150] or cell-cell contacts, are discussed in more detail in section 5.4.

## 5.6 Analyses of DC proliferation and DC precursors do not show compensatory effects

The effect of enhanced apoptosis described before did not match with the identical cell numbers of DCs observed in several organs (see chapter 4.3). Therefore, we investigated changes in DC proliferation (and turnover), which could compensate the loss of DCs by enhanced cell death and cause equal cell numbers.

For BrdU labeling experiments we observed inconsistent results between different experiments. In one experiment Ppef2<sup>-/-</sup> DCs seemed to incorporate more BrdU in the “pulse phase”, indicating an increase in proliferation, whereas in another experiment Ppef2 deficiency led to a decrease in the BrdU<sup>+</sup> DCs in the “chase phase”, suggesting a faster DC turnover. However, pooling data from individually performed experiments did not result in significant differences when it comes to DC proliferation or turnover. The same holds true for short time BrdU labeling experiments (Fig. 4.13 B). Also here pooling data from three independently performed experiments did not mark any significant differences, although some experiments indicated an increase in proliferation.

It was shown that DC-depleted mice, or mice with reduced cDCs numbers, have elevated serum Flt3L levels due to the decrease of cells consuming it [116, 117]. To check whether increased apoptosis would translate to an increase in the serum level of Flt3 ligand or its receptor we performed ELISAs of the serum, as well as flow cytometric stainings. Serum Flt3L showed only a small, non-statistically significant (p=0.0735) tendency to be elevated (Fig. 4.13). Staining of the receptor Flt3 revealed only minor, negligible difference of surface expression on CD11b<sup>+</sup> DCs (Fig. 4.13 D), and no differences in DC precursors (Fig. 4.13 E).

The mice generated by the group of Steffen Jung, where DCs are depleted by expression of diphtheria toxin A (DTA) when crossed to CD11c-Cre mice [116], deplete DCs after promoter activity of CD11c, which is already in the pre-DC state. On the other hand, Ppef2<sup>-/-</sup> mice show increased apoptosis in the state

of differentiated DCs but no impact on pre-DCs. Therefore, the mice of Steffen Jung influence the consumer of Flt3L on an earlier stage than *Ppef2*-deficiency does and DC-precursors of *Ppef2*<sup>-/-</sup> mice still differentiate into DCs and therefore consume Flt3L. That might be a reason why we can not observe increased serum levels of Flt3L to an extent comparable to CD11c:DTA mice, as increased Flt3L is rapidly consumed by DCs or their precursors in *Ppef2*<sup>-/-</sup> mice but not in the mice of Steffen Jung. Another factor influencing DC growth and survival is lymphotoxin (LT)- $\beta$ , which mainly acts on CD11b<sup>+</sup> DCs but not on CD8<sup>+</sup> DCs [72, 80]. However, we did not test for increased LT- $\beta$  in the serum of *Ppef2*<sup>-/-</sup> mice because of its exclusive effect on CD11b<sup>+</sup> DCs.

In conclusion, we did not observe any alterations of BrdU<sup>+</sup> DCs in the “pulse” or “chase” phase. Even short time BrdU labeling did not show any differences between *Ppef2*<sup>+/+</sup> and *Ppef2*<sup>-/-</sup> DCs. Only a small amount of *in situ* DCs is in cell cycle at any given time (ca. 5%) [72] and therefore the slight tendency of increased BrdU<sup>+</sup> DCs after short time labeling (Fig. 4.13 B) is unlikely to compensate for the increase in apoptosis. Effects on DC precursors might be more probable and we consequently checked for levels of Flt3L in the serum and the surface expression of its receptor, Flt3. Both were not markedly altered on fully differentiated DCs, as well as on DCs precursors. The frequencies of the DC precursors themselves were also not changed and a direct effect of *Ppef2* on DC precursors can be excluded as they do not express the protein (Fig. 4.13 E and F). With the methods available it was not possible to detect an increase in proliferation that would compensate the enhanced apoptosis and restore normal DC numbers. BrdU might be the wrong choice as the DCs themselves are not highly proliferative and the immediate precursors of the spleen also show only little proliferation capacity [154]. Additionally, investigation of one organ does take migratory precursors in consideration and the relation between precursors and differentiated DCs is complex to determine. Also the serum levels of Flt3L are hard to interpret and complex since it was shown that they might be regulated by feedback loops, as inhibition of Flt3L with an antibody results in increased serum Flt3L [77].

## 5.7 *Ppef2* controls the ability of DCs to transiently activate T cells *in vivo*

It was previously shown that changes in the lifespan of DCs influence the control of immunity and tolerance [1, 2, 3, 4]. Most studies artificially increased the lifespan of DCs to investigate the influence of DC longevity on immunity and tolerance.

Here we wanted to verify whether an impaired survival of CD8<sup>+</sup> DCs would lead to impaired transient T cell activation.

Transient CD8<sup>+</sup> T cell activation with OVA-pulsed DCs showed a dependency of *Ppef2*, since transfer of SIINFEKL-pulsed *Ppef2*<sup>-/-</sup> DCs resulted in a diminished T cell proliferation, observable by reduced numbers and frequencies of OVA-specific T cells. Signals important for the differentiation of naive T cells into effector cells include the triggering of the T cell receptor by MHCI-associated peptides on DCs (signal 1), costimulatory signals like e.g. triggering of CD28 on T cells by CD80 on DCs (signal 2) and the secretion of cytokines such as IL-12 by DCs (signal 3) (reviewed in [155, 156]). However, it has been suggested that DCs that are in an immature state, missing signal 2 and 3, induce tolerogenic T cells. Pulsing with peptide like performed here leads to immature DCs inducing tolerance [157, 158]. Therefore signal 2 and signal 3 do not play any role in the transfer of peptide-pulsed DCs like performed in this study. Because of the exaggerated T cell responses in systems with artificially increased DC lifespans [1, 3, 86, 87, 88] we hypothesize that the increased apoptosis of cDCs in *Ppef2*<sup>-/-</sup> mice leads to reduced numbers of DCs that are able to induce T proliferation.

*In vivo* expansion of DCs for peptide-pulsing was achieved by subcutaneous implantation of a Flt3L expressing tumor cell line. This leads to an increase of both CD8<sup>+</sup> and CD11b<sup>+</sup> DCs, since both populations are affected by Flt3L [159], although CD11b<sup>+</sup> DCs to a lesser extent than CD8<sup>+</sup> if Flt3 or Flt3L is missing [159, 74]. However, pulsing with peptide leads to presentation of the peptide-MHCI complex on both cDC subpopulations, but only the CD8<sup>+</sup> DCs are able to efficiently prime CD8<sup>+</sup> T cells [42]. To circumvent the influence of CD11b<sup>+</sup> DCs, we injected full OVA protein instead of pulsing with the peptide. Cross-presentation of extracellular antigens with MHCI to CD8<sup>+</sup> T cells is a unique feature of CD8<sup>+</sup> (and CD103<sup>+</sup>) DCs [42, 57, 59]. Cross-priming of OT-I cells was impaired in *Ppef2*<sup>-/-</sup> mice (Fig. 4.14 A and B). The half-life of CD8<sup>+</sup> DCs is approximately 1.5 days [52], and is shortened in case of *Ppef2* deficiency. This shortened lifespan of (CD8<sup>+</sup>) DCs directly influences the transient activation and proliferation of CD8<sup>+</sup> T cells.

In conclusion, we find an impaired transient T cell activation linked to *Ppef2* deficiency. This attenuated T cell proliferation was caused by an increased apoptosis of (CD8<sup>+</sup>) DCs.

## 5.8 Reduced expression of Trim2 leads to accumulation of pro-apoptotic Bim

Dephosphorylation of the pro-apoptotic kinase Ask1 was one of the few published specific targets for Ppef2 [97], which led us, in the first place, to the investigation of apoptosis in Ppef2<sup>-/-</sup> DCs. Nevertheless, western blot analyses of DCs lacking Ppef2 revealed no changes in the phosphorylation status of Ask1 (data not shown).

To find other mechanisms by which Ppef2 might drive apoptosis we performed mRNA sequencing of sorted CD8<sup>+</sup> and CD11b<sup>+</sup> DCs of the spleen (Fig. 4.15). Among the genes differentially expressed in Ppef2<sup>-/-</sup> CD8<sup>+</sup> DCs, Trim2 and Dll4 caught our interest (Fig. 4.15 C). Both mRNAs were reduced in Ppef2<sup>-/-</sup> CD8<sup>+</sup> DCs, which we were able to verify by qPCR (Fig. 4.15 E and F). None of the genes differentially expressed in CD11b<sup>+</sup> DCs lacking Ppef2 showed any connection to apoptosis or proliferation.

Dll4 is known to be a ligand for Notch receptors [121] and Notch signaling was shown to be important for the survival and homeostasis of CD11b<sup>+</sup> DCs [29]. The interaction of Dll4 with its receptor can function in cis and in trans whereat Notch is trans-activated and cis-inhibited [160, 161, 162]. Decreases in Dll4 on CD8<sup>+</sup> would lead to impaired Notch signaling in trans. In case of DC-DC interactions, as discussed in chapter 5.4, this could lead to effects similar to the ones observed when Notch-RBP-J signaling is knocked out by a CD11c specific Cre recombinase, leading to a breakdown of CD11b<sup>+</sup> homeostasis [29]. The limited effect on CD11b<sup>+</sup> DCs together with the postulated cis-inhibition of CD8<sup>+</sup> DCs makes it contradictory that Dll4 should influence survival of CD8<sup>+</sup> DCs. Nonetheless, we investigated alterations in surface expression of Dll4 on DCs, and did not observe any changes between Ppef2<sup>-/-</sup> and Ppef2<sup>+/+</sup> DCs (Fig. 4.16 D).

Trim2, an E3 Ligase, was shown to bind the Bcl-2-interacting Mediator of Cell Death (Bim) [120], which is an apoptotic activator [123]. Interaction of Trim2 with Bim leads to ubiquitination and proteasomal degradation of Bim [120]. Early reports, taking advantage of a mouse strain deficient in Bim, revealed an accumulation of lymphoid and myeloid cells, which led to autoimmunity and the conclusion that Bim is necessary for homeostasis of hematopoietic cells, as well as for the control of autoimmunity [163]. Maturation of DCs by TLR ligands was later shown to upregulate Bim and a DC specific Bim deficiency resulted in a decrease of cell death, overactivation of lymphocytes, and autoimmunity [86].

To investigate apoptosis pathways involving Trim2 and Bim we performed wes-

tern blot analyses of Bim in BMDCs that were either stimulated with LPS or left unstimulated (Fig. 4.16 A & B). Bim has three isoforms, Bim<sub>EL</sub>, Bim<sub>L</sub>, and Bim<sub>S</sub> [123]. All three isoforms are pro-apoptotic, with Bim<sub>S</sub> being the most cytotoxic and only transiently expressed during apoptosis. Ppef2<sup>-/-</sup> BMDCs showed an increase in all three isoforms that was comparable to the increase after LPS stimulus in Ppef2<sup>+/+</sup> BMDCs (Fig. 4.16 A & B). Also Ppef2<sup>-/-</sup> spleen DCs showed an increase in pro-apoptotic Bim (Fig. 4.16 C & D). Decrease in Trim2 would therefore lead to a intracellular accumulation of Bim, that then would drive apoptosis. Additionally, it was also shown that GM-CSF withdrawal in BMDC cultures increases pro-apoptotic Bim [86] and Ppef2<sup>-/-</sup> BMDCs were more prone to apoptosis after cytokine withdrawal (Fig. 4.9). However, the observed increase of Bim in CD11b<sup>+</sup> DCs argues for additional mechanisms of Bim regulation since Trim2 was not altered in the mRNA sequencing of CD11b<sup>+</sup> DCs.

Interestingly, Bim also is a downstream target of Jnk, which is activated by Ask1 [164, 165]. It is therefore difficult to rule out that Ask1 might also play a role in the increase in apoptosis seen in Ppef2<sup>-/-</sup> DCs, although the phosphorylation status of Ask1 was not altered in Ppef2<sup>-/-</sup> DCs (data not shown).

In conclusion, we showed that loss of Ppef2 led to a decrease of Trim2 mRNA which is known to influence the protein abundance of Bim. Being a regulator of DC apoptosis, Bim would therefore be responsible for the increase in apoptosis observed in this study.

## 5.9 Conclusion and Outlook

In this study, we identified Ppef2 as a crucial survival phosphatase, the presence of which controls DC survival and its disappearance acts as a molecular timer following DC maturation. In this model, DC maturation itself leads to downregulation of Ppef2 expression. This results in accumulation of pro-apoptotic Bim via a mechanism involving Trim2. Increase in cytoplasmic Bim eventually leads to apoptosis, limiting the time during which an activated DC is able to prime T cell responses. This mechanism limits antigen responses, and protects the organism from excessive immune activation that could lead to autoimmune disorders [1, 3, 86, 87, 88].

In addition to the experiments presented in this thesis, this model could also be tested with a system of Ppef2 overexpression. This could be achieved by lentiviral transduction of haematopoietic stem cells and adoptive transfer, to generate bone marrow chimeras, or by overexpression of Ppef2 in *in vitro* cultures (BMDCs or Hoxb8 cells). It would then be interesting to see whether constitutively expressed

Ppef2 protects DCs from apoptosis, and whether this can lead to autoimmunity. Furthermore, the same experiments performed with mutated versions of Ppef2 could allow to determine the specific protein motifs that are important for the function of Ppef2.

Another interesting question is whether Ppef2<sup>-/-</sup> mice are protected against DC-mediated autoimmunity, with their limited ability to induce tolerance. This can be evaluated by crossing Ppef2<sup>-/-</sup> mice with spontaneous autoimmune models, whereas the diminished T cell priming ability of Ppef2<sup>-/-</sup> DCs might hold the balance with the reduced induction of tolerance.

It would also be interesting to determine the direct substrates of Ppef2, by means of phosphoproteomics of Ppef2<sup>+/+</sup> and Ppef2<sup>-/-</sup> mice. Combining co-immunoprecipitation with a proteomic screening could also allow to identify the proteins that directly interact with Ppef2, still unknown.

The CD8<sup>+</sup> DC specific expression of Ppef2 could be used as a tool, e.g. to generate mouse models with highly specific CD8<sup>+</sup> DC expression of transgenes. Especially considering the maturation dependent promoter activity, this could be used to achieve not only cell specific expression, but also maturation dependent expression.

In the human, Ppef2 does not show an expression pattern similar to the one observed in mice [100]. Expression of human Ppef2 is limited to the retina. Therefore Ppef2 might not play a role in the human, although its sequence is highly conserved. However, the family of protein phosphatases is quite large and Ppef2 orthologues, like PPP3CC, which is expressed in BDCA4<sup>+</sup> DCs, might play a role in human DCs. It might thus be interesting to investigate the role of this or other phosphatases of the same family in human DC biology. Especially because Ppef2 was identified as a survival phosphatase in human cells in a screening utilizing RNA interference (RNAi) [166].

## 6 Material and Methods

### 6.1 Materials

#### 6.1.1 Devices

Analytic scale	Adventurer, Ohaus Corp., Pine Brooks, NJ, USA
automatic pipettors	Integra Biosciences, Baar, Switzerland
bench centrifuge	Centrifuge 5415 D, Eppendorf, Hamburg, Germany
cell counter	CASY cell counter and analyzer, OMNI life science, Bremen, Germany
centrifuge	Rotixa RP, Hettich, Tuttlingen, Germany
chemical scale	Kern, Albstadt, Germany
ELISA-reader	vmax kinetic microplate reader, Molecular Devices, Biberach, Germany
flow cytometer	FACSCalibur, FACSCantoII and FACS Aria, BD
incubator	Hera cell, Heraeus Kendro Laboratory Products, Hanau, Germany
irradiator	Gammacell 40, AECL, Mississauga, Canada
laminar airflow cabinet	Heraeus
magnetic stirrer	Ika Labortechnik, Staufen, Germany
PCR-machine	Biometra, Goettingen, Germany
pH-meter	Inolab, Weilheim, Germany
pipettes	Gilson, Middleton, WI, USA
power supply	Amersham Pharmacia, Piscataway, NJ, USA
real-time PCR machine	CFX96 Real Time System, BIO-RAD, Hercules, CA, USA
vacuum pump	KNF Neuberger, Munzingen, Germany
vortex-Genie2	Scientific Industries, Bohemia, NY, USA

water bath Grant Instruments Ltd., Barrington Cambridge,  
UK

### 6.1.2 Consumables

Disposable syringe filter (0.2 + 0.45 $\mu\text{m}$ )	Nalgene Nunc Int., Rochester, NJ, USA
Disposable injection needle (26 G x 1/2")	Terumo Medical Corporation, Tokyo, Japan
Disposable syringe (1+5 ml) Reaction	Braun, Melsungen, Germany
reaction container 5 ml (FACS)	BD, Franklin Lakes, NJ, USA
reaction container 15 ml and 50 ml	Greiner, Frickenhausen, Deutschland
BD Microtainer	BD, Franklin Lakes, NJ, USA
DuoSet mFlt3L ELISA	R&D Systems, MN, USA

### 6.1.3 Chemicals

Unless stated otherwise, chemicals were purchased from Merck (Darmstadt, Germany), Roth (Karlsruhe, Germany) or Sigma-Aldrich (St. Louis, MO, USA). All buffers and solutions were prepared using double distilled water.

### 6.1.4 Buffer and media

ACK:	8.29 g $\text{NH}_4\text{Cl}$
	1 g $\text{KHCO}_3$
	37.2 mg $\text{Na}_2\text{EDTA}$
	$\text{H}_2\text{O}$ ad 1 L
	pH 7.4

CFSE-staining buffer:	PBS 0.03% FCS
Cresol red buffer:	250 mM KCl 50 mM Tris-HCl (pH 8.3) 43% Glycerol 2 mM Cresol red 7.5 mM MgCl <sub>2</sub>
FACS buffer:	PBS 2% FCS 0.01% NaN <sub>3</sub>
Flt3L medium:	RPMI 1640 10% FCS 500 mM β-mercaptoethanol 100 U/ml Penicillin 100 g/ml Streptomycin 5 ml Glutamin 200 ng/ml Flt3L
GM-CSF medium:	IMDM 10% FCS 500 mM β-mercaptoethanol 100 U/ml Penicillin 100 g/ml Streptomycin 5 ml Glutamin 10 ml GM-CSF

HBSS:	137 mM NaCl
	5.4 mM KCl
	0.25 mM Na <sub>2</sub> HPO <sub>4</sub>
	0.1 g glucose
	0.44 mM KH <sub>2</sub> PO <sub>4</sub>
	1.3 mM CaCl <sub>2</sub>
	1.0 mM MgSO <sub>4</sub>
	4.2 mM NaHCO <sub>3</sub>
HBSS-EDTA:	HBSS
	8% FCS
	10 mM EDTA
	10 mM HEPES
PBS:	137 mM NaCl
	2.7 mM KCl
	10 mM Na <sub>2</sub> HPO <sub>4</sub>
	pH 7.4
50x TAE buffer:	242 g Tris-HCl
	57.1 ml 100% acetic acid (v/v)
	100 ml 0.5 M EDTA (pH 8.0)
	H <sub>2</sub> O ad 1 L
10x Gitocher:	670 mM Tris pH 8.8
	166 mM NH
	65 mM MgCl <sub>2</sub>

0.1% gelatin

1x Gitocher buffer: 5  $\mu$ l 10x Gitocher buffer  
 2.5  $\mu$ l 10% Triton X-100 (v/v)  
 0.5 $\mu$ l  $\beta$ -mecaptoethanol  
 3  $\mu$ l proteinase K (10 mg/ml)  
 39  $\mu$ l H<sub>2</sub>O

### 6.1.5 Antibodies

Antibodies and fluorochrome linked Streptavidin used for flow cytometry:

epitope	conjugate	clone	manufacturer
B220	Pacific Blue	RA3-6B2	eBioscience
	PE	RA3-6B2	BD
	PerCP	RA3-6B2	BioLegend
Bim	unlabeled	C34C5	Cell Signaling
BrdU	FITC		BD
CD3	biotin	145-2C11	BD
	FITC	145-2C11	eBioscience
	PE	145-2C11	eBioscience
	PerCP	145-2C11	BD
CD4	APC	RM4-5	eBioscience
	FITC	H129.19	BD
	PE	GK1.5	BD
	Pe-Cy7	GK1.5	eBioscience
	PerCP	RM4-5	BD
CD5	bio	53-7.3	BD
CD8	APC	53-6.7	eBioscience
	APC-Cy7	53-6.7	eBioscience

Continued on the next page.

<b>epitope</b>	<b>conjugate</b>	<b>clone</b>	<b>manufacturer</b>
	BV	53-6.7	BioLegend
	PE	53-6.7	BD
	PeCy7	53-6.7	eBioscience
CD9	FITC	MZ3	BioLegend
CD11b	APC-eFlour780	M1/70	eBioscience
CD11c	APC	N418	eBioscience
	PB	N418	eBioscience
	PeCy7	N418	BioLegend
CD16/32	unlabeled	2.4G2	BD
CD19	APC	1D3	BD
	biotin	1D3	BD
	PE	1D3	BD
	Pe-Cy7	1D3	BD
	PerCP	1D3	BD
CD21/35	PE	7G6	BD
CD23	APC	B3B4	BioLegend
CD24	APC	M1/69	BioLegend
CD40	APC	1C10	eBioscience
CD43	Biotin	S7	BD
	FITC	S7	BD
CD44	PE	IM7	eBioscience
CD45	Brilliant Violet	30-F11	BioLegend
	PE	30-F11	eBioscience
	PerCP	30-F11	BD
CD45.1	APC	A20	eBioscience
	bio	A20	BD
	FITC	A20	eBioscience

Continued on the next page.

<b>epitope</b>	<b>conjugate</b>	<b>clone</b>	<b>manufacturer</b>
	Pacific Blue	A20	BioLegend
	PE	A20	eBioscience
CD45.2	FITC	104	BioLegend
	APC	104	BioLegend
CD62L	APC	MEL-14	BD
CD64	APC	X54-5/7.1	BioLegend
CD69	PE	H1.2F3	BD
CD86	PE	GL-1	eBioscience
	PerCP	GL-1	BioLegend
CD90.1	PerCP	OX-7	BD
CD103	Brilliant Violet	M290	BD Horizon
	PE	M290	BD
CD115	APC	AFS98	eBioscience
	PeCy7	AFS98	eBioscience
CD135	PE	A2F10	eBioscience
CD161c	PE	PK136	BD
CD172a	APC	P84	BD
cl. Casp. 3	FITC	C92-605	BD
	unlabeled	D3E9	Cell Signaling
Dll4	PE	HMD4-1	BioLegend
EpCam (CD326)	APC	G8.8	BioLegend
ESAM	PE	1G8	eBioscience
F4/80	PE	BM8	eBioscience
	PeCy7	BM8	eBioscience
Fas	FITC	Jo2	Pharmingen
GL-7	PB	GL-7	eBioscience

Continued on the next page.

<b>epitope</b>	<b>conjugate</b>	<b>clone</b>	<b>manufacturer</b>
goat a-rabbit	PE		Life Technologies
Gr1	PE	RB6-8C5	BD
IgD	PB	11-26	eBioscience
	PE	11-26c.2a	BioLegend
IgM	PeCy7	II/41	eBioscience
IL-12 (p40/p70)	PE	C15.6	BD Pharmingen
KI67	PE	B56	BD Pharmingen
LAMP-1	PeCy7	1D48	BioLegend
Langerin	FITC	929F3.01	Dendritics
Ly6C	FITC	AL-21	BD
Ly6G	BV	1A8	BioLegend
	APC	1A8	BD
MHCII	APC	M5/114.15.2	eBioscience
	FITC	M5/114.15.2	BioLegend
	PE	M5/114.15.2	eBioscience
	PerCP	M5/114.15.2	BioLegend
PDC-TREM	PE	4A6	BioLegend
PDCA-I	APC	129c1	BioLegend
Siglec-H	APC	551	BioLegend
	FITC	551	BioLegend
	PerCP	551	BioLegend
Streptavidin	APC-Cy7		CALTAG
	PB		BioLegend
	PeCy7		eBioscience
	PerCP		BD
V-a2	APC	B20.1	eBioscience
V-b5	PE	MR9-4	BD

Antibodies used for Western-Blot analyses:

epitope	clone	isotype	manufacturer
Bim	C43C5	Rabbit IgG	Cell Signaling
GAPDH	14C10	Rabbit IgG	Cell Signaling

Anti-rabbit, HRP conjugated antibodies were purchased from Jackson Immuno-Research Laboratories (West Grove, PA, USA).

### 6.1.6 Oligonucleotides, peptides and proteins

All oligonucleotides were purchased at MWG-Biotech AG (Ebersberg, Germany). Ovalbumin protein grade VII was bought from Sigma-Aldrich (St. Louis, MO, USA).

target	primer name	sequence	probe
Ppef2	Ppef2_ex._11_fw	TTCTGTCACAACCGCAAGG	16
	Ppef2_ex._12_rv	TCTGTTGCTGCCAACTTCAT	
Ppef2	Ppef2_ex._2_fw	AGGAGGCGATGTACCTGGA	56
	Ppef2_ex._3_rv	CAAGGTAGCTGAAGAATTC- ATGG	
Ppef2	Ppef2_ex._4_fw	CTTCCTGACCATGCCACTG	31
	Ppef2_ex._5_rv	TATCGAGCATGGAGCTGT- TG	
CD11c	CD11c_fw	CCAGTTGGAGCTTCCAGT- AAA	46
	CD11c_rv	CCTTTTCTGAGGTTGAGA- AGTTAAG	

Continued on the next page.

target	primer name	sequence	probe
Trim2	Trim2_fw	TTTCCATAATCACTCTGTC-	12
	Trim2_rv	AAGGT CCATTGGAGCCAAACTTCA	
Dll4	Dll4_fw	AGGTGCCACTTCGGTTACAC	106
	Dll4_rv	GGGAGAGCAAATGGCTGATA	
HPRT	HPRT_fw	TCCTCCTCAGACCGCTTTT	95
	HPRT_rv	CCTGGTTCATCATCGCTAA- TC	
Frt site	5' FRT_fw	AGGCGCATAACGATAACCACGAT	
	5' FRT_rv	CCACAACGGGTTCTTCTGTT	
Ppef2	Ppef2_WT_fw	TAGTGCTCGCCAAGTTGAGA	
	Ppef2_WT_rv	TAACCCCTACCCCTCTGCTT	

### 6.1.7 Mouse strains

All mice except the H2-K<sup>bm1</sup> mice were bred and kept in the Institute for Immunology at the LMU Munich. H2-K<sup>bm1</sup> mice were bred and kept in the *Institut für Medizinische Mikrobiologie, Immunologie und Hygiene* at the TU munich, where the experiments with those animals were conducted.

#### C57BL/6

C57BL/6 mice were in-house bred as inbred line for several generations in the Institute for Immunology at the LMU Munich. Mice are Ppef2<sup>+/+</sup> and were used for breedings and as controls for Ppef2<sup>-/-</sup> mice.

#### Ly5.1

Ly5.1 mice express the Ly5.1 allele which serves as congenic marker and were kept on a C57BL/6 background.

**Ppef2<sup>-/-</sup>**

Alleles targeting Protein phosphatase with EF-hands 2 (Ppef2) and leading to a complete knockout were produced for the EUCOMM and EUCOMMTools projects by Wellcome Trust Sanger Institute (WTSI) [102]. Embryonic stem cells were purchased at EUCOMM and microinjection in C57BL/6 oocytes was performed by the Transgenic Core Facility at the MPI of Molecular Cell Biology and Genetics in Dresden. Chimeric mice were further crossed with C57BL/6 mice.

**OT-I**

This mouse strain carries a transgenic T cell receptor specific for the ovalbumin-derived peptide SIINFEKL that is presented to CD8<sup>+</sup> T cells in the context of H2-K<sup>b</sup> [167]. The T cell receptor of these mice uses the Vβ2 and the Vβ5 segments and T cells can be visualized using mAb directed against these two segments. For identification of OT-I cells in transfer experiments animals were either crossed to the congenic CD45.1 or CD90.1 strain.

**H2-K<sup>bm1</sup>**

The bm1 mutation of the H2-K<sup>b</sup> gene contains 7 nucleotide differences resulting in amino acid substitutions at codon 152 (glutamate to alanine), codon 155 (arginine to tyrosine) and codon 156 (leucine to tyrosine). This results in a failure to present the OVA peptide SIINFEKL via MHCI [119].

## 6.2 Methods

### 6.2.1 Immunological and cell biology methods

#### 6.2.1.1 Generation of BMDCs

BMDCs were either generated by addition of GM-CSF, or by addition of Flt3L to bone marrow cells. In both cases bone marrow was isolated as described in “Harvesting of blood and organs and single cell preparation” on page 74.

For GM-CSF BMDC cultures  $10^7$  cells were plated in 10 ml of GM-CSF containing medium (20 ng/ml GM-CSF) in a 100 mm plate and cultured under 37°C and 5% CO<sub>2</sub> conditions. At day 3 of the culture, cells were harvested with Trypsin, counted, and again plated at a density of  $5 \cdot 10^6$  cells in a 10 mm plate in 10 ml of GM-CSF medium. For analysis, cells were harvested at day 8 of the culture with cold PBS.

For Flt3L cultures  $3 \cdot 10^6$  bone marrow cells were cultured with 2 ml Flt3L medium per well of a non-surface-treated 24 well plate. For analysis of Flt3L generated DCs, cells were harvested at day 8 with cold PBS.

Mature BMDCs were obtained by stimulation overnight with 2 µg/ml lipopolysaccharide (LPS, Sigma-Aldrich), 1 µg/ml Flagellin, 2.5 µg/ml Poly I:C, 1 µg/ml Pam3CSK4, 2.5 µg/ml CLO97, or 100 µg/ml antiCD40 respectively. To obtain higher percentages of matured BMDCs, antiCD40 stimulus (100 µg/ml) was combined with either TNFα (10 ng/ml), or LPS (2 µg/ml).

#### 6.2.1.2 Harvesting of blood and organs and single cell preparation

Animals were sacrificed either by CO<sub>2</sub> or by cervical dislocation after they had been sedated using Isoflurane. Organs were removed using scissors and fine tweezers and put into phosphate buffered saline (PBS) on ice. Blood was flushed out of lungs before by disruption of the aorta followed by injection of cold PBS in the right ventricle. Spleen, thymus, lymph nodes and lungs were then digested with DNase I (0.2 mg/ml) and Liberase (0.65 Wuensch units/ml, both Roche) for 30 min at 37°C. Afterwards the organs were passed through a 100 µm cell strainer, washed once with cold PBS and red blood cells were lysed using ACK buffer for 2 min at room temperature. Cells were washed once again and counted using CASY-counter (OMNI life science) and used for further analysis or experiments.

To analyze cells of the lamina propria, colon was taken from a mouse, fecal

content removed, the colon opened longitudinally and cut into approximately 5 mm big pieces. The pieces were then incubated with HBSS-EDTA for 10 min on a shaker at 37°C, the supernatant, containing epithelial cells, was discarded and gut parts were washed twice with ice-cold PBS. Afterwards, the colon was digested once for 30 min and then twice for 20 min with a mixture of Collagenase IV (157 Wuensch units/ml, Worthington), DNase I (0.2 mg/ml) and Liberase (0.65 Wuensch units/ml, both Roche), the supernatant was collected after each digestion and the cells were washed once with PBS.

Cells from all three digestions were combined and immune cells enriched using gradient centrifugation. To this end, cells were resuspended in 40% Percoll and this solution was overlayed onto a 80% Percoll solution. This was centrifuged for 20 min at 1800 rpm and 4°C without break. Cells at the interphase were collected, washed once and used for further analysis.

For analysis of dermal and epidermal cells ears were removed. The dorsal and ventral layers were separated with fine forceps and incubated dermal face down in 2 U/ml of Dispase II (Roche) in HBSS in 24 well plate for 90 min at 37°C. Skin sheets were separated into dermis and epidermis with fine forceps in cold PBS. Epidermal sheets were further incubated for 2 hours at 37°C in HBSS with 157 U/ml of collagenase IV (Worthington) and 10% FCS in 24 well plate. Dermal sheets were digested for 2 hours at 37°C in a solution containing 0.5 mg/ml of DNase I, 2.7 mg/ml of Collagenase XI, 27 µg/ml of Hylaronase VI and 10 mM of Hepes in RPMI.

The suspensions were passed through a cell strainer and the sheets were mashed on the cell strainer to obtain a homogeneous cell suspension. The cells were washed and counted. They were then stained for flow cytometric analyses.

Isolation of liver cells was carried out by mashing the organ through a 100 µm mesh in PBS. Afterwards, mononuclear cells were enriched by applying a gradient using Lymphoprep (STEMCELL Technologies). Hepatocytes and other cells were cleared out and positively enriched cell fraction was further used for counting and stainings.

For the isolation of bone marrow the terminal parts of femurs and tibiae were cut open and the bone marrow was flushed out with needle and syringe using medium containing 10% FCS. Red blood cells were lysed for 2 min in ACK buffer and the cell suspension was passed over a cell strainer to remove debris. Cells

were subsequently subjected to cell culture, or frozen for future use in BMDC medium supplemented with 10% extra FCS and 10% dimethyl sulfoxide (DMSO) at  $-80^{\circ}\text{C}$ .

### 6.2.1.3 Flow Cytometry staining

For flow cytometric analysis  $2 \cdot 10^6$  cells were used per staining in a FACS acquisition tube. Cells were washed once with 200  $\mu\text{l}$  FACS buffer and then stained for 20 min at  $4^{\circ}\text{C}$  in the dark in 100  $\mu\text{l}$  of antibody mix in FACS buffer. Each antibody has been titrated for optimal use. After the incubation cells were washed once with 200  $\mu\text{l}$  FACS buffer and either directly acquired at the FACS, or fixed for overnight storage using FACS buffer containing 2% paraformaldehyde. Cells that have been stained with a biotinylated mAb were stained in a second step with a fluorescently labeled streptavidin, also in a volume of 100  $\mu\text{l}$  at  $4^{\circ}\text{C}$  in dark for additional 20 min.

For intracellular stainings cell were fixed and permeabilized after they have been stained for all extracellular markers. For the staining of cleaved caspase-3 cells were washed once and then resuspended in 200  $\mu\text{l}$  4% PFA for 15 min at room temperature in the dark. After washing twice with 1x fixation/permeabilisation buffer (BD) cells were blocked for 10 min with an anti CD16/32 antibody (Fc block) and 0.1% goat serum at  $4^{\circ}\text{C}$ . After 10 min of blocking, 100  $\mu\text{l}$  anti cleaved caspase-3 antibody was added and cells were incubated for 30 min at  $4^{\circ}\text{C}$ . Unbound antibody was washed away and cells were incubated with 100  $\mu\text{l}$  fluorochrome conjugated secondary antibody at  $4^{\circ}\text{C}$  for 30 min. Afterwards cells were washed once and acquired at the FACS.

Acquisition was performed using a FACSCanto II. Cell sorting was performed at FACS Aria (all BD). Data analysis was performed using FlowJo version 8 and 9 (TreeStar, Ashland, OR, USA).

Flow cytometric analyses as performed by the Centre d'Immunophénomique (CI-PHE) were performed in two different panels to identify various cell population with the markers listed below. Following cell populations were defined as possible dump population for gating out:

<b>dump populations</b>	<b>marker</b>
Eosinophils	CD5- CD19- CD11b+ MHCII- SSChi
Neutrophils	CD5- CD19- Eosino- Macro- CD11b+ Ly6Cint

Continued on the next page.

<b>dump populations</b>	<b>marker</b>
Monocytes	CD11b+ Ly6G- Ly6Chi
pDC	CD5- CD19- Eosino- Macro- Mono- CD11clo CD317+ CD45R+ Ly6C+
Macrophages	CD11bint Ly6G- Ly6C- F4/80hi

The following markers were used by CIPHE to define populations of the spleen in two different staining panels:

<b>population</b>	<b>marker</b>
Eosinophils (Panel 4)	CD5- CD19- CD11b+ MHCII- SSChi
Infl. DCs	CD5- CD19- Eosino- Macro- Mono- pDC- CD11c+ MHCII+ CD64+
Stage I (% pDC)	CD5- CD19- Eosino- Macro- Mono- CD11clo CD317+ CD45R+ Ly6C+ CD4- CD8-
gd T cells	CD161- Ly6G- CD317- CD5+ CD3+ TCRd+
CD4 shedding [CD4 CD44-CD62L- (Shed- ding)]	CD161- Ly6G- CD317- CD5+ CD3+ TCRd- CD4+ CD44- CD62L-
Eosinophils (Panel 1)	CD11b+ Ly6G- Ly6Clo SSChi
CD4 Naive	CD161- Ly6G- CD317- CD5+ CD3+ TCRd- CD4+ CD44- CD62L+
Cellularity	-
B1 B cells	CD161- Ly6G- CD317- CD19+ MHCII+ CD5+
Xcr1 cDCs	CD5- CD19- Eosino- Macro- Mono- pDC- CD11c+ MHCII+ CD64- CD24+ CD172a- CD8a+
IgDlo B2 B cells	CD161- Ly6G- CD317- CD19+ MHCII+ CD5- IgDlo
CD8 naive	CD161- Ly6G- CD317- CD5+ CD3+ TCRd- CD8+ CD44- CD62L+
gd Naive	CD161- Ly6G- CD317- CD5+ CD3+ TCRd+ CD44- CD62L+

Continued on the next page.

<b>population</b>	<b>marker</b>
CD4- CD8+ (%pDCs)	CD5- CD19- Eosino- Macro- Mono- CD11clo CD317+ CD45R+ Ly6C+ CD4- CD8+
CD8 shedding [CD8 CD44-CD62L- (Shed- ding)]	CD161- Ly6G- CD317- CD5+ CD3+ TCRd- CD8+ CD44- CD62L-
gd shedding [gd cd44- cd62l- (Shedding)]	CD161- Ly6G- CD317- CD5+ CD3+ TCRd+ CD44- CD62L-
NKT	CD161+ Ly6G- CD317- CD5+
IgDhi B2 B cells	CD161- Ly6G- CD317- CD19+ MHCII+ CD5- IgDhi
CD8	CD161- Ly6G- CD317- CD5+ CD3+ TCRd- CD8+
CD4 CM	CD161- Ly6G- CD317- CD5+ CD3+ TCRd- CD4+ CD44+ CD62L+
NK CD11b+Ly6C+	CD161+ Ly6G- CD317- CD5- CD11b+ Ly6C+
CD4 EM	CD161- Ly6G- CD317- CD5+ CD3+ TCRd- CD4+ CD44+ CD62L-
NK	CD161+ Ly6G- CD317- CD5-
CD8 CM	CD161- Ly6G- CD317- CD5+ CD3+ TCRd- CD8+ CD44+ CD62L+
B cells	CD161- Ly6G- CD317- CD19+ MHCII+
Viability	-
B2 B cells	CD161- Ly6G- CD317- CD19+ MHCII+ CD5-
ab T cells	CD161- Ly6G- CD317- CD5+ CD3+ TCRd-
CD4	CD161- Ly6G- CD317- CD5+ CD3+ TCRd- CD4+
CD11b+ DCs	CD5- CD19- Eosino- Macro- Mono- pDC- CD11c+ MHCII+ CD64- CD24+/- CD172a+ CD11b+
Imm CD11b+ DCs	CD5- CD19- Eosino- Macro- Mono- pDC- CD11c+ MHCII+ CD64- CD24+/- CD172a+ CD11b+ CD117+

Continued on the next page.

<b>population</b>	<b>marker</b>
Imm Xcr1 DCs	CD5- CD19- Eosino- Macro- Mono- pDC- CD11c+ MHCIIlo CD64- CD24+ CD172a- CD8a+ CD117+
gd CM	CD161- Ly6G- CD317- CD5+ CD3+ TCRd+ CD44+ CD62L+
CD11b-type DC	CD11b- Ly6G- CD11b- CD317- CD11c+ MHCII+ CD11b+
NK CD11b-Ly6C+	CD161+ Ly6G- CD317- CD5- CD11b- Ly6C+
Stage III (%pDCs)	CD5- CD19- Eosino- Macro- Mono- CD11clo CD317+ CD45R+ Ly6C+ CD4+ CD8-
gd EM	CD161- Ly6G- CD317- CD5+ CD3+ TCRd+ CD44+ CD62L-
Stage II (%pDC)	CD5- CD19- Eosino- Macro- Mono- CD11clo CD317+ CD45R+ Ly6C+ CD4+ CD8+
CD8 EM	CD161- Ly6G- CD317- CD5+ CD3+ TCRd- CD8+ CD44+ CD62L-
Mat Xcr1 DC	CD5- CD19- Eosino- Macro- Mono- pDC- CD11c+ MHCIIlo CD64- CD24+ CD172a- CD8a+ CD117-
Mat CD11b+ DC	CD5- CD19- Eosino- Macro- Mono- pDC- CD11c+ MHCII+ CD64- CD24+/- CD172a+ CD11b+ CD117-
Xcr1 DC	CD5- CD19- Eosino- Macro- Mono- pDC- CD11c+ MHCII+ CD64- CD24+ CD172a- CD8a+
Macrophages	CD5- CD19- CD24+ CD172a+ CD64+
cDC (Panel 4)	CD5- CD19- Eosino- Macro- Mono- pDC- CD11c+ MHCII+
Neutrophils (Panel 1)	CD11b+ Ly6G+
Neutrophils (Panel 4)	CD5- CD19- Eosino- Macro- CD11b+ Ly6Cint
Monocytes	CD5- CD19- Eosino- Macro- CD11b+ Ly6C+
NK CD11b-Ly6C-	CD161+ Ly6G- CD317- CD5- CD11b- Ly6C+

Continued on the next page.

---

population	marker
Monocytes	CD11b+ Ly6G- Ly6Chi
pDC (Panel 1)	CD11b- Ly6G- Ly6Chi CD317+
pDC (Panel 4)	CD5- CD19- Eosino- Macro- Mono- CD11clo CD317+ CD45R+ Ly6C+
Other Mac	CD11bhi Ly6G- Ly6C- F4/80hi
RP Macrophages	CD11bint Ly6G- Ly6C- F4/80hi

---

#### 6.2.1.4 Measurement of $\beta$ -galactosidase (**lacZ**) expression and activity

Measurement of the expression of the bacterial  $\beta$ -galactosidase gene (**lacZ**) was carried out by using the FluoReporter **lacZ** Flow Cytometry Kit (Thermo Fisher Scientific Inc.) according to the manufacturers protocol. Therefore the activity of the enzyme was measured by adding Fluorescein isothiocyanate (FITC) coupled substrate (fluorescein di-V-galactoside (FDG)) for 2 min at 37°C and stopping of the reaction by addition of cold staining medium. Followed by normal surface antibody staining samples were analyzed using a FACSCanto II.

#### 6.2.1.5 Enzym-linked immunosorbent assay (**ELISA**) for **Flt3L**

Blood of animals was taken by cardiac puncture after sacrificing the mice by cervical dislocation and directly transferred into microtainer tubes (BD). After incubation for 30 min at room temperature blood coagulated and was spun down 1.5 min at 8000 rpm. Serum was stored at -20°C until use.

Serum was diluted 1:20 with PBS and ELISA was carried out according to the manufacturers protocol (DuoSet mFlt3L ELISA, R&D Systems, Minneapolis, USA).

#### 6.2.1.6 Generation of bone marrow chimeras

To generate bone marrow chimeras, recipient mice were irradiate with two separate doses of 550 rad using a Cesium source (Gammacell 40, AECL, Mississauga, Canada). Irradiated animals were reconstituted with  $5 \cdot 10^6$  bone marrow cells, 1:1 mixed from Ly5.1<sup>+</sup> and Ly5.2<sup>+</sup> bone marrow. To prevent infection, animals received 1.2 g/l neomycin in water ad libitum for 4 weeks. Animals were analyzed 8 to 10 weeks after reconstitution.

### 6.2.1.7 Magnetic cell sorting

To purify cell populations based on surface marker expression magnetic cell sorting (MACS, Miltenyi Biotec) was employed. This technique uses antibodies reactive to certain surface antigens and coupled to magnetic beads. After cells have been incubated with these antibodies for the appropriate amount of time they can be applied to a column that is placed in a paramagnetic field. Labeled cells are retained on the column, while unlabeled cells are washed away. Columns are rinsed three times and the eluted fraction can be collected.

This technique was actually employed when CD8<sup>+</sup> T cells were purified for adoptive transfer experiment (CD8<sup>+</sup> T cell Isolation Kit, negative selection), for depletion of T and B cells before sorting of DCs (biotin conjugated antibodies against CD3 and CD19 and anti-biotin microbeads), or for the enrichment of DCs (CD11c microbeads). All procedures were performed according to the manufacturers instructions.

### 6.2.1.8 Adoptive T cell transfer

To transfer transgenic T cells into experimental animals spleens from transgenic animals were taken and the respective T cells purified using a CD8 T cell enrichment kit (see 6.2.1.7). Purity of the cell suspension was checked using anti-CD8 antibody in combination with an appropriate V $\beta$  antibody specific for the respective TCR.

If not stated otherwise 0.5·10<sup>6</sup> CD8<sup>+</sup> T cells were transferred intravenously into the syngenic and sex-matched mice. Transferred cells could be followed by analyzing the congenic markers CD45.1 or CD90.1.

### 6.2.1.9 Immunofluorescence staining

Organs were directly embedded in Tissue-Tek OCT compound (Sakura Finetek, Zoeterwoude, The Netherlands) and snap frozen in liquid nitrogen. Sections of 5-7  $\mu$ m were cut using a cryostat instrument (Leica Microsystems, Wetzlar, Germany), fixed for 20 min at -20 °C using acetone and subsequently dried over night in the dark.

Before staining the slides were adjusted to room temperature and rehydrated for 15 min with PBS containing 0.25% bovine serum albumin (BSA). To minimize unspecific binding the slides were then incubated with PBS, 0.25% BSA containing 10% mouse serum.

Staining was performed in a moist chamber in the dark for 30 min at room tem-

perature. After staining the slides were washed and cover slides put on. The slides were analyzed using a BX41 microscope equipped with a F-view II camera and cellF software (all from Olympus, Hamburg, Germany).

#### 6.2.1.10 Cytokine bead array

Blood of animals was taken via puncturing the heart, the blood was transferred into a microtainer tube (BD, Franklin Lakes, NJ, USA) and incubated at room temperature for 30 min, so that the blood could coagulate. Afterwards the tube was centrifuged at 8000 rpm for 1.5 min at room temperature and the serum was frozen at  $-20^{\circ}\text{C}$  until use.

To measure up to six different cytokines in the same amount of serum the BD Cytokine Bead Array mouse inflammation kit was employed. Serum samples were titered in the beginning to ensure an optimal concentration for the assay. The assay procedure was then performed according to manufacturers instructions.

Acquisition of the samples was performed using a FACSCantoII. Results were analyzed using FCAP Array Software (Soft Flow Inc.).

#### 6.2.1.11 DC vaccination

DCs of Ppef2<sup>+/+</sup> or Ppef2<sup>-/-</sup> mice were *in vivo* expanded for up to ten days by subcutaneously injecting a Flt3L secreting tumor cell line. After *in vivo* expansion, DCs were magnetically purified by using a DC isolation kit (see 6.2.1.7) and  $1.5 \cdot 10^5$  SIINFEKL pulsed DCs were transferred into K<sup>bm1</sup> recipient mice. One day later, recipient mice received congenitally marked (CD45<sup>+</sup>) OT-I cells intravenously. Three days after adoptive T cell transfer mice were analyzed for T cell proliferation by flow cytometry. Experiments were carried out by the group of Veit Buchholz/Dirk Busch at the *Institut für Medizinische Mikrobiologie, Immunologie und Hygiene* at the TU munich.

### 6.2.2 Molecular biology

#### 6.2.2.1 Gel electrophoresis

To visualize DNA fragments and to separate them according to their size they were applied to gelelectrophoresis on an agarose gel. Gel was prepared by dissolving 0.8-2% agarose in TAE buffer, depending of the fragment size that was supposed to be visualized. To estimate the size of the fragments either a 100bp or a 1kb ladder was used (New England Biolabs, Ipswich, MA, USA). PCR fragments either already contained loading buffer or a buffer consisting of 10% glycerol and xylene cyanol

FF was added directly before applying the sample to the gel. The DNA samples were visualized using ethidium bromide (0.5 µg/ml) that was added to the gel followed by examination with UV light (312 nm, Intas, Goettingen, Germany).

#### **6.2.2.2 Isolation of genomic DNA**

To isolate genomic DNA for genotyping 2-5 mm of mouse tail tip was cut, put into 50 µl 1x Gitocher buffer, and incubated at 55 °C for 6h. Proteinase K was inactivated at 95 °C for 5 min.

#### **6.2.2.3 Isolation of total Ribonucleic acid (RNA)**

Total RNA was isolated by resuspending a pellet of up to 10<sup>7</sup> cells in 1 ml of Trizol. After incubation for 10 min on ice 300 µl chloroform was added and incubated another 15 min on ice. Suspension was spun down 10 min at 1300 rpm in a cooled tabletop centrifuge. The upper aqueous phase was transferred in a new 2 ml reaction tube and 2 volumes of chloroform were added on top. After centrifugation for 10 min under the conditions mentioned before the aqueous phase was transferred into a new 2 ml reaction tube. To precipitate the RNA 1 volume of isopropanol and, for better visualization of the RNA pellet, 1 µl of Glycoblue was added. Samples were then incubated for at least 2 h at -80 °C or overnight at -20 °C. After centrifugation for 30 min at 1300 rpm in a cooled tabletop centrifuge the supernatant was removed carefully and pellet was washed by adding 400 µl 70% ethanol followed by centrifugation for 10 min. To dry the pellet the supernatant got poured off and the pellet air dried. According to the expected final RNA concentration the pellet got resuspended in an appropriate amount of water and concentration was determined by spectrophotometry (NanoDrop 1000, Thermo Fischer Scientific, Waltham, Massachusetts, USA).

#### **6.2.2.4 cDNA synthesis**

Equal amounts of RNA were used to generated cDNA using the QuantiTect Reverse Transcription Kit (Qiagen, Venlo, Netherlands) according to the manufacturers protocol.

#### **6.2.2.5 Polymerase Chain Reaction (PCR)**

For genotyping of Ppof2 deficient mice PCRs were performed with the primers listed in Oligonucleotides, peptides and proteins on page 71 with small amounts

of genomic DNA isolated from tail biopsies. The reaction mix contained

Cresol red buffer with MgCl <sub>2</sub>	6 $\mu$ l
forward primer (100 pmol/ $\mu$ l)	0.2 $\mu$ l
reverse primer (100 pmol/ $\mu$ l)	0.2 $\mu$ l
dNTPs (2.5 mM)	2 $\mu$ l
PANScript DNA Polymerase (5 U/ml)	0.25 $\mu$ l
H <sub>2</sub> O	20.35 $\mu$ l
template DNA	1 $\mu$ l

PCR reactions were performed with a T3 Thermocycler (Biometra). After an initialization step of 5 min at 94 °C the samples were amplified for 35 cycles beginning with a denaturation step at 94 °C for 30 sec followed by an annealing step of 58 °C for another 30 sec and ended with extension/elongation step for 45 sec at 72 °C. After the 35 cycles a final elongation step for 5 min at 72 °C was performed and amplified fragments were stored at 4 °C until loading on a 1.8% agarose gel.

#### 6.2.2.6 qPCR

qPCRs were performed on a CFX96 Real Time System (BIO-RAD) using the LightCycler 480 Probes Master kit (Roche) according to the manufacturer's protocol. The primers and probes used are depicted in the section "Oligonucleotides, peptides and proteins" on page 71. Expression levels were, unless stated otherwise, normalized to HPRT and relative quantification was calculated using either the  $2^{-\Delta C^t}$  method [104, 105], or the  $\Delta\Delta C^t$  method.

#### 6.2.2.7 mRNA-Sequencing

Samples for mRNA-Sequencing were FACS sorted of spleens of Ppof2<sup>+/+</sup> and Ppof2<sup>-/-</sup> mice. Up to 10<sup>6</sup> sorted cells were resuspended in 1 ml of Trizol and snap frozen in liquid nitrogen. Further sample preparation and mRNA-Sequencing was performed by the lab of Joachim Schultze (Life & Medical Sciences Institute, University of Bonn), as well as the data analysis.

### 6.2.2.8 Western Blot analysis

Cellular protein was purified by washing the cells once with PBS to remove extracellular proteins, pelleted and resuspended at a concentration of  $1 \cdot 10^6$  cells per 15  $\mu$ l of Nonidet P-40 (NP-40) cell lysis buffer in the presence of protease inhibitors (Protease Inhibitor Cocktail P8340 and phenylmethylsulfonyl fluoride (PMSF) (both Sigma-Aldrich). Cells were lysed for 15 min on ice, followed by 5 min. centrifugation at 2500g to remove intact nuclei and insoluble cellular debris. Both, total cell lysates and supernatants were quantified using the QuantiT Protein Assay Kit (Molecular Probes) to determine the exact protein concentration. Equal amounts of protein were then denatured using sodium dodecyl sulfate (SDS) sample buffer at 95 °C for 7 min. and further subjected to SDS Page and Western blot.

Equal amounts of protein were loaded onto a 12-15% SDS gel prepared as described in the Current Protocols in Immunology (Unit 8.9) and separated by gel electrophoresis for 1.5 h at 80-100 V. PageRuler prestained protein ladder (Thermo Scientific, Rockford, IL USA) was loaded as a protein standard. Separated proteins were transferred onto a nitrocellulose membrane (Whatman) using a tank transfer system (BIO-RAD) as described in the Current Protocols in Immunology (Unit 8.10); transfer time was adjusted to 1.5 h at 80 V. Membranes were blocked overnight in PBS supplemented with 0.5% Tween-20 and 5% milk.

After incubation with specific primary and secondary antibodies, membranes were developed using enhanced chemiluminescence (ECL) Western blotting substrate (PerkinElmer Inc., MA, USA) followed by exposure to Amersham Hyperfilm (GE Healthcare). Specific bands were quantified relative to GAPDH as indicated in the figure legends, using the free online tool ImageJ.

### 6.2.3 Statistics

Statistical analysis was performed using PRISM software (GraphPad software, La Jolla, CA, USA). Unless stated otherwise all bar graphs represent mean  $\pm$  standard error of mean (SEM) and significance was analyzed using Student's *t*-test, with \*:  $p < 0.01$  to 0.05, \*\*:  $p < 0.001$  to 0.01 and \*\*\*:  $p < 0.001$ .

---

## References

- [1] M. Chen, Y.-H. Wang, Y. Wang, L. Huang, H. Sandoval, Y.-J. Liu, and J. Wang, “Dendritic cell apoptosis in the maintenance of immune tolerance.,” *Science*, vol. 311, no. 5764, pp. 1160–1164, 2006.
- [2] R. Josien, H. L. Li, E. Ingulli, S. Sarma, B. R. Wong, M. Vologodskaja, R. M. Steinman, and Y. Choi, “TRANCE, a tumor necrosis factor family member, enhances the longevity and adjuvant properties of dendritic cells in vivo.,” *The Journal of Experimental Medicine*, vol. 191, no. 3, pp. 495–502, 2000.
- [3] A. Nopora and T. Brocker, “Bcl-2 controls dendritic cell longevity in vivo.,” *The Journal of Immunology*, vol. 169, pp. 3006–14, sep 2002.
- [4] J. Wang, L. Zheng, A. Lobito, F. K. M. Chan, J. Dale, M. Sneller, X. Yao, J. M. Puck, S. E. Straus, and M. J. Lenardo, “Inherited human caspase 10 mutations underlie defective lymphocyte and dendritic cell apoptosis in autoimmune lymphoproliferative syndrome type II,” *Cell*, vol. 98, pp. 47–58, 1999.
- [5] S. L. Edelman, P. J. Nelson, and T. Brocker, “Comparative promoter analysis in vivo: identification of a dendritic cell-specific promoter module.,” *Blood*, vol. 118, pp. e40–9, sep 2011.
- [6] O. Takeuchi and S. Akira, “Pattern Recognition Receptors and Inflammation,” *Cell*, vol. 140, no. 6, pp. 805–820, 2010.
- [7] T. Kawasaki, T. Kawai, and S. Akira, “Recognition of nucleic acids by pattern-recognition receptors and its relevance in autoimmunity,” *Immunological Reviews*, vol. 243, no. 1, pp. 61–73, 2011.
- [8] R. M. Steinman and Z. A. Cohn, “Identification of a novel cell type in peripheral lymphoid organs of mice. I. Morphology, quantitation, tissue distribution.,” *The Journal of Experimental Medicine*, vol. 137, pp. 1142–1162, 1973.
- [9] R. M. Steinman and Z. a. Cohn, “Identification of a novel cell type in peripheral lymphoid organs of mice. II. Functional properties in vitro.,” *The Journal of Experimental Medicine*, vol. 139, no. 2, pp. 380–397, 1973.
- [10] R. M. Steinman and M. D. Witmer, “Lymphoid dendritic cells are potent stimulators of the primary mixed leukocyte reaction in mice.,” *Proceedings of*

- 
- the National Academy of Sciences of the United States of America*, vol. 75, no. 10, pp. 5132–6, 1978.
- [11] D. Traver, K. Akashi, M. Manz, M. Merad, T. Miyamoto, E. G. Engleman, and I. L. Weissman, “Development of CD8 $\alpha$ -positive dendritic cells from a common myeloid progenitor.,” *Science*, vol. 290, no. 1995, pp. 2152–2154, 2000.
- [12] M. G. Manz, D. Traver, T. Miyamoto, I. L. Weissman, and K. Akashi, “Dendritic cell potentials of early lymphoid and myeloid progenitors,” *Blood*, vol. 97, no. 11, pp. 3333–3341, 2001.
- [13] C. Ardavin, L. Wu, C. L. Li, and K. Shortman, “Thymic dendritic cells and T cells develop simultaneously in the thymus from a common precursor population.,” *Nature*, vol. 362, no. 6422, pp. 761–763, 1993.
- [14] D. K. Fogg, C. Sibon, C. Miled, S. Jung, P. Aucouturier, D. R. Littman, A. Cumano, and F. Geissmann, “A Clonogenic Bone Marrow Progenitor Specific for Macrophages and Dendritic Cells,” *Science*, vol. 311, no. March, pp. 83–88, 2006.
- [15] N. Onai, A. Obata-Onai, M. a. Schmid, T. Ohteki, D. Jarrossay, and M. G. Manz, “Identification of clonogenic common Flt3+ M-CSFR+ plasmacytoid and conventional dendritic cell progenitors in mouse bone marrow.,” *Nature Immunology*, vol. 8, no. 11, pp. 1207–16, 2007.
- [16] K. Liu, G. D. Victora, T. A. Schwickert, P. Guernonprez, M. M. Meredith, K. Yao, F.-F. Chu, G. J. Randolph, A. Y. Rudensky, and M. Nussenzweig, “In vivo analysis of dendritic cell development and homeostasis.,” *Science*, vol. 324, no. 5925, pp. 392–397, 2009.
- [17] S. H. Naik, D. Metcalf, A. van Nieuwenhuijze, I. Wicks, L. Wu, M. O’Keeffe, and K. Shortman, “Intrasplenic steady-state dendritic cell precursors that are distinct from monocytes.,” *Nature Immunology*, vol. 7, no. 6, pp. 663–71, 2006.
- [18] K. L. Lewis, M. L. Caton, M. Bogunovic, M. Greter, L. T. Grajkowska, D. Ng, A. Klinakis, I. F. Charo, S. Jung, J. L. Gommerman, I. I. Ivanov, K. Liu, M. Merad, and B. Reizis, “Notch2 receptor signaling controls functional differentiation of dendritic cells in the spleen and intestine,” *Immunity*, vol. 35, no. 5, pp. 780–791, 2011.
-

- 
- [19] H. Karsunky, M. Merad, A. Cozzio, I. L. Weissman, and M. G. Manz, "Flt3 Ligand Regulates Dendritic Cell Development from Flt3+ Lymphoid and Myeloid-committed Progenitors to Flt3+ Dendritic Cells In Vivo," *The Journal of Experimental Medicine*, vol. 198, no. 2, pp. 305–313, 2003.
- [20] D. Vremec, G. J. Lieschke, A. R. Dunn, L. Robb, D. Metcalf, and K. Shortman, "The influence of granulocyte/macrophage colony-stimulating factor on dendritic cell levels in mouse lymphoid organs.," *The European Journal of Immunology*, vol. 27, pp. 40–44, 1997.
- [21] M. Greter, J. Helft, A. Chow, D. Hashimoto, A. Mortha, J. Agudo-Cantero, M. Bogunovic, E. L. Gautier, J. Miller, M. Leboeuf, G. Lu, C. Aloman, B. D. Brown, J. W. Pollard, H. Xiong, G. J. Randolph, J. E. Chipuk, P. S. Frenette, and M. Merad, "GM-CSF controls nonlymphoid tissue dendritic cell homeostasis but is dispensable for the differentiation of inflammatory dendritic cells.," *Immunity*, vol. 36, pp. 1031–46, jun 2012.
- [22] T. Tamura, P. Taylor, K. Yamaoka, H. J. Kong, H. Tsujimura, J. J. O'Shea, H. Singh, and K. Ozato, "IFN regulatory factor-4 and -8 govern dendritic cell subset development and their functional diversity," *The Journal of Immunology*, vol. 174, no. 5, pp. 2573–2581, 2005.
- [23] K. Hildner, B. T. Edelson, W. E. Purtha, M. Diamond, H. Matsushita, M. Kohyama, B. Calderon, B. U. Schraml, E. R. Unanue, M. S. Diamond, R. D. Schreiber, T. L. Murphy, and K. M. Murphy, "Batf3 deficiency reveals a critical role for CD8 $\alpha$ + dendritic cells in cytotoxic T cell immunity," *Science*, vol. 322, no. 5904, pp. 1097–1100, 2008.
- [24] M. Cella, D. Jarrossay, F. Facchetti, O. Alebardi, H. Nakajima, A. Lanzavecchia, and M. Colonna, "Plasmacytoid monocytes migrate to inflamed lymph nodes and produce large amounts of type I interferon.," *Nature Medicine*, vol. 5, no. 8, pp. 919–923, 1999.
- [25] V. Hornung, S. Rothenfusser, S. Britsch, A. Krug, B. Jahrsdorfer, T. Giese, S. Endres, and G. Hartmann, "Quantitative Expression of Toll-Like Receptor 1-10 mRNA in Cellular Subsets of Human Peripheral Blood Mononuclear Cells and Sensitivity to CpG Oligodeoxynucleotides," *The Journal of Immunology*, vol. 168, no. 9, pp. 4531–4537, 2002.
- [26] A. Krug, A. R. French, W. Barchet, J. A. A. Fischer, A. Dzionek, J. T. Pingel, M. M. Orihuela, S. Akira, W. M. Yokoyama, and M. Colonna, "TLR9-
-

- dependent recognition of MCMV by IPC and DC generates coordinated cytokine responses that activate antiviral NK cell function,” *Immunity*, vol. 21, no. 1, pp. 107–119, 2004.
- [27] A. Blasius, W. Vermi, A. Krug, F. Facchetti, M. Cella, and M. Colonna, “A cell-surface molecule selectively expressed on murine natural interferon-producing cells that blocks secretion of interferon-alpha,” *Blood*, vol. 103, no. 11, pp. 4201–4206, 2004.
- [28] C. Asselin-Paturel, G. Brizard, J.-J. Pin, F. Brière, and G. Trinchieri, “Mouse strain differences in plasmacytoid dendritic cell frequency and function revealed by a novel monoclonal antibody,” *The Journal of Immunology*, vol. 171, no. 12, pp. 6466–6477, 2003.
- [29] M. L. Caton, M. R. Smith-Raska, and B. Reizis, “Notch-RBP-J signaling controls the homeostasis of CD8- dendritic cells in the spleen,” *The Journal of Experimental Medicine*, vol. 204, no. 7, pp. 1653–1664, 2007.
- [30] M. M. Meredith, K. Liu, G. Darrasse-Jeze, a. O. Kamphorst, H. a. Schreiber, P. Guermonprez, J. Idoyaga, C. Cheong, K.-H. Yao, R. E. Niec, and M. C. Nussenzweig, “Expression of the zinc finger transcription factor zDC (Zbtb46, Btbd4) defines the classical dendritic cell lineage,” *The Journal of Experimental Medicine*, vol. 209, no. 6, pp. 1153–1165, 2012.
- [31] A. T. Satpathy, W. Kc, J. C. Albring, B. T. Edelson, N. M. Kretzer, D. Bhattacharya, T. L. Murphy, and K. M. Murphy, “Zbtb46 expression distinguishes classical dendritic cells and their committed progenitors from other immune lineages,” *The Journal of Experimental Medicine*, vol. 209, no. 6, pp. 1135–1152, 2012.
- [32] X. Wu, C. G. Briseño, V. Durai, J. C. Albring, M. Haldar, P. Bagadia, K.-W. Kim, G. J. Randolph, T. L. Murphy, and K. M. Murphy, “<i>Mafb</i> lineage tracing to distinguish macrophages from other immune lineages reveals dual identity of Langerhans cells,” *The Journal of Experimental Medicine*, vol. 213, no. 12, pp. 2553–2565, 2016.
- [33] M. Merad, P. Sathe, J. Helft, J. Miller, and A. Mortha, “The Dendritic Cell Lineage: Ontogeny and Function of Dendritic Cells and Their Subsets in the Steady State and the Inflamed Setting,” *Annual Review of Immunology*, vol. 31, pp. 563–604, jan 2013.

- 
- [34] A. T. Satpathy, X. Wu, J. C. Albring, and K. M. Murphy, “Re(de)fining the dendritic cell lineage.,” *Nature Immunology*, vol. 13, pp. 1145–54, dec 2012.
- [35] A. Mildner and S. Jung, “Development and function of dendritic cell subsets,” *Immunity*, vol. 40, no. 5, pp. 642–656, 2014.
- [36] M. Crowley, K. Inaba, M. Witmer-Pack, and R. M. Steinman, “The cell surface of mouse dendritic cells: FACS analyses of dendritic cells from different tissues including thymus,” *Cellular Immunology*, vol. 118, no. 1, pp. 108–125, 1989.
- [37] D. Vremec, M. Zorbas, R. Scollay, D. J. Saunders, C. F. Ardavin, L. Wu, and K. Shortman, “The surface phenotype of dendritic cells purified from mouse thymus and spleen: investigation of the CD8 expression by a subpopulation of dendritic cells,” *The Journal of Experimental Medicine*, vol. 176, no. 1, pp. 47–58, 1992.
- [38] L. S. Bursch, L. Wang, B. Igyarto, A. Kissenpfennig, B. Malissen, D. H. Kaplan, and K. A. Hogquist, “Identification of a novel population of Langerin+ dendritic cells.,” *The Journal of Experimental Medicine*, vol. 204, no. 13, pp. 3147–56, 2007.
- [39] M.-L. del Rio, J.-I. Rodriguez-Barbosa, E. Kremmer, and R. Förster, “CD103- and CD103+ Bronchial Lymph Node Dendritic Cells Are Specialized in Presenting and Cross-Presenting Innocuous Antigen to CD4+ and CD8+ T Cells,” *The Journal of Immunology*, vol. 178, no. 11, pp. 6861–6866, 2007.
- [40] K. Crozat, R. Guiton, V. Contreras, V. Feuillet, C.-A. Dutertre, E. Ventre, T.-P. Vu Manh, T. Baranek, A. K. Storset, J. Marvel, P. Boudinot, A. Hosmalin, I. Schwartz-Cornil, and M. Dalod, “The XC chemokine receptor 1 is a conserved selective marker of mammalian cells homologous to mouse CD8 $\alpha$ + dendritic cells.,” *The Journal of Experimental Medicine*, vol. 207, no. 6, pp. 1283–92, 2010.
- [41] A. Bachem, E. Hartung, S. Güttler, A. Mora, X. Zhou, A. Hegemann, M. Plantinga, E. Mazzini, P. Stoitzner, S. Gurka, V. Henn, H. W. Mages, and R. A. Kroczeck, “Expression of XCR1 characterizes the Batf3-dependent lineage of dendritic cells capable of antigen cross-presentation,” *Frontiers in Immunology*, vol. 3, no. JUL, pp. 1–12, 2012.
-

- 
- [42] D. Dudziak, A. O. Kamphorst, G. F. Heidkamp, V. R. Buchholz, C. Trumppeller, S. Yamazaki, C. Cheong, K. Liu, H.-W. Lee, C. G. Park, R. M. Steinman, and M. C. Nussenzweig, “Differential Antigen Processing by Dendritic Cell Subsets in Vivo,” *Science*, vol. 315, no. January, pp. 107–112, 2007.
- [43] B. U. Schraml, J. Van Blijswijk, S. Zelenay, P. G. Whitney, A. Filby, S. E. Acton, N. C. Rogers, N. Moncaut, J. J. Carvajal, and C. Reis E Sousa, “Genetic tracing via DNGR-1 expression history defines dendritic cells as a hematopoietic lineage,” *Cell*, vol. 154, no. 4, pp. 843–858, 2013.
- [44] C. Reis e Sousa, S. Hieny, T. Scharton-Kersten, D. Jankovic, H. Charest, R. N. Germain, and A. Sher, “In vivo microbial stimulation induces rapid CD40 ligand-independent production of interleukin 12 by dendritic cells and their redistribution to T cell areas.,” *The Journal of Experimental Medicine*, vol. 186, no. 11, pp. 1819–1829, 1997.
- [45] R. Grumont, H. Hochrein, M. O’Keeffe, R. Gugasyan, C. White, I. Caminschi, W. Cook, and S. Gerondakis, “c-Rel regulates interleukin 12 p70 expression in CD8(+) dendritic cells by specifically inducing p35 gene transcription.,” *The Journal of Experimental Medicine*, vol. 194, no. 8, pp. 1021–32, 2001.
- [46] D. A. Jaitin, E. Kenigsberg, H. Keren-Shaul, N. Elefant, F. Paul, I. Zaretsky, A. Mildner, N. Cohen, S. Jung, A. Tanay, and I. Amit, “Massively parallel single-cell RNA-seq for marker-free decomposition of tissues into cell types.,” *Science*, vol. 343, no. 6172, pp. 776–9, 2014.
- [47] C.-H. Qiu, Y. Miyake, H. Kaise, H. Kitamura, O. Ohara, and M. Tanaka, “Novel subset of CD8 $\alpha$ + dendritic cells localized in the marginal zone is responsible for tolerance to cell-associated antigens,” *The Journal of Immunology*, vol. 182, no. 7, pp. 4127–4136, 2009.
- [48] J. Idoyaga, N. Suda, K. Suda, C. G. Park, and R. M. Steinman, “Antibody to Langerin/CD207 localizes large numbers of CD8 $\alpha$ + dendritic cells to the marginal zone of mouse spleen.,” *Proceedings of the National Academy of Sciences of the United States of America*, vol. 106, pp. 1524–1529, 2009.
- [49] C. A. Bernhard, C. Ried, S. Kochanek, and T. Brocker, “CD169 + macrophages are sufficient for priming of CTLs with specificities left out by cross-priming dendritic cells,” *Proceedings of the National Academy of Sciences of the United States of America*, vol. 112, no. 17, 2015.
-

- 
- [50] K. Inaba, M. Witmer-Pack, M. Inaba, K. S. Hathcock, H. Sakuta, M. Azuma, H. Yagita, K. Okumura, P. S. Linsley, S. Ikehara, S. Muramatsu, R. J. Hodes, and R. M. Steinman, "The Tissue Distribution of the B7-2 Costimulator in Mice: Abundant Expression on Dendritic Cells In Situ and During Maturation In Vitro," *The Journal of Experimental Medicine*, vol. 180, no. November, pp. 1849–1860, 1994.
- [51] D. Vremec and K. Shortman, "Dendritic cell subtypes in mouse lymphoid organs: cross-correlation of surface markers, changes with incubation, and differences among thymus, spleen, and lymph nodes.," *The Journal of Immunology*, vol. 159, pp. 565–573, 1997.
- [52] A. T. Kamath, J. Pooley, M. a. O’Keeffe, D. Vremec, Y. Zhan, a. M. Lew, A. D’Amico, L. Wu, D. F. Tough, and K. Shortman, "The development, maturation, and turnover rate of mouse spleen dendritic cell populations.," *The Journal of Immunology*, vol. 165, no. 165, pp. 6762–6770, 2000.
- [53] N. S. Wilson, D. El-Sukkari, G. T. Belz, C. M. Smith, R. J. Steptoe, W. R. Heath, K. Shortman, and J. A. Villadangos, "Most lymphoid organ dendritic cell types are phenotypically and functionally immature," *Blood*, vol. 102, no. 6, pp. 2187–2194, 2003.
- [54] B. T. Edelson, T. R. Bradstreet, K. Hildner, J. a. Carrero, K. E. Frederick, W. Kc, R. Belizaire, T. Aoshi, R. D. Schreiber, M. J. Miller, T. L. Murphy, E. R. Unanue, and K. M. Murphy, "CD8 $\alpha$ (+) dendritic cells are an obligate cellular entry point for productive infection by *Listeria monocytogenes*," *Immunity*, vol. 35, pp. 236–48, aug 2011.
- [55] G. T. Belz, K. Shortman, M. J. Bevan, and W. R. Heath, "CD8 $\alpha$ + dendritic cells selectively present MHC class I-restricted noncytolytic viral and intracellular bacterial antigens in vivo.," *The Journal of Immunology*, vol. 175, no. 1, pp. 196–200, 2005.
- [56] T. Iyoda, S. Shimoyama, K. Liu, Y. Omatsu, Y. Akiyama, Y. Maeda, K. Takahara, R. M. Steinman, and K. Inaba, "The CD8+ dendritic cell subset selectively endocytoses dying cells in culture and in vivo.," *The Journal of Experimental medicine*, vol. 195, no. 10, pp. 1289–302, 2002.
- [57] J. M. den Haan, S. M. Lehar, and M. J. Bevan, "CD8(+) but not CD8(-) dendritic cells cross-prime cytotoxic T cells in vivo.," *The Journal of Experimental Medicine*, vol. 192, no. 12, pp. 1685–96, 2000.
-

- 
- [58] S. Bedoui, P. G. Whitney, J. Waithman, L. Eidsmo, L. Wakim, I. Caminschi, R. S. Allan, M. Wojtasiak, K. Shortman, F. R. Carbone, A. G. Brooks, and W. R. Heath, “Cross-presentation of viral and self antigens by skin-derived CD103+ dendritic cells,” *Nature Immunology*, vol. 10, no. 5, pp. 488–495, 2009.
- [59] P. Schnorrer, G. M. N. Behrens, N. S. Wilson, J. L. Pooley, C. M. Smith, D. El-Sukkari, G. Davey, F. Kupresanin, M. Li, E. Maraskovsky, G. T. Belz, F. R. Carbone, K. Shortman, W. R. Heath, and J. A. Villadangos, “The dominant role of CD8+ dendritic cells in cross-presentation is not dictated by antigen capture,” *Proceedings of the National Academy of Sciences of the United States of America*, vol. 103, no. 28, pp. 10729–34, 2006.
- [60] J. M. M. den Haan and M. J. Bevan, “Constitutive versus activation-dependent cross-presentation of immune complexes by CD8(+) and CD8(-) dendritic cells in vivo,” *The Journal of Experimental Medicine*, vol. 196, no. 6, pp. 817–27, 2002.
- [61] A. Ballesteros-Tato, B. León, F. E. Lund, and T. D. Randall, “Temporal changes in dendritic cell subsets, cross-priming and costimulation via CD70 control CD8(+) T cell responses to influenza,” *Nature Immunology*, vol. 11, no. 3, pp. 216–224, 2010.
- [62] L. Delamarre, “Differential Lysosomal Proteolysis in Antigen-Presenting Cells Determines Antigen Fate,” *Science*, vol. 307, no. 5715, pp. 1630–1634, 2005.
- [63] A.-M. Lennon-Duménil, A. H. Bakker, R. Maehr, E. Fiebiger, H. S. Overkleeft, M. Roseblatt, H. L. Ploegh, and C. Lagaudrière-Gesbert, “Analysis of protease activity in live antigen-presenting cells shows regulation of the phagosomal proteolytic contents during dendritic cell activation,” *The Journal of Experimental Medicine*, vol. 196, no. 4, pp. 529–40, 2002.
- [64] M. Kovacsovics-Bankowski and K. L. Rock, “A phagosome-to-cytosol pathway for exogenous antigens presented on MHC class I molecules,” *Science*, vol. 267, no. 5195, pp. 243–246, 1995.
- [65] L. Klein, M. Hinterberger, G. Wirnsberger, and B. Kyewski, “Antigen presentation in the thymus for positive selection and central tolerance induction,” *Nature Reviews Immunology*, vol. 9, no. 12, pp. 833–844, 2009.
-

- 
- [66] C.-S. Hsieh, H.-M. Lee, and C.-W. J. Lio, “Selection of regulatory T cells in the thymus,” *Nature Reviews Immunology*, vol. 12, no. 3, pp. 157–167, 2012.
- [67] K. Liu, T. Iyoda, M. Saternus, Y. Kimura, K. Inaba, and R. M. Steinman, “Immune tolerance after delivery of dying cells to dendritic cells in situ,” *The Journal of Experimental Medicine*, vol. 196, no. 8, pp. 1091–1097, 2002.
- [68] N. Luckashenak, S. Schroeder, K. Endt, D. Schmidt, K. Mahnke, M. F. Bachmann, P. Marconi, C. a. Deeg, and T. Brocker, “Constitutive crosspresentation of tissue antigens by dendritic cells controls CD8+ T cell tolerance in vivo.,” *Immunity*, vol. 28, pp. 521–32, apr 2008.
- [69] C.-M. Sun, J. a. Hall, R. B. Blank, N. Bouladoux, M. Oukka, J. R. Mora, and Y. Belkaid, “Small intestine lamina propria dendritic cells promote de novo generation of Foxp3 T reg cells via retinoic acid.,” *The Journal of Experimental Medicine*, vol. 204, no. 8, pp. 1775–1785, 2007.
- [70] J. L. Coombes, K. R. R. Siddiqui, C. V. Arancibia-Cárcamo, J. Hall, C.-M. Sun, Y. Belkaid, and F. Powrie, “A functionally specialized population of mucosal CD103+ DCs induces Foxp3+ regulatory T cells via a TGF-beta and retinoic acid-dependent mechanism.,” *The Journal of Experimental Medicine*, vol. 204, no. 8, pp. 1757–1764, 2007.
- [71] C. Ruedl, P. Koebel, M. Bachmann, M. Hess, and K. Karjalainen, “Anatomical origin of dendritic cells determines their life span in peripheral lymph nodes.,” *The Journal of Immunology*, vol. 165, no. 9, pp. 4910–4916, 2000.
- [72] K. Kabashima, T. a. Banks, K. M. Ansel, T. T. Lu, C. F. Ware, and J. G. Cyster, “Intrinsic lymphotoxin-beta receptor requirement for homeostasis of lymphoid tissue dendritic cells.,” *Immunity*, vol. 22, pp. 439–50, apr 2005.
- [73] K. Liu, C. Waskow, X. Liu, K. Yao, J. Hoh, and M. Nussenzweig, “Origin of dendritic cells in peripheral lymphoid organs of mice.,” *Nature Immunology*, vol. 8, pp. 578–83, jun 2007.
- [74] C. Waskow, K. Liu, G. Darrasse-Jèze, P. Guermonprez, F. Ginhoux, M. Merad, T. Shengelia, K. Yao, and M. Nussenzweig, “The receptor tyrosine kinase Flt3 is required for dendritic cell development in peripheral lymphoid tissues.,” *Nature Immunology*, vol. 9, no. 6, pp. 676–83, 2008.
-

- 
- [75] E. Maraskovsky, K. Brasel, M. Teepe, E. R. Roux, S. D. Lyman, K. Shortman, and H. J. McKenna, “Dramatic increase in the numbers of functionally mature dendritic cells in Flt3 ligand-treated mice: multiple dendritic cell subpopulations identified,” *The Journal of Experimental Medicine*, vol. 184, no. 5, pp. 1953–62, 1996.
- [76] K. Brasel, H. J. McKenna, P. J. Morrissey, K. Charrier, a. E. Morris, C. C. Lee, D. E. Williams, and S. D. Lyman, “Hematologic effects of flt3 ligand in vivo in mice.,” *Blood*, vol. 88, no. 6, pp. 2004–2012, 1996.
- [77] R. Tussiwand, N. Onai, L. Mazzucchelli, and M. G. Manz, “Inhibition of natural type I IFN-producing and dendritic cell development by a small molecule receptor tyrosine kinase inhibitor with Flt3 affinity,” *The Journal of Immunology*, vol. 175, no. 6, pp. 3674–3680, 2005.
- [78] K. A. Whartenby, P. A. Calabresi, E. McCadden, B. Nguyen, D. Kardian, T. Wang, C. Mosse, D. M. Pardoll, and D. Small, “Inhibition of FLT3 signaling targets DCs to ameliorate autoimmune disease.,” *Proceedings of the National Academy of Sciences of the United States of America*, vol. 102, no. 46, pp. 16741–6, 2005.
- [79] Q. Wu, Y. Wang, J. Wang, E. O. Hedgeman, J. L. Browning, and Y. X. Fu, “The requirement of membrane lymphotoxin for the presence of dendritic cells in lymphoid tissues.,” *The Journal of Experimental Medicine*, vol. 190, no. 5, pp. 629–38, 1999.
- [80] Y.-G. Wang, K. D. Kim, J. Wang, P. Yu, and Y.-X. Fu, “Stimulating lymphotoxin beta receptor on the dendritic cells is critical for their homeostasis and expansion.,” *The Journal of Immunology*, vol. 175, pp. 6997–7002, 2005.
- [81] Y. Y. Kong, H. Yoshida, I. Sarosi, H. L. Tan, E. Timms, C. Capparelli, S. Morony, a. J. Oliveira-dos Santos, G. Van, A. Itie, W. Khoo, A. Wakeham, C. R. Dunstan, D. L. Lacey, T. W. Mak, W. J. Boyle, and J. M. Penninger, “OPGL is a key regulator of osteoclastogenesis, lymphocyte development and lymph-node organogenesis.,” *Nature*, vol. 397, no. 6717, pp. 315–323, 1999.
- [82] B. B. R. Wong, R. Josien, S. Y. Lee, B. Sauter, H.-l. Li, R. M. Steinman, and Y. Choi, “TRANCE (Tumor Necrosis Factor [TNF]-related Activation-induced Cytokine), a New TNF Family Member Predominantly Expressed
-

- in T cells, Is a Dendritic Cell-specific Survival Factor,” *The Journal of Experimental Medicine*, vol. 186, no. 12, pp. 2075–2080, 1997.
- [83] K. Inaba, M. Inaba, N. Romani, H. Aya, M. Deguchi, S. Ikehara, S. Muramatsu, and R. M. Steinman, “Generation of large numbers of dendritic cells from mouse bone marrow cultures supplemented with granulocyte/macrophage colony-stimulating factor,” *The Journal of Experimental Medicine*, vol. 176, pp. 1693–1702, 1992.
- [84] D. Metcalf, “Hematopoietic cytokines,” *Blood*, vol. 111, no. 2, pp. 485–491, 2009.
- [85] A. T. Kamath, S. Henri, F. Battye, D. F. Tough, and K. Shortman, “Developmental kinetics and lifespan of dendritic cells in mouse lymphoid organs.,” *Blood*, vol. 100, pp. 1734–41, sep 2002.
- [86] M. Chen, L. Huang, and J. Wang, “Deficiency of Bim in dendritic cells contributes to overactivation of lymphocytes and autoimmunity,” *Blood*, vol. 109, no. 10, pp. 4360–4367, 2007.
- [87] P. B. Stranges, J. Watson, C. J. Cooper, C. M. Choisy-Rossi, A. C. Stonebraker, R. a. Beighton, H. Hartig, J. P. Sundberg, S. Servick, G. Kaufmann, P. J. Fink, and A. V. Chervonsky, “Elimination of Antigen-Presenting Cells and Autoreactive T Cells by Fas Contributes to Prevention of Autoimmunity,” *Immunity*, vol. 26, no. 5, pp. 629–641, 2007.
- [88] D. Park, N. Lapteva, M. Seethammagari, K. M. Slawin, and D. M. Spencer, “An essential role for Akt1 in dendritic cell function and tumor immunotherapy.,” *Nature Biotechnology*, vol. 24, no. 12, pp. 1581–1590, 2006.
- [89] E. Montini, E. I. Rugarli, E. Van de Vosse, G. Andolfi, M. Mariani, a. a. Puca, G. G. Consalez, J. T. den Dunnen, A. Ballabio, and B. Franco, “A novel human serine-threonine phosphatase related to the Drosophila retinal degeneration C (rdgC) gene is selectively expressed in sensory neurons of neural crest origin.,” *Human Molecular Genetics*, vol. 6, pp. 1137–45, jul 1997.
- [90] F. Steele and J. E. O’Tousa, “Rhodopsin activation causes retinal degeneration in drosophila rdgC mutant,” *Neuron*, vol. 4, no. 6, pp. 883–890, 1990.
- [91] P. M. Sherman, H. Sun, J. P. Macke, J. Williams, P. M. Smallwood, and J. Nathans, “Identification and characterization of a conserved family of

- protein serine y threonine phosphatases homologous to *Drosophila* retinal degeneration C (rdgC),” *Proceedings of the National Academy of Sciences of the United States of America*, vol. 94, no. October, pp. 11639–11644, 1997.
- [92] P. Ramulu, M. Kennedy, W.-h. Xiong, M. Cowan, D. Blesh, K.-w. Yau, B. Hurley, J. Nathans, J. Williams, and J. B. Hurley, “Normal Light Response, Photoreceptor Integrity, and Rhodopsin Dephosphorylation in Mice Lacking Both Protein Phosphatases with EF Hands (PPEF-1 and PPEF-2),” *Molecular And Cellular Biology*, vol. 21, no. 24, pp. 8605–8614, 2001.
- [93] P. Ramulu and J. Nathans, “Cellular and subcellular localization, N-terminal acylation, and calcium binding of *Caenorhabditis elegans* protein phosphatase with EF-hands,” *The Journal of Biological Chemistry*, vol. 276, pp. 25127–35, jul 2001.
- [94] M. a. Kutuzov, O. V. Solov’eva, A. V. Andreeva, and N. Bennett, “Protein Ser/Thr phosphatases PPEF interact with calmodulin,” *Biochemical and Biophysical Research Communications*, vol. 293, pp. 1047–52, may 2002.
- [95] X. Huang and R. E. Honkanen, “Molecular cloning, expression, and characterization of a novel human serine/ threonine protein phosphatase, PP7, that is homologous to *Drosophila* retinal degeneration C gene product (rdgC),” *The Journal of Biological Chemistry*, vol. 273, no. 3, pp. 1462–1468, 1998.
- [96] A. V. Andreeva and M. a. Kutuzov, “PPEF/PP7 protein Ser/Thr phosphatases,” *Cellular and Molecular Life Sciences*, vol. 66, pp. 3103–10, oct 2009.
- [97] M. a. Kutuzov, N. Bennett, and A. V. Andreeva, “Protein phosphatase with EF-hand domains 2 (PPEF2) is a potent negative regulator of apoptosis signal regulating kinase-1 (ASK1),” *The International Journal of Biochemistry & Cell Biology*, vol. 42, pp. 1816–22, nov 2010.
- [98] K. I. Morita, M. Saitoh, K. Tobiume, H. Matsuura, S. Enomoto, H. Nishitoh, and H. Ichijo, “Negative feedback regulation of ASK1 by protein phosphatase 5 (PP5) in response to oxidative stress,” *The EMBO Journal*, vol. 20, no. 21, pp. 6028–6036, 2001.
- [99] T. S. P. Heng, M. W. Painter, and I. G. P. Consortium, “The Immunological Genome Project: networks of gene expression in immune cells,” *Nature Immunology*, vol. 9, no. 10, pp. 1091–1094, 2008.

- [100] J. E. Lattin, K. Schroder, A. I. Su, J. R. Walker, J. Zhang, T. Wiltshire, K. Saijo, C. K. Glass, D. A. Hume, S. Kellie, and M. J. Sweet, "Expression analysis of G Protein-Coupled Receptors in mouse macrophages," *Immuno-meme Research*, vol. 4, no. 1, pp. 1–13, 2008.
- [101] G. Testa, J. Schaft, F. Van Der Hoeven, S. Glaser, K. Anastassiadis, Y. Zhang, T. Hermann, W. Stremmel, and A. F. Stewart, "A Reliable lacZ Expression Reporter Cassette for Multipurpose, Knockout-First Alleles," *Genesis*, vol. 38, no. 3, pp. 151–158, 2004.
- [102] W. C. Skarnes, B. Rosen, A. P. West, M. Koutsourakis, W. Bushell, V. Iyer, A. O. Mujica, M. Thomas, J. Harrow, T. Cox, D. Jackson, J. Severin, P. Biggs, J. Fu, M. Nefedov, P. J. de Jong, a. F. Stewart, and A. Bradley, "A conditional knockout resource for the genome-wide study of mouse gene function.," *Nature*, vol. 474, pp. 337–42, jun 2011.
- [103] G. P. Nolan, S. Fiering, J. F. Nicolas, and L. A. Herzenberg, "Fluorescence-activated cell analysis and sorting of viable mammalian cells based on b-D-galactosidase activity after transduction of E. Coli LacZ," *Proceedings of the National Academy of Sciences of the United States of America*, vol. 85, no. April, pp. 2603–2607, 1988.
- [104] K. J. Livak and T. D. Schmittgen, "Analysis of relative gene expression data using real-time quantitative PCR and," *Methods*, vol. 25, pp. 402–408, 2001.
- [105] T. D. Schmittgen and K. J. Livak, "Analyzing real-time PCR data by the comparative CT method," *Nature Protocols*, vol. 3, no. 6, pp. 1101–1108, 2008.
- [106] B. C. Caux, C. Massacrier, B. Vanbervliet, B. Dubois, C. V. Kooten, I. Durand, and J. Banchereau, "Activation of Human Dendritic Cells through CD40 Cross-linking," *The Journal of Experimental Medicine*, vol. 180, no. October, pp. 1263–1272, 1994.
- [107] M. Celia, D. Scheidegger, K. Palmer-Lehmann, P. Lane, A. Lanzavecchia, and G. Alber, "Ligation of CD40 on Dendritic Cells Triggers Production of High Levels of Interleukin-12 and Enhances T Cell Stimulatory Capacity: T-T Help via APC Activation," *The Journal of Experimental Medicine*, vol. 184, no. August, pp. 747–752, 1996.

- [108] S.-I. Fujii, K. Liu, C. Smith, A. J. Bonito, and R. M. Steinman, "The linkage of innate to adaptive immunity via maturing dendritic cells in vivo requires CD40 ligation in addition to antigen presentation and CD80/86 costimulation.," *The Journal of Experimental Medicine*, vol. 199, no. 12, pp. 1607–18, 2004.
- [109] B. J. Weigel, N. Nath, P. A. Taylor, A. Panoskaltsis-Mortari, W. Chen, A. M. Krieg, K. Brasel, and B. R. Blazar, "Comparative analysis of murine marrow-derived dendritic cells generated by Flt3L or GM-CSF/IL-4 and matured with immune stimulatory agents on the in vivo induction of antileukemia responses," *Blood*, vol. 100, no. 12, pp. 4169–4176, 2002.
- [110] B. F. Sallusto and A. Lanzavecchia, "Efficient Presentation of Soluble Antigen by Cultured Human Dendritic Cells is Maintained by Granulocyte/Macrophage Colony-stimulating Factor Plus Interleukin-4 and Downregulated by Tumor Necrosis Factor- $\alpha$ ," *The Journal of Experimental Medicine*, vol. 179, no. April, pp. 1109–1118, 1994.
- [111] O. Schulz, a. D. Edwards, M. Schito, J. Aliberti, S. Manickasingham, a. Sher, and C. Reis e Sousa, "CD40 triggering of heterodimeric IL-12 p70 production by dendritic cells in vivo requires a microbial priming signal.," *Immunity*, vol. 13, no. 4, pp. 453–62, 2000.
- [112] A. Jiang, O. Bloom, S. Ono, W. Cui, J. Unternaehrer, S. Jiang, J. A. Whitney, J. Connolly, J. Banchereau, and I. Mellman, "Disruption of E-cadherin-mediated adhesion induces a functionally distinct pathway of dendritic cell maturation.," *Immunity*, vol. 27, pp. 610–24, oct 2007.
- [113] S. Tamoutounour, S. Henri, H. Lelouard, B. de Bovis, C. de Haar, C. J. van der Woude, A. M. Woltman, Y. Reyat, D. Bonnet, D. Sichien, C. C. Bain, A. M. Mowat, C. Reis e Sousa, L. F. Poulin, B. Malissen, and M. Guillems, "CD64 distinguishes macrophages from dendritic cells in the gut and reveals the Th1-inducing role of mesenteric lymph node macrophages during colitis.," *The European Journal of Immunology*, vol. 42, pp. 3150–66, dec 2012.
- [114] G. Trinchieri, "Interleukin-12: A proinflammatory cytokine with immunoregulatory functions that bridge innate resistance and antigen-specific adaptive immunity," *Annual Review of Immunology*, no. 13, pp. 251–176, 1995.

- 
- [115] S. J. Martin, C. P. Reutelingsperger, a. J. McGahon, J. a. Rader, R. C. van Schie, D. M. LaFace, and D. R. Green, “Early redistribution of plasma membrane phosphatidylserine is a general feature of apoptosis regardless of the initiating stimulus: inhibition by overexpression of Bcl-2 and Abl,” *The Journal of Experimental Medicine*, vol. 182, no. November, pp. 1545–1556, 1995.
- [116] T. Birnberg, L. Bar-On, A. Sapoznikov, M. L. Caton, L. Cervantes-Barragán, D. Makia, R. Krauthgamer, O. Brenner, B. Ludewig, D. Brockschnieder, D. Riethmacher, B. Reizis, and S. Jung, “Lack of Conventional Dendritic Cells Is Compatible with Normal Development and T Cell Homeostasis, but Causes Myeloid Proliferative Syndrome,” *Immunity*, vol. 29, no. 6, pp. 986–997, 2008.
- [117] S. Li, B. Dislich, C. H. Brakebusch, F. Stefan, T. Brocker, S. Li, B. Dislich, C. H. Brakebusch, and S. F. Lichtenthaler, “Control of Homeostasis and Dendritic Cell Survival by the GTPase RhoA,” *The Journal of Immunology*, vol. 195, no. 9, pp. 4244–4256, 2015.
- [118] B. A. M. Turner, N. L. Lin, S. Issarachai, S. D. Lyman, and C. Virginia, “FLT3 receptor expression on the surface of normal and malignant human hematopoietic cells,” *Blood*, vol. 88, no. 9, pp. 3383–3390, 1996.
- [119] J. Nikolić-Zugić and F. R. Carbone, “The effect of mutations in the MHC class I peptide binding groove on the cytotoxic T lymphocyte recognition of the Kb-restricted ovalbumin determinant,” *European journal of immunology*, vol. 20, no. 11, pp. 2431–7, 1990.
- [120] S. Thompson, A. N. Pearson, M. D. Ashley, V. Jessick, B. M. Murphy, P. Gafken, D. C. Henshall, K. T. Morris, R. P. Simon, and R. Meller, “Identification of a novel Bcl-2-interacting mediator of cell death (Bim) E3 ligase, tripartite motif-containing protein 2 (TRIM2), and its role in rapid ischemic tolerance-induced neuroprotection,” *The Journal of Biological Chemistry*, vol. 286, no. 22, pp. 19331–19339, 2011.
- [121] J. R. Shutter, “Dll4, a novel Notch ligand expressed in arterial endothelium,” *Genes and Development*, vol. 14, pp. 1313–1318, 2000.
- [122] I. Maillard, T. Fang, and W. S. Pear, “Regulation of Lymphoid Development, Differentiation, and Function By the Notch Pathway,” *Annual Review of Immunology*, vol. 23, no. 1, pp. 945–974, 2005.
-

- 
- [123] L. O'Connor, A. Strasser, L. A. O'Reilly, G. Hausmann, J. M. Adams, S. Cory, and D. C. S. Huang, "Bim: A novel member of the Bcl-2 family that promotes apoptosis," *The EMBO Journal*, vol. 17, no. 2, pp. 384–395, 1998.
- [124] R. de Sousa Abreu, L. O. Penalva, E. M. Marcotte, and C. Vogel, "Global signatures of protein and mRNA expression levels," *Molecular BioSystems*, vol. 5, no. 12, pp. 1512–1526, 2009.
- [125] C. Vogel and E. M. Marcotte, "Insights into the regulation of protein abundance from proteomic and transcriptomic analyses," *Nature Reviews Genetics*, vol. 13, no. 4, pp. 227–232, 2012.
- [126] T. Ishida, S. Mizushima, S. Azuma, N. Kobayashi, T. Tojo, K. Suzuki, S. Aizawa, T. Watanabe, G. Mosialos, E. Kieff, T. Yamamoto, and J. Inoue, "Identification of TRAF6, a novel tumor necrosis factor receptor-associated factor protein that mediates signaling from an amino-terminal domain of the CD40 cytoplasmic region," *The Journal of Biological Chemistry*, vol. 271, no. 15, pp. 28745–28748, 1996.
- [127] T. Kobayashi, P. T. Walsh, M. C. Walsh, K. M. Speirs, E. Chiffolleau, C. G. King, W. W. Hancock, J. H. Caamano, C. A. Hunter, P. Scott, L. A. Turka, and Y. Choi, "TRAF6 is a critical factor for dendritic cell maturation and development," *Immunity*, vol. 19, no. 3, pp. 353–363, 2003.
- [128] B. J. O'Sullivan and R. Thomas, "CD40 Ligation Conditions Dendritic Cell Antigen-Presenting Function Through Sustained Activation of NF-kappaB," *The Journal of Immunology*, vol. 168, no. 11, pp. 5491–5498, 2002.
- [129] N. Tsukamoto, N. Kobayashi, S. Azuma, T. Yamamoto, and J. Inoue, "Two differently regulated nuclear factor kappaB activation pathways triggered by the cytoplasmic tail of CD40.," *Proceedings of the National Academy of Sciences of the United States of America*, vol. 96, no. 4, pp. 1234–9, 1999.
- [130] J. R. Arron, M. Vologodskaja, B. R. Wong, M. Naramura, N. Kim, H. Gu, and Y. Choi, "A Positive Regulatory Role for Cbl Family Proteins in Tumor Necrosis Factor-related Activation-induced Cytokine (TRANCE) and CD40L-mediated Akt Activation," *Journal of Biological Chemistry*, vol. 276, no. 32, pp. 30011–30017, 2001.
- [131] L. a. J. O'Neill, D. Golenbock, and A. G. Bowie, "The history of Toll-like receptors - redefining innate immunity.," *Nature reviews. Immunology*, vol. 13, pp. 453–60, jun 2013.
-

- 
- [132] T. Akiyama, M. Shinzawa, and N. Akiyama, “TNF receptor family signaling in the development and functions of medullary thymic epithelial cells,” *Frontiers in Immunology*, vol. 3, no. SEP, pp. 1–9, 2012.
- [133] C. Hull, G. McLean, F. Wong, P. J. Duriez, and A. Karsan, “Lipopolysaccharide signals an endothelial apoptosis pathway through TNF receptor-associated factor 6-mediated activation of c-Jun NH2-terminal kinase.,” *Journal of Immunology*, vol. 169, no. 5, pp. 2611–8, 2002.
- [134] S. K. Zaidi, W.-J. Shen, S. Bittner, A. Bittner, M. P. McLean, J. Han, R. J. Davis, F. B. Kraemer, and S. Azhar, “p38 MAPK regulates steroidogenesis through transcriptional repression of StAR gene,” *Journal of Molecular Endocrinology*, vol. 41, no. 3, pp. 1120–1131, 2008.
- [135] M. Kelleher and P. C. L. Beverley, “Lipopolysaccharide Modulation of Dendritic Cells Is Insufficient to Mature Dendritic Cells to Generate CTLs from Naive Polyclonal CD8+ T Cells In Vitro, Whereas CD40 Ligation Is Essential,” *The Journal of Immunology*, vol. 167, pp. 6247–6255, dec 2001.
- [136] J. Helft, J. Böttcher, P. Chakravarty, S. Zelenay, J. Huotari, B. U. Schraml, D. Goubau, and C. Reis e Sousa, “GM-CSF Mouse Bone Marrow Cultures Comprise a Heterogeneous Population of CD11c+MHCII+ Macrophages and Dendritic Cells,” *Immunity*, vol. 42, no. 6, pp. 1197–1211, 2015.
- [137] K. Brasel, T. D. Smedt, J. L. Smith, and C. R. Maliszewski, “Generation of murine dendritic cells from flt3-ligand-supplemented bone marrow cultures.,” *Blood*, vol. 96, no. 9, pp. 3029–3039, 2014.
- [138] S. H. Naik, A. I. Proietto, N. S. Wilson, A. Dakic, P. Schnorrer, M. Fuchsberger, M. H. Lahoud, M. O’Keeffe, Q.-x. Shao, W.-f. Chen, J. a. Villadangos, K. Shortman, and L. Wu, “Cutting edge: generation of splenic CD8+ and CD8- dendritic cell equivalents in Fms-like tyrosine kinase 3 ligand bone marrow cultures.,” *The Journal of Immunology*, vol. 174, no. 11, pp. 6592–6597, 2005.
- [139] E. Riedl, J. Stöckl, O. Majdic, C. Scheinecker, W. Knapp, and J. Sto, “Ligation of E-cadherin on in vitro-generated immature Langerhans-type dendritic cells inhibits their maturation,” *Blood*, vol. 96, no. 13, pp. 4276–4284, 2000.
- [140] B. vander Lugt, Z. T. Beck, R. C. Fuhlbrigge, N. Hacohen, J. J. Campbell, and M. Boes, “Tgf- $\beta$  suppresses  $\beta$ -catenin-dependent tolerogenic activation program in dendritic cells,” *PLoS ONE*, vol. 6, no. 5, pp. 1–9, 2011.
-

- 
- [141] D. Vremec, M. O’Keeffe, A. Wilson, I. Ferrero, U. Koch, F. Radtke, B. Scott, P. Hertzog, J. Villadangos, and K. Shortman, “Factors determining the spontaneous activation of splenic dendritic cells in culture.,” *Innate Immunity*, vol. 17, no. 3, pp. 338–52, 2011.
- [142] C. Ocaña-Morgner, A. Götz, C. Wahren, and R. Jessberger, “SWAP-70 restricts spontaneous maturation of dendritic cells.,” *The Journal of Immunology*, vol. 190, pp. 5545–58, jun 2013.
- [143] J. Riepsaame, A. van Oudenaren, B. J. H. den Broeder, W. F. J. van Ijcken, J. Pothof, and P. J. M. Leenen, “MicroRNA-Mediated Down-Regulation of M-CSF Receptor Contributes to Maturation of Mouse Monocyte-Derived Dendritic Cells.,” *Frontiers in Immunology*, vol. 4, no. October, p. 353, 2013.
- [144] C. L. Ahonen, C. L. Doxsee, S. M. McGurran, T. R. Riter, W. F. Wade, R. J. Barth, J. P. Vasilakos, R. J. Noelle, and R. M. Kedl, “Combined TLR and CD40 triggering induces potent CD8+ T cell expansion with variable dependence on type I IFN.,” *The Journal of Experimental Medicine*, vol. 199, no. 6, pp. 775–84, 2004.
- [145] P. J. Sanchez, J. a. McWilliams, C. Haluszczak, H. Yagita, and R. M. Kedl, “Combined TLR/CD40 stimulation mediates potent cellular immunity by regulating dendritic cell expression of CD70 in vivo.,” *The Journal of Immunology*, vol. 178, no. 3, pp. 1564–1572, 2007.
- [146] A. L. Olex, E. M. Hiltbold, X. Leng, and J. S. Fetrow, “Dynamics of dendritic cell maturation are identified through a novel filtering strategy applied to biological time-course microarray replicates.,” *BMC Immunology*, vol. 11, pp. 1–19, jan 2010.
- [147] A. M. Woltman, S. W. Van der Kooij, P. J. Coffey, R. Offringa, M. R. Daha, and C. Van Kooten, “Rapamycin specifically interferes with GM-CSF signaling in human dendritic cells, leading to apoptosis via increased p27KIP1 expression,” *Blood*, vol. 101, no. 4, pp. 1439–1445, 2003.
- [148] M. B. Yamaoka K Zhou YJ, Paul WE, O’shea JJ., “Jak3 negatively regulates dendritic-cell cytokine production and survival.,” *Blood*, vol. 106, no. 9, pp. 3227–3234, 2005.
- [149] L. Lozza, M. Farinacci, K. Faé, M. Bechtle, M. Stäber, A. Dorhoi, M. Bauer, C. Ganoza, S. Weber, and S. H. E. Kaufmann, “Crosstalk between human
-

- DC subsets promotes antibacterial activity and CD8+ T-cell stimulation in response to bacille Calmette-Guérin,” *The European Journal of Immunology*, vol. 44, no. 1, pp. 80–92, 2014.
- [150] S. Kuwajima, T. Sato, K. Ishida, H. Tada, H. Tezuka, and T. Ohteki, “Interleukin 15-dependent crosstalk between conventional and plasmacytoid dendritic cells is essential for CpG-induced immune activation.” *Nature Immunology*, vol. 7, no. 7, pp. 740–6, 2006.
- [151] R. S. Allan, J. Waithman, S. Bedoui, C. M. Jones, J. A. Villadangos, Y. Zhan, A. M. Lew, K. Shortman, W. R. Heath, and F. R. Carbone, “Migratory Dendritic Cells Transfer Antigen to a Lymph Node-Resident Dendritic Cell Population for Efficient CTL Priming,” *Immunity*, vol. 25, no. 1, pp. 153–162, 2006.
- [152] A. Chen, H. Xu, Y. Choi, B. Wang, and G. Zheng, “TRANCE counteracts FasL-mediated apoptosis of murine bone marrow-derived dendritic cells,” *Cellular Immunology*, vol. 231, no. 1-2, pp. 40–48, 2004.
- [153] A. J. Miga, S. R. Masters, B. G. Durell, M. Gonzalez, M. K. Jenkins, C. Maliszewski, H. Kikutani, W. F. Wade, and R. J. Noelle, “Dendritic cell longevity and T cell persistence is controlled by CD154-CD40 interactions,” *European Journal of Immunology*, vol. 31, pp. 959–965, 2001.
- [154] J. Diao, E. Winter, C. Cantin, W. Chen, L. Xu, D. Kelvin, J. Phillips, and M. S. Cattral, “In situ replication of immediate dendritic cell (DC) precursors contributes to conventional DC homeostasis in lymphoid tissue.” *Journal of immunology (Baltimore, Md : 1950)*, vol. 176, no. 12, pp. 7196–7206, 2006.
- [155] R. Maldonado and U. V. Andrian, *How tolerogenic dendritic cells induce regulatory T cells*, vol. 108. *Advances in Immunology*, 2010.
- [156] S. J. F. Cronin and J. M. Penninger, “From T-cell activation signals to signaling control of anti-cancer immunity,” *Immunological Reviews*, vol. 220, no. 1, pp. 151–168, 2007.
- [157] M. V. Dhodapkar, R. M. Steinman, J. Krasovsky, C. Munz, and N. Bhardwaj, “Antigen-specific inhibition of effector T cell function in humans after injection of immature dendritic cells,” *J Exp Med*, vol. 193, no. 2, pp. 233–238, 2001.

- 
- [158] M. V. Dhodapkar and R. M. Steinman, “Antigen-bearing immature dendritic cells induce peptide-specific CD8+ regulatory T cells in vivo in humans,” *Blood*, vol. 100, no. 1, pp. 174–177, 2002.
- [159] H. J. McKenna, K. L. Stocking, R. E. Miller, K. Brasel, T. De Smedt, E. Maraskovsky, C. R. Maliszewski, D. H. Lynch, J. Smith, B. Pulendran, E. R. Roux, M. Teepe, S. D. Lyman, and J. J. Peschon, “Mice lacking flt3 ligand have deficient hematopoiesis affecting hematopoietic progenitor cells, dendritic cells, and natural killer cells.,” *Blood*, vol. 95, no. 11, pp. 3489–3497, 2000.
- [160] Vincent C. Luca, K. M. Jude, N. W. Pierce, M. V. Nachury, S. Fischer, and C. K. Garcia, “Structural basis for Notch1 engagement of Delta-like 4,” *Science*, vol. 347, no. 6224, pp. 847–854, 2015.
- [161] D. Sprinzak, A. Lakhanpal, L. Lebon, L. A. Santat, M. E. Fontes, G. A. Anderson, J. Garcia-Ojalvo, and M. B. Elowitz, “Cis-interactions between Notch and Delta generate mutually exclusive signalling states,” *Nature*, vol. 465, no. 7294, pp. 86–90, 2010.
- [162] J. F. de Celis and S. Bray, “Feed-back mechanisms affecting Notch activation at the dorsoventral boundary in the *Drosophila* wing.,” *Development*, vol. 124, no. 17, pp. 3241–3251, 1997.
- [163] P. Bouillet, D. Metcalf, D. C. S. Huang, D. M. Tarlinton, T. W. H. Kay, F. Köntgen, J. M. Adams, and A. Strasser, “Proapoptotic Bcl-2 Relative Bim Required for Certain Apoptotic Responses, Leukocyte Homeostasis, and to Preclude Autoimmunity,” *Science*, vol. 286, no. 5445, pp. 1735–1738, 1999.
- [164] X. Deng, L. Xiao, W. Lang, F. Gao, P. Ruvolo, and W. S. May, “Novel Role for JNK as a Stress-activated Bcl2 Kinase,” *The Journal of Biological Chemistry*, vol. 276, no. 26, pp. 23681–23688, 2001.
- [165] K. Lei and R. J. Davis, “JNK phosphorylation of Bim-related members of the Bcl2 family induces Bax-dependent apoptosis,” *Proceedings of the National Academy of Sciences of the United States of America*, vol. 100, no. 5, pp. 2432–2437, 2003.
- [166] J. P. MacKeigan, L. O. Murphy, and J. Blenis, “Sensitized RNAi screen of human kinases and phosphatases identifies new regulators of apoptosis and chemoresistance.,” *Nature cell biology*, vol. 7, pp. 591–600, jun 2005.
-

- [167] H. Kristin, S. Jameson, William Heath, J. Howard, M. Bevan, and F. Carbone, “T cell receptor antagonist peptides induce positive selection,” *Cell*, vol. 76, no. 1, pp. 17–27, 1994.

## **Acknowledgements**

Besonders herzlich möchte ich mich bei Herrn Prof. Dr. Thomas Brocker für die Überlassung des Themas, die stets offene Tür und den unerschütterlichen Glauben an den erfolgreichen Ausgang des Projekts bedanken.

Herrn Dr. Veit Buchholz an der TU München bin ich für die erfolgreiche Kooperation und die Diskussion der Daten und des Projekts ebenfalls zu Dank verpflichtet.

Bei Herrn Dr. Thomas Ulas bedanke ich mich für die mehreren Telefonate und erläuternden E-Mails zum mRNA sequencing. Ohne seine Bereitschaft immer wieder weitere Analysen durchzuführen wären wir nicht weiter gekommen.

Herrn Andrea Musumeci danke ich für das kritische Lesen des Manuskripts.

Frau Christine Ried danke ich für ihre Unterstützung beim Anfertigen der immunhistologischen Analysen, sowie für die äußerst arbeitserleichternde Organisation der alltäglich im Hintergrund laufenden Labor-Organisation.

Den Mitarbeitern der Tierhaltung, namentlich besonders Frau Andrea Bohl und Frau Tamara Weinberger, möchte ich ebenfalls meinen Dank aussprechen. Ihre Arbeit hat die meinige deutlich erleichtert.

Den restlichen Mitarbeitern des Instituts für Immunologie möchte ich ebenfalls für die tolle Zeit und den Zusammenhalt meinen Dank aussprechen. Ebenso dem SFB1054 und insbesondere dem IRTG. Nicht nur für den wissenschaftlichen Austausch, sondern auch für die dort entstandenen Freundschaften.